GAUGED U(1) EXTENSION OF THE STANDARD MODEL AND PHENOMENOLOGY

by

DIGESH RAUT

NOBUCHIKA OKADA, COMMITTEE CHAIR
BENJAMIN HARMS
PAOLO RUMERIO
QAISAR SHAFI
ALLEN B. STERN
DEAN TOWNSLEY

A DISSERTATION

Submitted in partial fulfillment of the requirements
for the degree of Doctor of Philosophy
in the Department of Physics and Astronomy
in the Graduate School of
The University of Alabama

TUSCALOOSA, ALABAMA

2018

ABSTRACT

Despite the tremendous success of the Standard Model (SM), it needs to be extended to explain the origin of cosmological inflation, dark matter (DM) and neutrino masses. We consider gauged $U(1)_X$ extended SM, where in addition to the SM particles, the model includes a $U(1)_X$ scalar, Z' gauge boson, and three generations of right-handed neutrinos (RHNs), where the $U(1)_X$ charges of all the particles are defined by a single free parameter x_H. In this model context, we discuss the complementarity between the cosmological inflation, the DM physics, and new physics searches at the Large Hadron Colliders (LHC). With the identification of the $U(1)_X$ scalar as an inflaton field, we consider the cosmological inflation scenario. For an effective inflaton potential to develop an inflection-point with predictions consistent with cosmological observations, the mass ratios among the Z' boson, the RHNs, and the inflaton are fixed. Requiring the inflationary prediction to be consistent with the current cosmological observation and collider experimental results, we show that our scenario can be tested at the future collider experiments such as the High Luminosity-LHC and the SHiP experiment. We also consider $SU(5)\times U(1)_X$ scenario, where the SU(5) grand unification of the SM quarks and leptons is realized for $x_H = -4/5$. Hence, the $U(1)_X$ charge is quantized in this scenario. With an additional global Z_2 symmetry, one RHN, which is Z_2 odd particles, serves as the DM in the universe. We investigate the Z'-portal RHN DM scenario and find that the constraints from the DM relic abundance and the search results for a Z' boson resonance at the LHC Run-2 are complementary to narrow down the allowed parameter region, which will be fully covered by the future LHC experiments for the Z' boson mass < 5 TeV.

DEDICATION

This work is dedicated to my mother Sakuntala Katawal (Raut), father Durga B. Raut, and brother Nikesh Raut. No words can adequately describe how fortunate I am to receive your selfless, unwavering, and unconditional support throughout the years. To put it simply, none of my works and achievements so far would have been possible without you.

ACKNOWLEDGMENTS

First and foremost, I would like to express my most sincere gratitude to my adviser Prof. Nobuchika Okada, whose immense expertise in physics, in addition to his incredible academic/personal mentorship qualities, has been a constant source of my inspiration. It has always been pleasure to participate in prolonged and engaging discussions with Prof. Okada on diverse range of topics, mostly physics. With his guidance, I was able to branch out to many different area of particle physics research. I would also like to acknowledge all my collaborators, namely, Satomi Okada, Arindam Das, Desmond Villalba, Dai-suke Takahashi, Satsuki Oda, and Sudip Jana, whom I had pleasure working with during my PhD. In addition, I would also like to thank all the members of my thesis committee, Prof. Benjamin Harms, Prof. Paolo Rumerio, Prof. Qaisar Shafi, and Prof. Allen B. Stern for being considerate throughout these years. Particularly, I would like to thank Prof. Qaisar Shafi for the hospitality during my visit to University of Delaware. I would also like to thank Dr. Lee Sawyer, department chair at Louisiana Tech University, for his support during my undergraduate studies. I would also like to thank Prof. Raymond E. White and Prof. Patrick R. Leclair, past and current department chairs at the University of Alabama, respectively, as well as all the staff at the Department of Physics and Astronomy at the University of Alabama for all their support. Last but not least, I would like to thank all of my friends, far too many to name here, whom I had pleasure getting acquainted with during my years at high school, undergraduate and graduate school; I am personally indebted for all their support and encouragement throughout the years.

Chapter 2 has been previously published as "Inflection-point $B - L$ Higgs inflation" by D. Raut et al. in Physical Review D Journal, volume 95, issue 3, 2017, and it is reproduced here with a permission of the American Physical Society (APS). This work has

been supported in part by the United States Department of Energy (Award No. DE-SC0013680). Figures 2.1, 2.2, and 2.3 in Chapter 2 has been reproduced with permission from APS. Chapter 3 has been previously published as "Inflection-point inflation in hyper-charge oriented $U(1)_X$ model" by D. Raut et al. in Physical Review D Journal, volume 95, issue 5, 2017, and it is reproduced here with a permission of the APS. This work has been supported in part by the United States Department of Energy (Award No. DE-SC0013680). Figures 3.1, 3.2, 3.3, and 3.4 in Chapter 3 has been reproduced with permission from APS. Chapter 4 has been previously published as "$SU(5)\times U(1)_X$ grand unification with minimal seesaw and Z'-portal dark matter" by D. Raut et al. in Physics Letters B Journal, volume 780, pages 420-426, 2018, and it is reproduced here with a permission of Elsevier. This work has been supported in part by the United States Department of Energy (Award No. DE-SC0012447). Figures 4.1, and 4.2 in Chapter 4 has been reproduced with permission from Elsiver.

CONTENTS

ABSTRACT ii

DEDICATION iii

ACKNOWLEDGMENTS iv

LIST OF TABLES viii

LIST OF FIGURES ix

CHAPTER 1 INTRODUCTION 1

CHAPTER 2 INFLECTION-POINT $B - L$ HIGGS INFLATION 8

2.1 Introduction 8

2.2 Brief Review of Slow-roll Inflation 11

2.3 Inflection-point Inflation 13

2.4 The Inflection-point-like $B - L$ Higgs Inflation 15

2.5 Constraints from the Big Bang Nucleosynthesis and the Current Collider Experiments 23

2.6 Conclusion 28

2.7 Acknowledgments 29

2.8 References 29

CHAPTER 3 INFLECTION-POINT INFLATION IN HYPER-CHARGE ORIENTED $\mathrm{U}(1)_X$ MODEL 34

3.1 Introduction 34

3.2 Basics of Inflection-Point Inflation 38

3.3 The Inflection-point $\mathrm{U}(1)_X$ Higgs Inflation 41

3.4 LHC Run-2 Constraints 50
3.5 Constraints from the Big Bang Nucleosynthesis 53
3.6 Conclusions 55
3.7 Acknowledgments 56
3.8 References 57
Appendix 3.A RG equations in the minimal $U(1)_X$ model 62
CHAPTER 4 $SU(5)\times U(1)_X$ GRAND UNIFICATION WITH MINIMAL SEESAW AND Z'-PORTAL DARK MATTER 65
4.1 Introduction 65
4.2 $SU(5)\times U(1)_X$ Unification 67
4.3 Z'-portal Dark Matter 69
4.4 Gauge Coupling Unification 74
4.5 Conclusion and Discussion 76
4.6 Acknowledgments 77
4.7 References 77
CHAPTER 5 CONCLUSION 82
REFERENCES 85

LIST OF TABLES

2.1 Particle contents of the minimal $B - L$ model. 15

3.1 The particle content of the minimal $U(1)_X$ extended SM. 42

4.1 The particle content of the minimal $U(1)_X$ extended SM with Z_2-parity. . . . 68

LIST OF FIGURES

2.1 Gauge coupling (left) and inflaton quartic coupling (right) values at M plotted against M/M_P. 20

2.2 RG running of $B-L$ Higgs/inflaton quartic coupling (left) and RG improved inflaton potential (right). 21

2.3 Reheating temperature contours along with allowed parameter space of the minimal $B-L$ model, namely $m_{Z'}$ and g. 26

3.1 $\mathrm{U}(1)_X$ gauge coupling (left) and the inflaton quartic coupling (right) as a function of M/M_P. 47

3.2 RG running of $\mathrm{U}(1)_X$ Higgs/inflaton quartic coupling (left) and RG improved inflaton potential (right). 48

3.3 Reheating temperature contours along with the upper bounds on $\alpha_X\, x_H^2$ as a function of x_H from the CMS result. 52

3.4 Reheating temperature contours for fixed value $x_H = 400$ and $\xi = 0.1$. 55

4.1 Allowed parameter region (green shaded) for the Z'-portal RHN DM scenario in the context of our $\mathrm{SU}(5)\times\mathrm{U}(1)_X$ model ($x_H = -4/5$). 71

4.2 Allowed parameter region (green shaded) as a function of x_H, for $m_{Z'} = 4$ TeV in the minimal $\mathrm{U}(1)_X$ model with the Z'-portal RHN DM. 73

CHAPTER 1

INTRODUCTION

In theoretical particle physics, the construction of any particle physics model is based on the *gauge principle*, which requires the invariance of the Lagrangian under gauge transformations. This invariance of the Lagrangian necessitates the introduction of gauge fields which mediate the interactions between various elementary particles. The mathematical framework that neatly encapsulates our current understanding of the observed elementary particles in nature and their interactions is known as the Standard Model (SM) of particle physics. The SM is based on the gauge group $\mathrm{SU}(3)_c \times \mathrm{SU}(2)_L \times \mathrm{U}(1)_Y$, where the SM gauge interactions are mediated by gauge bosons, namely, gluons, $\mathrm{W}^{\pm}$ bosons, Z boson and photon. All the remaining fields (quarks, leptons, and Higgs fields) in the SM are then classified by their representation under the gauge group (see, for example, Refs. [1] and [2]). The predictions of the SM has been rigorously tested and confirmed by numerous experiments [3].

Despite the tremendous success of the SM in explaining most of the phenomena currently observed in nature, there are some experimental observational results that are completely unaccounted for in the SM, such as, the origin of cosmological inflation, the existence of dark matter (DM), and the neutrino masses and flavor mixings. Hence, it is quite clear that the SM is not the whole story and needs to be extended. The motivation of my dissertation research is to address these unresolved issues of the SM by considering an extension of the SM with new physics beyond the SM which can be tested at future collider experiments and cosmological observations.

Cosmological inflation is the standard paradigm in modern cosmology, according to which the universe experienced a period of accelerated expansion in the very early phase of its evolution (see Refs. [4, 5, 6] for a review). Successful inflation solves two major problems with the Standard Big Bang Cosmology (SBBC), namely, the *flatness/fine-tuning problem* and the *horizon problem*. According to various cosmological observations, the universe at the current epoch has very flat spatial curvature. However, this requires that the universe at very early epoch should be very finely tuned to be flat. This is known as the flatness/fine-tuning problem. On the other hand, the Wilkinson Microwave Anisotropy Probe (WMAP) [7] and the Planck satellite observations [8] of Cosmic Microwave Background indicate the universe was very homogenieous and isotropic at the large scale. However, to explain these observational results within the SBBC framework requires violation of *causaility*. This is the so-called horizon problem. During the inflationary epoch, the accelerated expansion of the universe dilutes any non-zero spatial curvature that was present before the inflationary epoch. At the same time, the accelerated expansion due to the inflation evolves a single causal region in the very early universe into the whole universe currently observed. The tiny inhomogeneities of the energy density in the early universe are crucial to seed the formation of large scale structure of the present universe such as the galaxies and galaxy clusters. Cosmological inflation can also naturally generate such inhomogeneities which are stretched over large cosmological scale during the inflation. A simple inflationary scenario is so-called slow-roll inflation [4, 5, 6], where the inflation is driven by a scalar field (inflaton) such that inflaton potential energy dominates over its kinetic energy during the inflation. However, the SM does not have a viable candidate for the inflaton.

The existence of the DM in the universe has been confirmed by numerous indirect astronomical observations, for example, the observations of flat galaxy rotation curves of stars orbiting their galaxies cannot be explained with just ordinary baryonic matter. This observation can be nicely explained by the existence of DM which interacts with the

ordinary baryonic matter only via gravitational interaction (see Refs. [4, 9] for a review). Observation of the matter distribution of the Bullet Cluster using gravitational lensing also confirmed the existence of DM. The ΛCDM (lambda cold dark matter) model is the standard paradigm of modern cosmology which nicely fits with the cosmological observations. According to various cosmological measurements, the matter energy density of the universe at large scale is only around 31.5% while the remaining 68.5 % associated with dark energy; of the 31.5% that constitute matter, only around 4.5 % are ordinary baryonic matter while the remainder is associated with the DM [8]. If one considers the DM to be weakly interacting particles in a thermal equilibrium with the SM particles in the early universe, then the observed DM can be naturally explained as thermal relics which decoupled from the thermal bath as the universe cooled down at later times. As measured by the Planck satellite experiment at 68% confidence, the relic abundance of DM at the current epoch is given by $\Omega_{DM}h^2 = 0.1198 \pm 0.0015$ [8]. However, the SM does not include a viable DM candidate.

Neutrinos are massless particles in the SM, and which unlike other particles in the SM only neutrinos with left-handed chirality are included in the SM framework while their right-handed partners are missing. However, the observation of the neutrino oscillation phenomena implies that neutrinos have tiny but non-zero masses and flavor mixings [3]. To explain the non-zero masses of neutrinos, the SM need to be supplemented with the missing right-handed neutrinos (RHNs). Another puzzle related to the masses of neutrinos is the fact that their masses are very small compared to the masses of the other particles in the SM. For example, their masses are $\mathcal{O}(10^{-6})$ times smaller than the mass of an electron. However, we cannot resolve the neutrino mass puzzle within the SM framework (see, for example, Ref. [28] for a review).

In the works presented here, we extended the SM with an additional U(1) gauge group with a minimal extension of the particles content of the SM. The model we consider is the so-called non-exotic U(1) extension of the SM [10] based on the gauge group, $SU(3)_c$

$\times$ SU(2)$_L\times$U(1)$_Y\times$ U(1)$_X$, where the U(1)$_X$ is the additional gauge group added to the SM. In the U(1)$_X$ extended SM, except for the U(1)$_X$ charge assignment, the structure is same as the minimal $B-L$ (baryon minus lepton number) model [11, 12, 13, 14, 15, 16], where the global $B-L$ symmetry of the SM is gauged. In addition to the SM particle content, this model includes three generations of RHNs required for the cancellation of the gauge and the mixed-gravitational anomalies, a new U(1)$_X$ Higgs field which breaks the U(1)$_X$ gauge symmetry, and a U(1)$_X$ gauge boson (Z'). The U(1)$_X$ charges of the particles are defined by a single free parameter x_H [17], and it is identical to the minimal $B-L$ model in the limit of $x_H = 0$. Hence, the minimal U(1)$_X$ extended SM is a generalization of the minimal $B-L$ model[1]. Even with such a minimal set of new particles, this model is well motivated and offers rich new physics phenomenologies. The U(1)$_X$ model can easily accommodate cosmological inflation scenario [19, 20, 21] and a suitable candidate for dark matter particle [22, 23, 24] as well as explain the origin of tiny neutrino masses [25, 26]. Hence, this model can address all three of the major unresolved mysteries of the SM. In doing so, we find interesting complementarities between various cosmological observations and the new physics searches at the Large Hadron Colliders (LHC), and this model can be tested in the future.

Let us consider the slow-roll inflation. From a theoretical point of view, if the inflaton value is trans-Planckian ($\phi_I > M_{Pl}$) during the inflation, where ϕ is the inflaton field, effective operators suppressed by the Planck mass (M_{Pl}) could significantly affect the inflaton potential during the inflation, and hence the inflationary predictions. To avoid this problem, in Refs. [19, 20], we have considered a small field inflation (SFI), where the inflaton value during inflation is smaller than the Planck mass ($\phi_I \lesssim M_{Pl}$). Inflection-point inflation is an interesting possibility to realize a successful slow-roll SFI scenario when the inflation is driven by a single scalar field. From a particle physics perspective it is interesting to consider a inflation scenario, where the scalar field (inflaton) plays the role of

[1]In fact this model is equivalent to the minimal $B-L$ model with a kinetic mixing between the SM U(1)$_Y$ and U(1)$_{B-L}$ gauge bosons (see, for example, Ref. [18]).

a Higgs field to spontaneously break some gauge symmetry in new physics models beyond the SM.

In Ref. [19], we have presented a general study of the inflection-point inflation scenario, where we have considered a general Higgs model, with the gauge and the Yukawa interactions, and identified the Higgs field to be the inflaton. In order for a renormalization group (RG) improved effective $\lambda\phi^4$ potential to develop an inflection-point, the running quartic coupling $\lambda(\phi)$ must exhibit a minimum with an almost vanishing value in its RG evolution, namely $\lambda(\phi_I) \simeq 0$ and $\beta_\lambda(\phi_I) \simeq 0$, where β_λ is the beta-function of the quartic coupling. Requiring the inflationary predictions to be consistent with the cosmological observation, the conditions, $\lambda(\phi_I) \simeq 0$ and $\beta_\lambda(\phi_I) \simeq 0$, lead to relations among the gauge, the Yukawa and the Higgs quartic couplings. Interestingly, we have found that inflection-point inflation provides a unique prediction for the running of the spectral index ($\alpha \simeq -2.7 \times 10^{-3}$), independently of the model parameters, which can be tested at the future cosmological experiments.

In Refs. [19, 20], as an example, we have considered the inflection-point inflation in the context of the minimal $\mathrm{U}(1)_X$ extended SM, and identified the $\mathrm{U}(1)_X$ Higgs field with the inflaton field. For a successful inflection-point inflation to be consistent with the current cosmological observations [8], the mass ratios among the Z' gauge boson, the RHNs, and the $\mathrm{U}(1)_X$ Higgs boson are fixed. Imposing the Big Bang Nucleosynthesis constraint on the reheating temperature at the end of inflation ($T_R > 1$ MeV) as well as the current collider experimental bounds, we have shown that the inflationary predictions are complementary to Z' boson searches at the LHC to identify the allowed parameter regions. In Ref. [19], we have considered the $B - L$ limit ($x_H = 0$). Requiring that the the inflationary prediction of the model to be consistent with the current cosmological observations, we have shown the allowed parameter region after considering the current results for the Z' boson narrow resonance search at the LHC for $m_{Z'} < 500$ GeV. The entire parameter region can be tested by the future collider experiments such as the High

Luminosity (HL)-LHC and the SHiP experiments [27]. On the other extreme, in Ref. [20], we have considered the scenario such that the $U(1)_X$ gauge symmetry is mostly oriented towards the SM $U(1)_Y$ direction ($|x_H| \gg 1$) and investigated a consistency between the inflationary predictions and the latest LHC Run-2 results for a Z' boson resonance search with di-lepton final states. Although the inflationary predictions requires gauge coupling to be very small, we have shown that a Z' mass of a few TeV can be explored at the LHC Run-2 for $|x_H| \gg 1$. This is in sharp contrast with the previous case with $x_H = 0$, where only $m_{Z'} < 500$ GeV can be explored in the future.

DM is another interesting possibility that one can consider in the context of the $U(1)_X$ extended SM [22, 23, 24]. With an introduction of a global Z_2 symmetry and assigning Z_2-odd parity to one of the RHNs, a unique Z_2-odd RHN is stable and serves as the DM in our setup, while the remaining two RHNs work to generate the SM neutrino masses[2] through the so-called type-I seesaw mechanism (see, for example, [28] for a review). In this model context, in Ref. [24], we have investigated the Z'-portal RHN DM scenario, where the RHN DM candidate interacts with the SM particles through the Z' boson mediated processes. We have shown that the constraints from the DM relic abundance and the search results for a Z' boson resonance at the LHC are complementary to narrow down the allowed parameter region, which will be fully covered by the future LHC experiments for the Z' boson mass < 5 TeV. In addition, in Ref. [24], we have also considered a $SU(5)\times U(1)_X$ scenario, and we have shown that the standard SU(5) grand unification of the SM quarks and leptons is realized for fixed $x_H = -4/5$. Hence, the $U(1)_X$ charge is quantized in this scenario. In our model, all the SM gauge couplings are successfully unified around $M_{\rm GUT} \simeq 4 \times 10^{16}$ GeV in the presence of two additional pairs of vector-like quarks,

[2]In Ref.[25, 26], we have shown that $U(1)_X$ model also provides significant enhancement of the production cross section of the RHNs from Z' decay in the future LHC experiments, which is crucial for the discovery of RHNs given that the production cross-section of Z' boson via di-lepton resonance is severely constrained. With this enhancement and realistic choice of parameters to reproduce the neutrino oscillation data, if we expect a 5σ discovery of RHNs in the future according to the simulation studies, the Z' boson must be discovered very soon at the LHC. In this setup, the tiny neutrino masses are naturally generated via so-called seesaw mechanism [28].

$D_L + D_R$ and $Q_L + Q_R$, with their mass of $\mathcal{O}(1$ TeV) in the representations of $(\mathbf{3}, \mathbf{1}, 1/3)$ and $(\mathbf{3}, \mathbf{2}, 1/6)$, respectively, under the SM gauge group of $\mathrm{SU}(3)_c \times \mathrm{SU}(2)_L \times \mathrm{U}(1)_Y$.

This organization of this thesis is as follows. The main body of this thesis is a compilation of three of my previously published works based on the minimal $\mathrm{U}(1)_X$ extension of the SM. Chapters 2 corresponds to my work [19] published in a peer reviewed journal Physical Review D, entitled *"Inflection-point $B - L$ Higgs Inflation"*, in collaboration with N. Okada. For a successful inflection-point inflation in the $\mathrm{U}(1)_X$ extended SM at the $B - L$ limit ($x_H = 0$), the entire parameter region for $m_{Z'} < 500$ GeV can be tested by the future collider experiments such as the HL-LHC and the SHiP experiments. Chapters 3 corresponds to my work [20] published in a peer reviewed journal Physical Review D entitled *"Inflection-point inflation in hyper-charge oriented U(1)$_X$ model"*, in collaboration with N. Okada and S. Okada. Although for a successful inflection-point inflation in the $\mathrm{U}(1)_X$ extended SM the $\mathrm{U}(1)_X$ gauge coupling has to be very small, we have shown that a Z' mass of a few TeV can be explored at the LHC Run-2 for $|x_H| \gg 1$. Chapters 4 corresponds to my work [24] published in the a peer reviewed journal Physics Letters B entitled *" SU(5)$\times$ U(1)$_X$ grand unification with minimal seesaw and Z'-portal dark matter"*, in collaboration with N. Okada and S. Okada. With an additional global Z_2 symmetry in the model, we have shown interesting complementarity between DM physics, collider searches and grand unification. Chapter 5 is an overall summary of the all the above works.

CHAPTER 2

INFLECTION-POINT $B - L$ HIGGS INFLATION

2.1 Introduction

Current understanding of the cosmic origin and the evolution is that our universe went through a period of rapid accelerated expansion at the beginning, which is known as inflation. Inflation [1, 2, 3, 4] solves several serious problems of the Standard Big Bang Cosmology, such as the horizon, flatness and monopole problems. More importantly, the primordial density fluctuations generated during inflation seed the formation of large scale structure of the universe we see today. In a simple inflationary scenario known as slow-roll inflation, inflation is driven by a single scalar field (inflaton) when it slowly rolls down to its potential. During the slow-roll, the energy density of the universe is dominated by the inflaton potential energy, which drives accelerated expansion of the universe. After the end of inflation, the inflaton decays to Standard Model (SM) particles to reheat the universe, and the Standard Big Bang Cosmology begins.

The slow-roll inflation requires the inflaton potential to be sufficiently flat in the inflationary epoch. In chaotic inflation, such a flat potential is realized by taking initial inflaton value to be of the trans-Planckian scale. From the field theoretical point of view, effective operators suppressed by the Planck mass ($M_{Pl} = 1.22 \times 10^{19}$ GeV) could significantly contribute to the inflaton potential and hence the inflationary predictions. For this reason, it may be more appealing to consider the small-field inflation (SFI) scenario, where the initial inflation value is smaller than the Planck mass. Hybrid inflation, which is

realized with multiple scalar fields, is a well known example of the SFI [5]. If one considers the SFI driven by a single scalar field, the so-called inflection-point inflation is an interesting possibility [6, 7, 8]. In this scenario the potential has an inflection-point, and hence slow-roll inflation can be realized if the initial inflaton value is taken in the immediate vicinity of the inflection-point.

An inflation scenario is more compelling if the inflaton field plays another important role in particle physics. It is then interesting to identify the inflaton (scalar) field with a Higgs field in a general Higgs model, which plays a crucial role to spontaneously break a gauge symmetry of the model. For example, in references [9, 10, 11], the SM Higgs field is identified with the inflaton field. In this Chapter, we investigate the inflection-point inflation in a general Higgs model, where the inflaton field is identified with the Higgs field and has both gauge and Yukawa interactions, just like the SM.

To realize the inflection-point in a Higgs/inflaton potential, we consider a Renormalization-Group (RG) improved effective Higgs/inflaton potential. During the inflation, we assume that inflaton value is much larger than its Vacuum Expectation Value (VEV) at the potential minimum, so that the inflaton potential is dominated by its quartic term. If the RG running of the inflaton quartic coupling first decreases towards high energy and then increases, inflection-point is realized in the vicinity of the minimum point of the running quartic coupling, where both the quartic coupling and its beta-function become vanishingly small [7, 8][1]. Interestingly, these boundary conditions lead to correlations between the very high energy physics of inflation and the low energy particle phenomenology.

For simplicity, let us consider a Higgs model with its RG improved effective potential given by

$$V(\phi) = \frac{1}{4}\lambda(\phi)\ \phi^4, \tag{2.1}$$

[1]In the context of the $\lambda\phi^4$ inflation with a non-minimal gravitational coupling [13], similar conditions have been derived to ensure the stability of the inflaton potential [14].

where ϕ denotes the inflaton field, $\lambda(\phi)$ is the running quartic coupling, and we have neglected the mass term assuming the initial inflaton value is much larger than the mass term. The running coupling coupling satisfies the (one-loop) RG equation of the form,

$$16\pi^2 \frac{d\lambda}{d\ln\mu} \simeq C_g\, g^4 - C_Y\, Y^4, \tag{2.2}$$

where g and Y are the gauge and Yukawa couplings, respectively, and C_g and C_Y are positive coefficients whose actual values are calculable once the particle contents of the model are defined. In Eq. (3.2) we have neglected terms proportional to λ (λ^2 term and the anomalous dimension term) because the SFI requires the quartic coupling $\lambda \propto g^6$, as will be shown later. Hence the quantum corrections to the effective Higgs potential are dominated by the gauge and Yukawa interactions. Realization of the inflection-point requires a vanishingly small beta-function at the initial inflaton value, namely $C_g\, g - C_Y\, Y = 0$. This condition leads to a relation between g and Y, or in other words, the mass ratio of gauge boson to the fermion in the Higgs model is fixed. Since the Higgs quartic coupling at low energy is evaluated by solving the RG equation, the resultant Higgs mass also has a unique relation to the gauge and the fermion masses.

As a concrete example of such a model, in this Chapter we consider the minimal gauged $B - L$ (baryon number minus lepton number) extension of the SM, where the global $B - L$ symmetry in the SM is gauged. The model has three right-handed neutrinos and the $B - L$ Higgs field (identified with inflaton), which are introduced for the cancellation of the gauge and gravitational anomaly and the $B - L$ gauge symmetry breaking, respectively. Associated with the $B - L$ gauge symmetry breaking, the $B - L$ gauge boson and the right-handed neutrinos acquire their masses. With the Majorana masses for the right-handed neutrinos, the seesaw mechanism [22], which naturally realizes the light neutrino mass generation, is automatically implemented in this model.

The Chapter is organized as follows. In the next section, we give a brief review of

the slow-roll inflation. In Sec. 3, we present the inflationary predictions for the scenario, where the inflaton potential exhibits an inflection-point-like behavior during the slow-roll. In Sec. 4, we consider the minimal gauged $B-L$ extension of the SM, where the $B-L$ Higgs field is identified with the inflaton field. To realize the inflection-point in a Higgs/inflaton potential, we consider the RG improved effective Higgs/inflaton potential. In Sec. 5, we consider the constraints on the model parameters from the Big Bang Nucleosynthesis and the current collider experiments. We also discuss the prospects of testing the scenario in the future collider experiments, such as the High-Luminosity LHC and SHiP experiments. Sec. 6 is devoted to conclusions.

Before moving on to the next section we comment on the differences between this work and the previous work in Ref. [8]. Although the parameterization of our inflaton potential is slightly different, our discussions in Sec. 3 and Sec. 4 are well overlapping with those in Ref. [8]. However, the authors in Ref. [8] mainly focus on the the inflection-point inflation with a large inflaton value beyond the Planck scale in the presence of non-minimal coupling while we focus on the SFI, so that our parameter regions are very different. More importantly our motivation for this work is to consider a complementarity between the inflection-point inflation and the new physics search at low energies as we will discuss in Sec. 5.

2.2 Brief Review of Slow-roll Inflation

The inflationary slow-roll parameters for the inflaton field (ϕ) are expressed as

$$\epsilon(\phi) = \frac{M_P^2}{2}\left(\frac{V'}{V}\right)^2, \quad \eta(\phi) = M_P^2\left(\frac{V''}{V}\right), \quad \zeta^2(\phi) = M_P^4\frac{V'V'''}{V^2}, \tag{2.3}$$

where $M_P = M_{Pl}/\sqrt{8\pi} = 2.43\times 10^{18}$ GeV is the reduced Planck mass, V is the inflation potential, and the prime denotes the derivative with respect to ϕ. The amplitude of the

curvature perturbation $\Delta^2_{\mathcal{R}}$ is given by

$$\Delta^2_{\mathcal{R}} = \frac{1}{24\pi^2}\frac{1}{M_P^4}\left.\frac{V}{\epsilon}\right|_{k_0}, \tag{2.4}$$

which should satisfy $\Delta^2_{\mathcal{R}} = 2.195 \times 10^{-9}$ from the Planck 2015 results [20] with the pivot scale chosen at $k_0 = 0.002$ Mpc^{-1}. The number of e-folds is defined as

$$N = \frac{1}{M_P^2}\int_{\phi_E}^{\phi_I}\frac{V}{V'}d\phi, \tag{2.5}$$

where ϕ_I is the inflaton value at a horizon exit corresponding to the scale k_0, and ϕ_E is the inflaton value at the end of inflation, which is defined by $\max[\epsilon(\phi_E), |\eta(\phi_E)|] = 1$. The value of N depends logarithmically on the energy scale during inflation as well as on the reheating temperature, and it is typically taken to be 50–60.

The slow-roll approximation is valid as long as the conditions $\epsilon \ll 1$, $|\eta| \ll 1$, and $\zeta^2 \ll 1$ hold. In this case, the inflationary predictions are given by

$$n_s = 1 - 6\epsilon + 2\eta, \quad r = 16\epsilon, \quad \alpha = 16\epsilon\eta - 24\epsilon^2 - 2\zeta^2, \tag{2.6}$$

where n_s and r and $\alpha \equiv \frac{dn_s}{dlnk}$ are the scalar spectral index, the tensor-to-scalar ratio and the running of the spectral index, respectively, which are evaluated at $\phi = \phi_I$. The Planck 2015 results [20] set an upper bound on the tensor-to-scalar ratio as $r \lesssim 0.11$, while the best fit value for the spectral index (n_s) and the running of spectral index (α) are 0.9655 ± 0.0062 and -0.0057 ± 0.0071, respectively, at 68% CL.

2.3 Inflection-point Inflation

In the SFI scenario, to realize the slow-roll inflation the inflaton potential must exhibit an inflection-point-like behavior, where the potential is very flat[2]. The initial inflaton value is set in the very flat region $\phi_I = M$. We consider the following expansion of an inflaton potential around the $\phi = M$ given by

$$V(\phi) \simeq V0 + V1(\phi - M) + \frac{V2}{2}(\phi - M)^2 + \frac{V3}{6}(\phi - M)^3, \tag{2.7}$$

where $V0$ is constant and $V1$, $V2$ and $V3$ are the first, second and third derivatives of the inflaton potential evaluated at $\phi = M$. To realize a very flat potential with a inflection-point-like behavior, we require $V1$ and $V2$ to be vanishingly small. From Eqs. (2.3) and (2.7), the slow-roll parameters are then given by

$$\epsilon(M) \simeq \frac{M_P^2}{2}\Big(\frac{V1}{V0}\Big)^2, \;\; \eta(M) \simeq M_P^2\Big(\frac{V2}{V0}\Big), \;\; \zeta^2(M) = M_P^4\frac{V1V3}{V0^2}, \tag{2.8}$$

where we have used the approximation $V(M) \simeq V0$. Similarly, the power-spectrum $\Delta^2_{\mathcal{R}}$ is expressed as

$$\Delta^2_{\mathcal{R}} \simeq \frac{1}{12\pi^2}\frac{1}{M_P^6}\frac{V0^3}{V1^2}. \tag{2.9}$$

Using the observational constraint, $\Delta^2_{\mathcal{R}} = 2.195 \times 10^{-9}$, and a fixed n_s value, we obtain

$$\begin{aligned} \frac{V1}{M^3} &\simeq 1961\left(\frac{M}{M_P}\right)^3\left(\frac{V0}{M^4}\right)^{3/2}, \\ \frac{V2}{M^2} &\simeq -1.725\times 10^{-2}\Big(\frac{1-n_s}{1-0.9655}\Big)\Big(\frac{M}{M_P}\Big)^2\left(\frac{V0}{M^4}\right), \end{aligned} \tag{2.10}$$

[2]For successful inflation scenario it is not necessary for the potential to realize an *exact* inflection-point. We only require the inflaton potential to exhibit a behavior of almost an inflection-point.

where we have used $V(M) \simeq V0$ and $\epsilon(M) \ll \eta(M)$ as we we see later. For the remainder of the analysis we set $n_s = 0.9655$ (the center value from the Planck 2015 results [20]). The inflaton value at the end of inflation is parameterized as $\phi_E/M = 1 - \delta_E$, where $\delta_E < 1$. We define the inflaton value (ϕ_E) at the end of inflation by $\epsilon(\phi_E) = 1$.

Using Eq. (2.5), the e-folding number (N) is given by

$$N = \frac{2V0}{M_P^2\sqrt{-V2^2 + 2V1V3}} \arctan\left(\frac{V2 + V3(\phi - M)}{\sqrt{-V2^2 + 2V1V3}}\right)\Big|_{\phi=M-M\delta_E}^{\phi=M}. \tag{2.11}$$

The inflection-point-like behavior requires $V1 \simeq 0$, $V2 \simeq 0$, and $V3 \neq 0$, so we approximate $-V2^2 + 2V1V3 \simeq 2V1V3$. We will confirm later that this is a good approximation. We will also show later that $V2, \sqrt{2V1V3} \ll V3M\delta_E$. Hence the e-folding number is approximated as

$$N \simeq 2\chi \arctan\left[\frac{V3M\delta_E}{\sqrt{2V1V3}}\right] \simeq \pi\chi, \tag{2.12}$$

where $\chi = \frac{V0}{M_P^2\sqrt{2V1V3}}$. Using Eq. (2.10), $V3$ is then given by

$$\frac{V3}{M} \simeq 6.989 \times 10^{-7}\Big(\frac{60}{N}\Big)^2\Big(\frac{V0^{1/2}}{MM_P}\Big). \tag{2.13}$$

From Eqs. (2.10) and (2.13), we obtain $2V1V3 \simeq 9.2(60/N)V2^2$. Hence, for $N \simeq 60$ $(-V2^2 + 2V1V3)^{1/2} \simeq (2V1V3)^{1/2}$ is a good approximation.

Using Eqs. (2.6), (2.10) and (2.13), we now express all the inflationary predictions in terms $V0$, M and N. From Eqs. (2.8) and (2.10), tensor-to-scalar ratio (r) is given by

$$r = 3.077 \times 10^7\Big(\frac{V0}{M_P^4}\Big). \tag{2.14}$$

The running of the spectral index (α) is given by

$$\alpha \simeq -2\zeta^2(M) = -\,2.742 \times 10^{-3} \left(\frac{60}{N}\right)^2, \tag{2.15}$$

which is independent of $V0$ and M. This prediction is consistent with the current experimental bound, $\alpha = -0.0057 \pm 0.0071$ [20]. Precision measurement of the running of the spectral index in future experiments can reduce the error to ± 0.002 [21]. Hence, the prediction can be tested in the future.

2.4 The Inflection-point-like $B - L$ Higgs Inflation

	$\mathrm{SU}(3)_c$	$\mathrm{SU}(2)_L$	$\mathrm{U}(1)_Y$	$\mathrm{U}(1)_{B-L}$
q_L^i	**3**	**2**	$+1/6$	$+1/3$
u_R^i	**3**	**1**	$+2/3$	$+1/3$
d_R^i	**3**	**1**	$-1/3$	$+1/3$
ℓ_L^i	**1**	**2**	$-1/2$	-1
N_R^i	**1**	**1**	0	-1
e_R^i	**1**	**1**	-1	-1
H	**1**	**2**	$-1/2$	0
φ	**1**	**1**	0	$+2$

Table 2.1: Particle contents of the minimal $B - L$ model. In addition to the SM particle contents, the right-handed neutrino N_R^i ($i = 1, 2, 3$ denotes the generation index) and a complex scalar φ are introduced.

As a simple example of the inflection-point Higgs inflation, in this section we consider the minimal $B - L$ extension of the SM. Here, anomaly-free $\mathrm{U}(1)_{B-L}$ gauge symmetry is introduced along with a scaler field φ ($B - L$ Higgs) and three right-handed neutrinos (N_R^i) which are necessary for the cancellation of all the anomalies. The particle contents of the model are listed in Table 2.1. For the right-handed neutrinos we add Majorana Yukawa interaction terms,

$$\mathcal{L} \supset -\frac{1}{2}\sum_{i=1}^{3} Y_i \varphi \overline{N_R^{i\,C}} N_R^i + \mathrm{h.c.} \tag{2.16}$$

Associated with the gauge symmetry breaking, all the new particles, $B-L$ gauge boson (Z'), the right-handed neutrinos (N_R) and the $B-L$ Higgs acquire their masses as follows:

$$m_{Z'} = 2\, g\, v_{BL}, \;\; m_{N^i} = \frac{1}{\sqrt{2}}\, Y_i\, v_{BL}, \;\; m_\phi = \sqrt{2\lambda}\, v_{BL}, \tag{2.17}$$

where $v_{BL} = \sqrt{2}\langle\varphi\rangle$ is the VEV of the $B-L$ Higgs field.

For simplicity, we consider a scenario where the $B-L$ Higgs sector is very weakly coupled to the SM Higgs doublet. Hence, for the inflationary analysis, the $B-L$ Higgs/inflaton sector can be treated independently. The tree level potential for the $B-L$ Higgs field is given by

$$V_{tree} = \lambda_{tree}\left(\varphi^\dagger\varphi - \frac{v_{BL}}{2}\right)^2. \tag{2.18}$$

We redefine the $B-L$ Higgs field as $\varphi = (\phi+v)/\sqrt{2}$ in the unitary gauge, where $\phi = \sqrt{2}\Re[\varphi]$ is the physical $B-L$ Higgs boson, identified as the inflaton. For the inflationary analysis, we consider $v_{BL} \ll \phi_I$, so that the inflaton potential is approximately given by $V_{tree} = (1/4)\lambda_{tree}\phi^4$, at the tree-level. In our analysis, we employ the RG improved effective potential given by

$$V(\phi) = \frac{1}{4}\lambda(\phi)\, \phi^4, \tag{2.19}$$

where $\lambda(\phi)$ is the solution to the following RG equations:

$$\begin{aligned}
\phi\frac{dg}{d\phi} &= \frac{1}{16\pi^2}12g^3, \\
\phi\frac{dY_i}{d\phi} &= \frac{1}{16\pi^2}\left(Y_i^3 + \frac{1}{2}Y_i\sum_j Y_j^2 - 6g^2Y_i\right), \\
\phi\frac{d\lambda}{d\phi} &= \beta_\lambda.
\end{aligned} \tag{2.20}$$

Here, the beta-function of the inflaton quartic coupling (β_λ) is expressed as

$$\beta_\lambda = \frac{1}{16\pi^2}\left(20\lambda^2 - 48\lambda g^2 + 2\lambda\sum_i Y_i^2 + 96g^4 - \sum_i Y_i^4\right). \tag{2.21}$$

We now turn to the inflationary analysis of the RG improved inflaton potential. At first, we simplify the model, and consider the degenerate mass spectrum for the right-handed neutrinos, $Y \equiv Y_1 = Y_2 = Y_3$. Thus the beta-function of the quartic coupling is

$$\beta_\lambda = \frac{1}{16\pi^2}\left(20\lambda^2 - (48g^2 - 6Y^2)\lambda + 96g^4 - 3Y^4\right). \tag{2.22}$$

Now we express the coefficients in the expansion of Eq. (2.7) as:

$$\begin{aligned}
\frac{V1}{M^3} &= \frac{1}{4}(4\lambda + \beta_\lambda), \\
\frac{V2}{M^2} &= \frac{1}{4}(12\lambda + 7\beta_\lambda + M\beta'_\lambda), \\
\frac{V3}{M} &= \frac{1}{4}(24\lambda + 26\beta_\lambda + 10M\beta'_\lambda + M^2\beta''_\lambda),
\end{aligned} \tag{2.23}$$

where the prime denotes $d/d\phi$. Using $V1/M^3 \simeq 0$ and $V2/M^2 \simeq 0$, we obtain

$$\beta_\lambda(M) \simeq -4\lambda(M), \qquad M\beta'_\lambda(M) \simeq 16\lambda(M). \tag{2.24}$$

For small values of the couplings, λ, g, and Y, we have $M^2\beta''_\lambda(M) \simeq -M\beta'_\lambda(M) \simeq -16\lambda(M)$, where we have neglected higher order coupling terms such as g^8, Y^8, and λ^4. Hence the last equation in Eq. (2.23) is simplified to $V3/M \simeq 16\ \lambda(M)$. Comparing it with Eq. (2.13), we obtain

$$\lambda(M) \simeq 4.770 \times 10^{-16}\Big(\frac{M}{M_P}\Big)^2\Big(\frac{60}{N}\Big)^4, \tag{2.25}$$

where we have approximated $V0 \simeq (1/4)\lambda(M)M^4$. Since the $\lambda(M)$ is extremely small, we approximate $\beta_\lambda(M) \simeq 0$, which leads to

$$Y(M) \simeq 32^{1/4}\, g(M), \tag{2.26}$$

assuming that the beta-function is dominated by the gauge and the Yukawa couplings. This equation implies that the mass ratio between the right-handed neutrinos and the $B-L$ gauge boson is fixed to realize a successful inflection-point inflation. Using the second equation in Eq. (2.24) and Eq. (2.26), we find $\lambda(M) \simeq 3.713 \times 10^{-3}\, g(M)^6$. Then from Eq. (2.25), $g(M)$ is expressed as

$$g(M) \simeq 7.107 \times 10^{-3} \left(\frac{M}{M_P}\right)^{1/3}. \tag{2.27}$$

Finally, from Eqs. (2.14) and (2.25), the tensor-to-scalar ratio (r) is given by

$$r \simeq 3.670 \times 10^{-9} \left(\frac{M}{M_P}\right)^6, \tag{2.28}$$

which is very small, as expected for the SFI scenario.

At the end of inflation $\epsilon(\phi_E)$ is explicitly given by

$$\epsilon(\phi_E) = \frac{{M_P}^2}{2V0^2}\left(V1 - V2\; M\delta_E + \frac{V3}{2}M^2{\delta_E}^2\right)^2 \simeq \frac{{M_P}^2\; M^6\; {\delta_E}^2}{2\; V0^2}\left(-\frac{V2}{M^2} + \frac{V3}{2M}\delta_E\right)^2. \tag{2.29}$$

We evaluate δ_E from $\epsilon(\phi_E) = 1$. If we assume that the first term dominates in the parenthesis of the final expression above we find $\delta_E \gg 1$ by using Eqs. (2.10) and (2.25), which is inconsistent. Therefore, the second term dominates, and hence we obtain

$$\delta_E \simeq 0.210 \left(\frac{M}{M_P}\right)^{1/2}, \tag{2.30}$$

by using Eqs. (2.13) and (2.25).

Before presenting our numerical analysis results, we check the consistency of our analysis. In our analysis in the previous section we have approximated the inflaton potential by Eq. (2.7), neglecting the higher order terms. For consistency, we need to check if the contribution of higher order terms can be neglected in our $B-L$ model. Consider the following expansion of inflaton potential at $\phi = M$,

$$V(\phi) = \sum_{n=0} \frac{V^{(n)}}{n!}(\phi - M)^n, \tag{2.31}$$

where $V^{(n)}$ is the n-th derivative of the potential evaluated at $\phi = M$. As before, $V1 = V^{(1)}$ and $V2 = V^{(2)}$ are uniquely fixed by the experimental values of scalar power-spectrum ($\Delta^2_{\mathcal{R}}$) and spectral index (n_s), respectively. For the consistency of our previous analysis, we require that the terms $V^{(4)} = V4$ and higher contribute negligibly in determination of δ_E. Using Eqs. (2.3) and (2.31) $\epsilon(\phi_E)$ is expressed as

$$\begin{aligned} \epsilon(\phi_E) &\simeq \frac{{M_P}^2}{2V0^2}\left(\sum_{n=1} \frac{V^{(n)}}{(n-1)!}(\phi - M)^{n-1}\right)^2 \\ &\simeq \frac{{M_P}^2}{2V0^2}\left(\frac{V3}{2}M^2{\delta_E}^2 + \sum_{n=4} \frac{V^{(n)}}{(n-1)!}(M\ \delta_E)^{n-1}\right)^2, \end{aligned} \tag{2.32}$$

where we have used $V(\phi_E) \simeq V0$. This leads to constraint

$${\delta_E}^{(p-3)} < \left|\frac{(p-1)!}{2}\frac{V^{(3)}}{V^{(p)}}M^{3-p}\right|. \tag{2.33}$$

where $p \geq 4$. To proceed further we need to evaluate Eq. (2.33) explicitly for the minimal $B-L$ model. As has been shown previously in this section, all the higher order derivatives of the potential can be approximately given by $V^{(n)}M^{n-4} \simeq C_n\lambda(M)$, where C_n is a constant; for example, $C_4 = 96$ and $C_5 = 184$. We find that the most severe bound for both cases is from $V^{(4)}$ term. Using Eqs. (2.30) we obtain upper bound on $M < 5.67M_P$.

Let us now present the numerical analysis of $B-L$ Higgs inflation scenario. For the

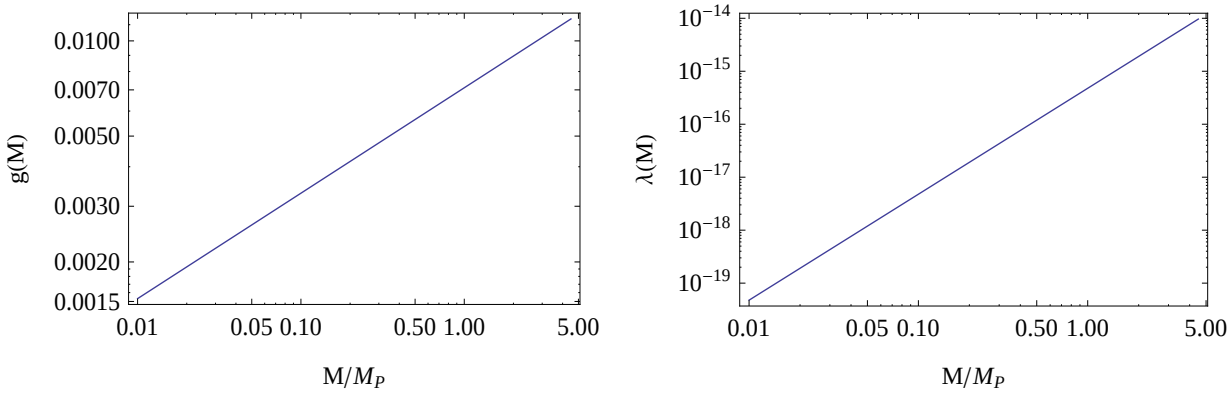

Figure 2.1: Left panel and right panels show gauge coupling g and inflaton quartic coupling λ values at M plotted against M/M_P, respectively.

rest of the Chapter, we set e-folding number $N = 60$, and hence M is the only free parameter in our analysis, and all the gauge, Yukawa and quartic coupling are expressed in terms of M. In Fig. 3.1, we show the gauge coupling (left) and the quartic coupling (right) as a function of M. Imposing $M < 5.67 M_P$, we obtain an upper-bound on the couplings,

$$g(M) < 1.261 \times 10^{-2}, \quad Y(M) < 3.001 \times 10^{-2}, \quad \lambda(M) < 1.486 \times 10^{-14}. \tag{2.34}$$

In Fig. 3.2, we plot the running quartic coupling (left) and the RG improved effective inflaton/Higgs potential (right). Here we have fixed $M = M_P$, which leads to $\lambda(M) \simeq 4.770 \times 10^{-16}$, $g(M) \simeq 7.107 \times 10^{-3}$ and $Y(M) \simeq 1.690 \times 10^{-2}$. In the left panel, the dashed line corresponds to $\lambda = 0$. In the right panel, we see inflection-point-like behavior of the inflaton potential around $\phi = M$, marked with dashed-dotted line.

Now we discuss the inflationary predictions of our scenario. The prediction for the tensor-to-scalar ratio (r) is given by Eq. (2.28). For the upper-bound on $M < 5.67 M_P$, the prediction for the tensor-to-scalar ratio is bounded by $r < 1.108 \times 10^{-4}$, which is very small. However, as discussed before the prediction for the running of the spectral index $\alpha \simeq -2.742 \times 10^{-3}$, which is independent of M, is within the reach of future precision measurements [21]. Note that this result is independent of the particle content of the

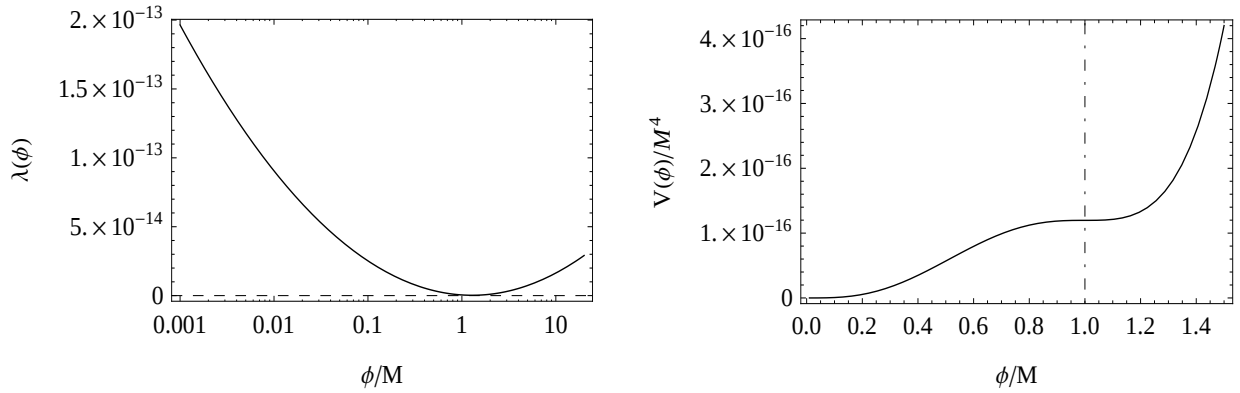

Figure 2.2: Left panel shows the RG running of $B-L$ Higgs/inflaton quartic coupling plotted against the normalized energy scale ϕ/M. Here we have fixed $M = M_P$, so that $g = 7.107 \times 10^{-3}$, $Y = 1.690 \times 10^{-2}$, and $\lambda(M) \simeq 4.770 \times 10^{-16}$. Dashed horizontal line corresponds to $\lambda = 0$. Right panel shows the corresponding RG improved inflaton potential, where the inflection-point-like point appears at $\phi = M$.

theory.

We now consider the particle mass spectrum of the model. At first, we evaluate the mass ratios of the right-handed neutrinos to the Z' gauge boson, $m_N/m_{Z'}$, where m_N is the degenerate right-handed neutrino mass. From the condition of almost vanishing $\beta_\lambda(M)$, we have $Y \simeq 32^{1/4} g$, and hence $m_N/m_{Z'} \simeq 0.84$ at M. This mass ratio remains almost the same at the $B-L$ Higgs VEV scale since the RG running effects for g and Y are negligible (see Eq. (2.34)).

As shown in Fig. 3.2, although the inflection-point-like behavior requires $\beta_\lambda(M) \simeq -4\lambda(M) \simeq 0$, RG running significantly changes the quartic coupling values at the low energies. In the following discussion we will derive an approximation formula for λ at the low energies. Since $g(M)$, $Y(M) \ll 1$, the solutions to their RG equations are approximately given by

$$\begin{aligned} g(\mu) &\simeq g(M) + \beta_g(M) \ln\left[\frac{\mu}{M}\right], \\ Y(\mu) &\simeq Y(M) + \beta_Y(M) \ln\left[\frac{\mu}{M}\right], \end{aligned} \tag{2.35}$$

where $\beta_g(M)$ and $\beta_Y(M)$ are the beta-functions of g and Y at M, respectively (see Eq. (2.20)). Hence, the beta-function of the quartic coupling is approximately described as

$$\begin{aligned}\beta_\lambda(\mu) &\simeq 96g^4(\mu) - 3Y^4(\mu), \\ &\simeq 4\left\{96g(M)^3\beta_g(M) - 3Y(M)^3\beta_Y(M)\right\}\ln\left[\frac{\mu}{M}\right], \\ &\simeq 5.941\times 10^{-2} g(M)^6 \ln\left[\frac{\mu}{M}\right], \end{aligned} \tag{2.36}$$

where we have used $96g^4(M) \simeq 3Y^4(M)$. Then we obtain the approximate solution to the RG equation as

$$\begin{aligned}\lambda(v_{BL}) &\simeq \lambda(M) + 3.868\times 10^{-15}\left(\frac{M}{M_P}\right)^2\left(\ln\left[\frac{v_{BL}}{M}\right]\right)^2, \\ &\simeq 3.868\times 10^{-15}\left(\frac{M}{M_P}\right)^2\left(\ln\left[\frac{v_{BL}}{M}\right]\right)^2, \end{aligned} \tag{2.37}$$

where $v_{BL} \ll M$. Using $m_{Z'} = 2g(v_{BL})v_{BL} \simeq 2g(M)v_{BL}$, the mass ratio of the $B-L$ Higgs boson/inflaton to the Z' boson is found to be

$$\frac{m_\phi}{m_{Z'}} \simeq 6.157\times 10^{-6}\Big(\frac{M}{M_P}\Big)^{2/3}\ln\left[\frac{M}{v_{BL}}\right]. \tag{2.38}$$

We now discuss a possibility of testing our scenario in the future collider experiments. In Ref. [17], the authors consider the heavy neutrino production at the High-Luminosity LHC [17] and the SHiP [18] experiments in the context of the minimal $B-L$ model. The process they have considered is a pair production of the heavy neutrinos via the decay of intermediate Z' boson, which is produced in proton-proton collisions. They focused on a simplified scenario where only one right-handed neutrino mixes with only one flavor of the SM neutrino via a small mixing angle. Since the lifetime of the heavy neutrino is long, its decay to the SM particles can be observed with a displaced vertex. For a fixed $m_{Z'}/m_N = 3$, it has been found that the LHC and the SHiP experiments can

explore the parameter regions, $g \gtrsim 10^{-4}$ and $1 \lesssim m_{Z'}[\mathrm{GeV}] \lesssim 500$. To implement this scenario, we extend our model with non-degenerate Majorana Yukawa couplings. For simplicity, we fix Y_1 to satisfy $m_{Z'}/m_{N^1} = 3$, following Ref. [17]. We consider the remaining Yukawas to be degenerate, $Y_2 = Y_3$. We repeat the same analysis as for the degenerate case, and find that $Y_{2,3} \simeq 2.63g$, or equivalently $m_{N^{2,3}}/m_{Z'} \simeq 0.929$. We find that the constant coefficients in Eqs. (2.27) and (2.36) change to 7.120×10^{-3} and 5.860×10^{-2}, respectively. These are coincidentally almost identical to those obtained in the degenerate case. As a result, the low energy value of the quartic coupling, and hence the mass ratio $m_\phi/m_{Z'}$ is almost the same as that of the degenerate case. In the next section, we focus on this non-degenerate scenario.

2.5 Constraints from the Big Bang Nucleosynthesis and the Current Collider Experiments

Let us now consider a reheating scenario after the end of inflation to connect our inflation scenario with the Standard Big Bang Cosmology. This occurs via inflaton decay into the SM particles while the inflaton oscillates around its potential minimum. We estimate the reheating temperature (T_R) as

$$T_R \simeq 0.2 \left(\frac{100}{g_*}\right)^{1/4} \sqrt{\Gamma M_P}. \tag{2.39}$$

For the successful Big Bang Nucleosynthesis (BBN), we impose a model-independent lower bound on the reheating temperature as $T_R \gtrsim 1$ MeV.

The general, renormalizable scalar potential for the $B-L$ Higgs/inflaton field and the SM Higgs doublet (H) is given by

$$V(|H|,|\varphi|) = \lambda\left(|\varphi|^2 - \frac{v_{BL}^2}{2}\right)^2 + \lambda_H\left(|H|^2 - \frac{v_H^2}{2}\right)^2 + \lambda'\left(|H|^2 - \frac{v_H^2}{2}\right)\left(|\varphi|^2 - \frac{v_{BL}^2}{2}\right), \tag{2.40}$$

where $\lambda' > 0$ is the mixing term between the two scalar fields. The vacuum of the system is

located at $\langle\varphi\rangle = v_{BL}/\sqrt{2}$ and $\langle H\rangle = (\frac{v_H}{\sqrt{2}}\ \ 0)^T$. After the breaking of the $B-L$ and the electroweak symmetries, the mass matrix is given by

$$\mathcal{L} \supset -\frac{1}{2}\begin{bmatrix} h & \phi \end{bmatrix}\begin{bmatrix} m_h^2 & \lambda' v_{BL} v_H \\ \lambda' v_{BL} v_H & m_\phi^2 \end{bmatrix}\begin{bmatrix} h \\ \phi \end{bmatrix}, \tag{2.41}$$

where $m_\phi^2 = 2\lambda v_{BL}^2$, h is the SM Higgs boson with mass $m_h = \sqrt{2\lambda_H} v_H = 125$ GeV, where λ_H is the SM Higgs quartic coupling and $v_H = 246$ GeV. We diagonalize the mass matrix by

$$\begin{bmatrix} h \\ \phi \end{bmatrix} = \begin{bmatrix} \cos\theta & \sin\theta \\ -\sin\theta & \cos\theta \end{bmatrix}\begin{bmatrix} \phi_1 \\ \phi_2 \end{bmatrix}, \tag{2.42}$$

where ϕ_1 and ϕ_2 are the mass eigenstates. The relations among the mass parameters and the mixing angle (θ) are the following:

$$\begin{aligned} 2 v_{BL} v_H \lambda' &= (m_h^2 - m_\phi^2)\tan 2\theta, \\ m_{\phi_1}^2 &= m_h^2 - \left(m_\phi^2 - m_h^2\right)\tfrac{\sin^2\theta}{1-2\sin^2\theta}, \\ m_{\phi_2}^2 &= m_\phi^2 + \left(m_\phi^2 - m_h^2\right)\tfrac{\sin^2\theta}{1-2\sin^2\theta}\ . \end{aligned} \tag{2.43}$$

Since the inflaton is much lighter than the Z' boson and the heavy neutrinos, it decays to the SM particles mainly through the mixing with the SM Higgs boson. We calculate the inflaton decay width as

$$\Gamma_{\phi_2} = \sin^2\theta \times \Gamma_h(m_{\phi_2}), \tag{2.44}$$

where $\Gamma_h(m_{\phi_2})$ is the SM Higgs boson decay width if the SM Higgs boson mass were m_{ϕ_2}.

There are constraints on the mixing angle. Firstly, the introduction of the mixing coupling modifies the beta-function of the inflaton quartic coupling in Eq. (2.21) as $16\pi^2\beta_\lambda \to 16\pi^2\beta_\lambda + 2\lambda'^2$. In order not to change our results in the previous sections, λ'^2

should be negligibly small in the beta-function i.e $\lambda'^2 \ll 48g^4$, evaluated at M. Another constraint on the mixing angle is from requiring positive definiteness of mass squared eigenvalues of the mass matrix in Eq. (2.41), which leads to $\lambda'^2 < 4\lambda_H\lambda_\phi$. We find that the latter constraint is more severe and requires $\theta \ll 1$. Hence ϕ_1 and ϕ_2 are mostly the SM Higgs and the B-L Higgs mass eigenstates, respectively.

In the following analysis we parameterize $\lambda'^2 = 4\lambda_H\lambda_\phi\xi$, with a new parameter $0 < \xi < 1$. From Eq. (2.43), we obtain

$$\theta^2 \simeq \xi \left(\frac{m_\phi}{m_h}\right)^2, \tag{2.45}$$

where we have used $m_\phi^2 \ll m_h^2$ for the parameter region we are interested in, namely $1 \lesssim m_{Z'}[\text{GeV}] \lesssim 500$. We also find that $m_{\phi 2} \simeq m_\phi\sqrt{1-\xi}$. From Eqs. (2.38) and (2.45), we can express the reheating temperature as a function of M, $m_{Z'}$ and ξ. For maximum value of $M = 4.6M_P$ and a fixed ξ, there is a lower bound on the mass of Z' from the BBN constraint on reheating temperature, for example if $\xi = 0.5$, 0.1, and 0.01 we find $m_{Z'} \gtrsim$ 13.6, 21.5, 46.5 GeV, respectively.

Our results are shown in Fig. 3.3. In both panels, from left to right, the diagonal lines are contours corresponding to $T_R = 1$ MeV for fixed $\xi = 0.5$, 0.1 and 0.05, respectively. The regions to the left of each contour are excluded by the BBN constraint. For the current experimental constraints and the future search reach we have referred to the results presented in Ref. [17]. Here, for fixed $m_{Z'}/m_N = 3$, the authors have shown all the current experimental constraints and the future search reach constraints on the parameter space of the minimal $B - L$ model, namely $m_{Z'}$ and g. In Fig. 3.3, we have re-parameterized the gauge coupling (g) in terms of M/M_P according to Eq. (2.27). In both of the panels, the excluded regions by the current LHC experiments are shown by the (Grey) shaded regions bounded by the solid lines. The very narrow regions bounded by the horizontal solid lines are excluded by the LEP experiment. In the left panel, the (yellow)

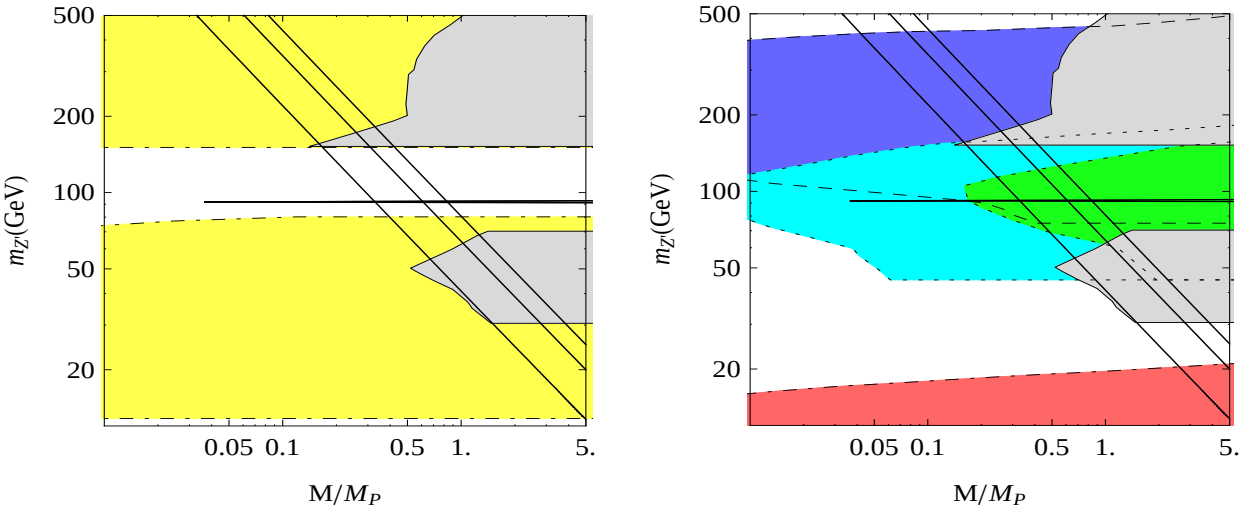

Figure 2.3: In both panels, the diagonal lines from left to right are the contours for the reheating temperature of $T_R = 1$ MeV for fixed $\xi = 0.5$, 0.1, and 0.05, respectively. The regions to the left of the diagonal lines are excluded by the BBN constraint. For $m_{Z'}/m_N = 3$, the (Grey) shaded regions bounded by the solid lines are excluded by the current LHC experiments. The very narrow regions bounded by the horizontal solid lines are excluded by the LEP experiment. The remaining regions bounded by broken lines are the future reach of different experiments, where the left (right) panel shows the future reach using direct (displaced vertex) searches.

shaded regions bounded by the dashed-dotted lines can be tested by the Z' resonance search at the High-Luminosity LHC. In the right panel, the regions bounded by the dashed and the dotted lines (dashed-dotted line) can be tested through the observation of the displaced vertex of the heavy neutrino decay at the High-Luminosity LHC (SHiP) experiment. For details about the correspondence of each shaded region to the individual experimental search, see Ref. [17]. Combining the left and the right panels, all the allowed regions of our scenario for $13.6 \lesssim m_{Z'}[\mathrm{GeV}] \lesssim 500$ can be tested at the future experiments.

So far in our analysis, the inflaton is considered to be mostly the $B-L$ Higgs boson with a small mixing with the SM Higgs boson, which allows the inflaton to decay into the SM particles. Since the inflection-point-like inflation scenario requires $\lambda(v_{BL}) \ll 1$, we expect the reheating temperature to be small. We find that $T_R \lesssim 1$ GeV, for $m_{Z'} \lesssim 500$ GeV. In terms of baryogenesis and dark matter physics, a reheating temperature $T_R \gg 1$ GeV is desirable. Note that when we carefully consider the inflation trajectory on the scalar potential in Eq. (2.40), the reheating process would be more involved. During the inflation, the inflaton tracks the trajectory with $H = 0$. When the inflaton field rolls down to $\phi \simeq \sqrt{\lambda_H/\lambda'}\, v_H$, the potential starts to develop a minimum away from $H = 0$ in the H direction. As the ϕ rolls down further, the minimum becomes deeper. Because the $\lambda \ll \lambda_H$, the potential is very flat along the ϕ direction at $H = 0$, while it sharply drops in the H direction at $\phi \simeq v_{BL}$. Hence, the SM Higgs field behaves like the waterfall field in the hybrid inflation scenario [5]. In this case the decaying inflaton should have a sizable amount of the SM Higgs component. If the decaying inflaton field is mostly the SM Higgs field, the reheating temperature is evaluated by the decay width of the SM Higgs boson ($\Gamma_h \simeq 4.07$ MeV), so that we find $T_R \simeq 10^7$ GeV. Although the true reheating temperature must be less than 10^7 GeV, we may expect the actual reheating temperature sufficiently high, say, $T_R \gg 1$ TeV, which is desirable for the (thermal) baryogenesis and the dark matter physics.

If the reheating temperature is high, the $B-L$ Higgs boson ϕ can be in thermal equilibrium through its interactions with the SM Higgs boson and the heavy neutrinos.

The interaction is so weak that ϕ decouples in the relativistic regime. We requires that ϕ decays before the BBN era, namely the lifetime of ϕ must be shorter than 1 second ($\tau_\phi = 1/\Gamma_\phi < 1$ s), not to ruin the success of the BBN scenario. This condition is mathematically the same as requiring the reheating temperature $T_R > 1$ MeV from the inflaton ϕ decay. Hence, the results shown in the Fig. 3.3 are also applied to the scenario with a very high reheating temperature.

2.6 Conclusion

From a theoretical point of view, if the inflaton value is trans-Planckian, effective operators suppressed by the Planck mass could significantly affect the inflaton potential, and hence the inflationary predictions. To avoid this problem, we may consider slow-roll inflation with a small initial inflaton value ($\phi_I < M_{Pl}$). In this case, the inflection-point inflation is an interesting possibility to realize a successful slow-roll inflation when inflation is driven by a single scalar field. To realize the inflection-point-like behavior for the renormalization group (RG) improved effective $\lambda\phi^4$ potential, the running quartic coupling $\lambda(\phi)$ must exhibit a minimum with an almost vanishing value in its RG evolution, namely $\lambda(\phi_I) \simeq 0$ and $\beta_\lambda(\phi_I) \simeq 0$, where β_λ is the beta-function of the quartic coupling.

From a particle physics perspective, it is more compelling to consider an inflationary scenario, where the inflaton field plays another important role. We have considered a general Higgs model, with the gauge and the Yukawa interactions, and identified the Higgs field with the inflaton. In this case, the conditions, $\lambda(\phi_I) \simeq 0$ and $\beta_\lambda(\phi_I) \simeq 0$, lead to relations among the model parameters, the gauge, the Yukawa and the Higgs quartic couplings. Using the relations and requiring the inflationary predictions to be consistent with the Planck 2015 results [20], we have found that all the couplings depend only on ϕ_I. Hence, the low energy mass spectrum of the model is uniquely determined by only two free parameters, ϕ_I and the inflaton/Higgs VEV. Hence the inflationary predictions are complimentary to the low energy mass spectrum. We have also shown that the

inflection-point inflation provides a unique prediction for the running of the spectral index $\alpha \simeq -2.7 \times 10^{-3} \left(\frac{60}{N}\right)^2$, where N is the e-folding number, independently of the model parameters. The future experiments can test this prediction for α.

As an example Higgs model, we have considered the minimal gauged $B-L$ extension of the Standard Model, and identified the $B-L$ Higgs field as the inflaton field. Hence, we have obtained our predictions for the mass spectrum for the $B-L$ gauge boson, the right-handed neutrinos, and the $B-L$ Higgs boson as a function of ϕ_I and the inflaton/Higgs VEV. We then considered the reheating after inflation. Imposing the Big Bang Nucleosynthesis constraint and the current collider experimental bounds, we have identified the allowed parameter regions. The entire parameter region for $m_{Z'} < 500$ GeV can be tested by the future collider experiments such as the High-Luminosity LHC and the SHiP experiments.

2.7 Acknowledgments

This work is supported in part by the United States Department of Energy (Award No. DE-SC0013680).

2.8 References

[1] A. A. Starobinsky, "A New Type of Isotropic Cosmological Models Without Singularity," Phys. Lett. B **91**, 99 (1980).

[2] A. H. Guth, "The Inflationary Universe: A Possible Solution to the Horizon and Flatness Problems," Phys. Rev. D **23**, 347 (1981).

[3] A. D. Linde, "Chaotic Inflation," Phys. Lett. B **129**, 177 (1983).

[4] A. Albrecht and P. J. Steinhardt, "Cosmology for Grand Unified Theories with Radiatively Induced Symmetry Breaking," Phys. Rev. Lett. **48**, 1220 (1982).

[5] A. D. Linde, "Hybrid inflation," Phys. Rev. D **49**, 748 (1994) doi:10.1103/PhysRevD.49.748 [astro-ph/9307002].

[6] R. Allahverdi, K. Enqvist, J. Garcia-Bellido and A. Mazumdar, "Gauge invariant MSSM inflaton," Phys. Rev. Lett. **97**, 191304 (2006) doi:10.1103/PhysRevLett.97.191304 [hep-ph/0605035]; R. Allahverdi, K. Enqvist, J. Garcia-Bellido, A. Jokinen and A. Mazumdar, "MSSM flat direction inflation: Slow roll, stability, fine tunning and reheating," JCAP **0706**, 019 (2007) doi:10.1088/1475-7516/2007/06/019 [hep-ph/0610134]; J. C. Bueno Sanchez, K. Dimopoulos and D. H. Lyth, "A-term inflation and the MSSM," JCAP **0701**, 015 (2007) doi:10.1088/1475-7516/2007/01/015 [hep-ph/0608299]; D. Baumann, A. Dymarsky, I. R. Klebanov, L. McAllister and P. J. Steinhardt, "A Delicate universe," Phys. Rev. Lett. **99**, 141601 (2007) doi:10.1103/PhysRevLett.99.141601 [arXiv:0705.3837 [hep-th]]; D. Baumann, A. Dymarsky, I. R. Klebanov and L. McAllister, "Towards an Explicit Model of D-brane Inflation," JCAP **0801**, 024 (2008) doi:10.1088/1475-7516/2008/01/024 [arXiv:0706.0360 [hep-th]]; M. Badziak and M. Olechowski, "Volume modulus inflection point inflation and the gravitino mass problem," JCAP **0902**, 010 (2009) doi:10.1088/1475-7516/2009/02/010 [arXiv:0810.4251 [hep-th]]; K. Enqvist, A. Mazumdar and P. Stephens, "Inflection point inflation within supersymmetry," JCAP **1006**, 020 (2010) doi:10.1088/1475-7516/2010/06/020 [arXiv:1004.3724 [hep-ph]]; R. Cerezo and J. G. Rosa, "Warm Inflection," JHEP **1301**, 024 (2013) doi:10.1007/JHEP01(2013)024 [arXiv:1210.7975 [hep-ph]]; S. Choudhury, A. Mazumdar and S. Pal, "Low & High scale MSSM inflation, gravitational waves and constraints from Planck," JCAP **1307**, 041 (2013) doi:10.1088/1475-7516/2013/07/041 [arXiv:1305.6398 [hep-ph]]; S. Choudhury and A. Mazumdar, "Reconstructing inflationary potential from BICEP2 and running of tensor modes," arXiv:1403.5549 [hep-th].

[7] G. Ballesteros and C. Tamarit, "Radiative plateau inflation," JHEP **1602**, 153 (2016) doi:10.1007/JHEP02(2016)153 [arXiv:1510.05669 [hep-ph]].

[8] S. M. Choi and H. M. Lee, "Inflection point inflation and reheating," Eur. Phys. J. C **76**, no. 6, 303 (2016) doi:10.1140/epjc/s10052-016-4150-5 [arXiv:1601.05979 [hep-ph]].

[9] F. L. Bezrukov and M. Shaposhnikov, "The Standard Model Higgs boson as the inflaton," Phys. Lett. B **659**, 703 (2008) [arXiv:0710.3755 [hep-th]]; J. Garcia-Bellido, D. G. Figueroa and J. Rubio, "Preheating in the Standard Model with the Higgs-Inflaton coupled to gravity," Phys. Rev. D **79**, 063531 (2009) doi:10.1103/PhysRevD.79.063531 [arXiv:0812.4624 [hep-ph]]; F. Bezrukov, D. Gorbunov and M. Shaposhnikov, "On initial conditions for the Hot Big Bang," JCAP **0906**, 029 (2009) [arXiv:0812.3622 [hep-ph]]; F. L. Bezrukov, A. Magnin and M. Shaposhnikov, "Standard Model Higgs boson mass from inflation," Phys. Lett. B **675**, 88 (2009) [arXiv:0812.4950 [hep-ph]]; F. Bezrukov and M. Shaposhnikov, "Standard Model Higgs boson mass from inflation: two loop analysis," JHEP **0907**, 089 (2009) [arXiv:0904.1537 [hep-ph]]; F. Bezrukov, A. Magnin, M. Shaposhnikov and S. Sibiryakov, "Higgs inflation: consistency and generalisations," JHEP **1101**, 016 (2011) [arXiv:1008.5157 [hep-ph]]; F. Bezrukov and M. Shaposhnikov, "Higgs inflation at the critical point," Phys. Lett. B **734**, 249 (2014) doi:10.1016/j.physletb.2014.05.074 [arXiv:1403.6078 [hep-ph]]; Y. Hamada, H. Kawai, K. y. Oda and S. C. Park, "Higgs Inflation is Still Alive after the Results from BICEP2," Phys. Rev. Lett. **112**, no. 24, 241301 (2014) doi:10.1103/PhysRevLett.112.241301 [arXiv:1403.5043 [hep-ph]].

[10] A. O. Barvinsky, A. Y. Kamenshchik and A. A. Starobinsky, "Inflation scenario via the Standard Model Higgs boson and LHC," JCAP **0811**, 021 (2008) [arXiv:0809.2104 [hep-ph]]; A. O. Barvinsky, A. Y. Kamenshchik, C. Kiefer, A. A. Starobinsky and C. Steinwachs, "Asymptotic freedom in inflationary cosmology with a non-minimally coupled Higgs field," JCAP **0912**, 003 (2009) [arXiv:0904.1698 [hep-ph]]; "Higgs boson, renormalization group, and naturalness in cosmology," Eur. Phys. J. C **72**, 2219 (2012) [arXiv:0910.1041 [hep-ph]].

[11] A. De Simone, M. P. Hertzberg and F. Wilczek, "Running Inflation in the Standard Model," Phys. Lett. B **678**, 1 (2009) [arXiv:0812.4946 [hep-ph]]; T. E. Clark, B. Liu, S. T. Love and T. ter Veldhuis, "The Standard Model Higgs Boson-Inflaton and Dark Matter," Phys. Rev. D **80**, 075019 (2009) [arXiv:0906.5595 [hep-ph]].

[12] See, for example, N. Okada, M. U. Rehman and Q. Shafi, "Tensor to Scalar Ratio in Non-Minimal ϕ^4 Inflation," Phys. Rev. D **82**, 043502 (2010) [arXiv:1005.5161 [hep-ph]]; N. Okada, V. N. Senoguz and Q. Shafi, "The Observational Status of Simple Inflationary Models: an Update," arXiv:1403.6403 [hep-ph]; T. Inagaki, R. Nakanishi and S. D. Odintsov, "Non-Minimal Two-Loop Inflation," Phys. Lett. B **745**, 105 (2015) [arXiv:1502.06301 [hep-ph]].

[13] K. Kannike, G. Hütsi, L. Pizza, A. Racioppi, M. Raidal, A. Salvio and A. Strumia, "Dynamically Induced Planck Scale and Inflation," JHEP **1505**, 065 (2015) doi:10.1007/JHEP05(2015)065 [arXiv:1502.01334 [astro-ph.CO]]; N. Okada and D. Raut, "Running Non-Minimal Inflation with Stabilized Inflaton Potential," PoS DSU **2015**, 013 (2016) [arXiv:1509.04439 [hep-ph]]; K. Kannike, A. Racioppi and M. Raidal, JHEP **1601**, 035 (2016) doi:10.1007/JHEP01(2016)035 [arXiv:1509.05423 [hep-ph]].

[14] P. Minkowski, Phys. Lett. B **67**, 421 (1977); T. Yanagida, in *Proceedings of the Workshop on the Unified Theory and the Baryon Number in the Universe* (O. Sawada and A. Sugamoto, eds.), KEK, Tsukuba, Japan, 1979, p. 95; M. Gell-Mann, P. Ramond, and R. Slansky, *Supergravity* (P. van Nieuwenhuizen et al. eds.), North Holland, Amsterdam, 1979, p. 315; S. L. Glashow, *The future of elementary particle physics*, in *Proceedings of the 1979 Cargèse Summer Institute on Quarks and Leptons* (M. Lévy et al. eds.), Plenum Press, New York, 1980, p. 687; R. N. Mohapatra and G. Senjanović, "Neutrino Mass and Spontaneous Parity Violation," Phys. Rev. Lett. **44**, 912 (1980); J. Schechter and J. W. F. Valle, "Neutrino Masses in SU(2) x U(1) Theories," Phys. Rev. D **22**, 2227 (1980).

[15] P. A. R. Ade *et al.* [Planck Collaboration], "Planck 2015 results. XIII. Cosmological parameters," Astron. Astrophys. **594**, A13 (2016) doi:10.1051/0004-6361/201525830 [arXiv:1502.01589 [astro-ph.CO]].

[16] K. N. Abazajian *et al.*, "Inflation Physics from the Cosmic Microwave Background and Large Scale Structure," Astropart. Phys. **63**, 55 (2015) doi:10.1016/j.astropartphys.2014.05.013 [arXiv:1309.5381 [astro-ph.CO]].

[17] B. Batell, M. Pospelov and B. Shuve, "Shedding Light on Neutrino Masses with Dark Forces," JHEP **1608**, 052 (2016) doi:10.1007/JHEP08(2016)052 [arXiv:1604.06099 [hep-ph]].

[18] B. Schmidt, "The High-Luminosity upgrade of the LHC: Physics and Technology Challenges for the Accelerator and the Experiments," J. Phys. Conf. Ser. **706**, no. 2, 022002 (2016). doi:10.1088/1742-6596/706/2/022002

[19] M. Anelli *et al.* [SHiP Collaboration], "A facility to Search for Hidden Particles (SHiP) at the CERN SPS," arXiv:1504.04956 [physics.ins-det].

CHAPTER 3

INFLECTION-POINT INFLATION IN HYPER-CHARGE ORIENTED $U(1)_X$ MODEL

3.1 Introduction

Inflationary universe is the standard paradigm in the modern cosmology [1, 2, 3, 4] which provides not only solutions to various problems in the Standard Big Bang Cosmology, such as the flatness and horizon problems, but also the primordial density fluctuations which seed the formation of large scale structure of the universe we see today. In a simple inflationary scenario known as slow-roll inflation, inflation is driven by a single scalar field (inflaton) when it slowly rolls down to its potential minimum. During the slow-roll, the energy density of the universe is dominated by the inflaton potential energy, which drives accelerated expansion of the universe, namely, cosmological inflation. After the end of inflation, the inflaton decays to Standard Model (SM) particles to reheat the universe to initiate the Standard Big Bang Cosmology.

The slow-roll inflation requires the inflaton potential to be sufficiently flat in the inflationary epoch. In a simple inflationary scenario such as chaotic inflation, a flat potential is realized by taking an initial inflaton value to be of the trans-Planckian scale. However, the field theoretical point of view, it may be more appealing to consider the small-field inflation (SFI) scenario, where the initial inflaton value is smaller than the Planck mass and possible higher-dimensional Planck suppressed operators are less important to the inflationary predictions. Hybrid inflation [5] is a well known example of the SFI [5], where a flat direction of the scalar potential is realized with multiple scalar

fields. When one considers the SFI driven by a single scalar field, the so-called inflection-point inflation [6, 7, 8] is an interesting possibility. If the inflaton potential exhibits an inflection-point, the slow-roll inflation epoch can be realized with the initial inflaton value in the immediate vicinity of the inflection-point.

From a particle physics point of view, an inflation scenario seems more compelling if the inflaton field plays another important role in particle physics models, such as the Higgs inflation scenario [9, 10, 11] in which the SM Higgs field is identified with the inflaton field. When the SM is extended with some extra gauge groups or unified gauged groups, such models always include an extra Higgs field, in addition to the SM Higgs field, to spontaneously break the gauge symmetries down to the SM one. Similarly to the Higgs inflation scenario, it is interesting if we can identify the extra Higgs field with the inflaton. The extra Higgs field usually has Yukawa couplings with some fermions in addition to the gauge and the quartic couplings, just like the SM Higgs doublet. As will be discussed below, this gauge-Higgs-Yukawa system is essential to realize the inflection-point inflation with the identification of the Higgs field as the inflaton.

Let us consider a Renormalization-Group (RG) improved effective Higgs/inflaton potential [12]. During the inflation, we assume that inflaton value is much larger than its Vacuum Expectation Value (VEV) at the potential minimum, so that the inflaton potential is dominated by its quartic term of the form,

$$V(\phi) = \frac{1}{4}\lambda(\phi)\ \phi^4, \tag{3.1}$$

where ϕ denotes the inflaton field, and $\lambda(\phi)$ is the running quartic coupling. If the RG running of the inflaton quartic coupling first decreases towards high energy and then increases, inflection-point is realized in the vicinity of the minimum point of the running quartic coupling, where both the quartic coupling and its beta-function become vanishingly small [7, 8].[1] In the vicinity of the inflection-point, the running quartic coupling obeys the

[1] In the context of the $\lambda\phi^4$ inflation with non-minimal gravitational coupling [13], similar conditions have

(one-loop) RG equation of the form,

$$16\pi^2 \frac{d\lambda}{d\ln\phi} \simeq C_g\, g^4 - C_Y\, Y^4, \tag{3.2}$$

where g and Y are the gauge and Yukawa couplings, respectively, and C_g and C_Y are positive coefficients whose actual values are calculable once the particle content of the model is defined. Here, we have neglected terms proportional to λ (λ^2 term and the anomalous dimension term) because the SFI requires the quartic coupling $\lambda \propto g^6$, as will be shown later. Hence the quantum corrections to the effective Higgs potential are dominated by the gauge and Yukawa interactions. Realization of the inflection-point requires a vanishingly small beta-function at the initial inflaton value, namely $C_g\, g^4 - C_Y\, Y^4 = 0$. This condition leads to a relation between g and Y, or in other words, the mass ratio of gauge boson to the fermion in the Higgs model is fixed. Since the Higgs quartic coupling at low energy is evaluated by solving the RG equation, the resultant Higgs mass also has a unique relation to the gauge and the fermion masses. Therefore, in the inflection-point inflation scenario with the Higgs field as the inflaton, there is a correlation between the very high energy physics of inflation and the low energy particle phenomenology.

Recently, two of the authors of this paper (N.O. and D.R.) have investigated the inflection-point inflation in the minimal gauged $B-L$ (baryon number minus lepton number) extension of the SM [15], where the $B-L$ Higgs field as the inflaton field [16]. In order to realize the successful inflection-point inflation, we have obtained the predictions for the mass spectrum for the $B-L$ gauge boson (Z' boson), the right-handed neutrinos, and the $B-L$ Higgs boson as a function of the initial inflaton value (ϕ_I) and the inflaton/Higgs VEV (v_{BL}). Considering the reheating after inflation with the fixed particle mass spectrum, we have identified the allowed parameter regions to satisfy the Big Bang Nucleosynthesis constraint. We have found that the entire parameter region for $m_{Z'} \lesssim 500$ GeV can be tested by the future collider experiments such as the High-Luminosity Large

been derived to ensure the stability of the inflaton potential [14].

Hadron Collider (LHC) [17] and the SHiP [18] experiments.

In this Chapter, we generalize the minimal $B-L$ model to the so-called non-exotic $\mathrm{U}(1)_X$ extension of the SM [19]. The non-exotic $\mathrm{U}(1)_X$ model is the most general extension of the SM with an extra anomaly-free U(1) gauge symmetry, which is described as a linear combination of the SM $\mathrm{U}(1)_Y$ and the $\mathrm{U}(1)_{B-L}$ gauge groups. The particle content of the model is the same as the one in the minimal $B-L$ model except for the generalization of the $\mathrm{U}(1)_X$ charge assignment for particles. The orientation of the $\mathrm{U}(1)_X$ gauge group is characterized by a $\mathrm{U}(1)_X$ charge of the SM Higgs doublet (x_H). For example, $x_H = 0$ is the $\mathrm{U}(1)_{B-L}$ limit, while the $\mathrm{U}(1)_{B-L}$ gauge group is oriented to the SM $\mathrm{U}(1)_Y$ direction for $|x_H| \gg 1$. In this context, we investigate the inflection-point inflation with the identification of the $\mathrm{U}(1)_X$ Higgs field as the inflaton. As we will discuss in the following, the inflation analysis weakly depends on x_H and hence our results are similar to those in Ref. [16]. However, there is a sharp contract in low energy phenomenologies, in particular, the $\mathrm{U}(1)_X$ gauge boson phenomenology at the LHC. An upper bound on the $\mathrm{U}(1)_{B-L}$ gauge coupling, $g_{BL} \lesssim 0.01$, has been obtained from theoretical consistencies in Ref. [16]. The Z' boson with such a small coupling can be explored in future collider experiments only for a small mass region such as $m_{Z'} \lesssim 500$ GeV. For this case in the inflection-point inflation scenario, the reheating temperature is estimated to be $T_R \lesssim 1$ GeV [16]. Such a low reheating temperature may not be desirable in terms of thermal dark matter physics and baryogenesis scenario. On the other hand, in the $\mathrm{U}(1)_X$ generalization, the coupling of the Z' boson with the SM fermions is controlled by $g_X x_H$ for $|x_H| \gtrsim 1$ with g_X being the $\mathrm{U}(1)_X$ gauge coupling, and therefore the Z' boson coupling becomes sizable for $|x_H| \gg 1$. In this Chapter, we will investigate the inflection-point inflation for this hyper-charge oriented $U(1)_X$ extension of the SM, which opens up a possibility to explore the mass region of $m_{Z'} > 1$ TeV at the LHC Run-2 while successfully realizing the inflection-point inflation.

The Chapter is organized as follows. In the next section, we give a brief review of the slow-roll inflation. In Sec. 3, we present the inflationary predictions for the scenario,

where the inflaton potential exhibits an inflection-point-like behavior during the slow-roll. In Sec. 4, we consider the minimally gauged $B-L$ extension of the SM, where the $B-L$ Higgs field is identified with the inflaton field. To realize the inflection-point in a Higgs/inflaton potential, we consider the RG improved effective Higgs/inflaton potential. In Sec. 5, we consider the constraints on the model parameters from the Big Bang Nucleosynthesis and the current collider experiments. We also discuss the prospects of testing the scenario in the future collider experiments, such as the High-Luminosity LHC and SHiP experiments. Sec. 6 is devoted to conclusions.

3.2 Basics of Inflection-Point Inflation

The inflationary slow-roll parameters for the inflaton field (ϕ) are given by

$$\epsilon(\phi) = \frac{M_P^2}{2}\left(\frac{V'}{V}\right)^2, \quad \eta(\phi) = M_P^2\left(\frac{V''}{V}\right), \quad \zeta^2(\phi) = M_P^4\frac{V'V'''}{V^2}, \tag{3.3}$$

where $M_P = M_{Pl}/\sqrt{8\pi} = 2.43\times 10^{18}$ GeV is the reduced Planck mass, V is the inflaton potential, and the prime denotes the derivative with respect to ϕ. The amplitude of the curvature perturbation $\Delta_{\mathcal{R}}^2$ is given by

$$\Delta_{\mathcal{R}}^2 = \frac{1}{24\pi^2}\frac{1}{M_P^4}\left.\frac{V}{\epsilon}\right|_{k_0}, \tag{3.4}$$

which should satisfy $\Delta_{\mathcal{R}}^2 = 2.195\times 10^{-9}$ from the Planck 2015 results [20] with the pivot scale chosen at $k_0 = 0.002$ Mpc^{-1}. The number of e-folds is defined as

$$N = \frac{1}{M_P^2}\int_{\phi_E}^{\phi_I} d\phi\,\frac{V}{V'}, \tag{3.5}$$

where ϕ_I is the inflaton value at a horizon exit corresponding to the scale k_0, and ϕ_E is the inflaton value at the end of inflation, which is defined by $\epsilon(\phi_E) = 1$. The value of N depends logarithmically on the energy scale during inflation as well as on the reheating

temperature, and it is typically taken to be $50 - 60$.

The slow-roll approximation is valid as long as the conditions $\epsilon \ll 1$, $|\eta| \ll 1$, and $\zeta^2 \ll 1$ hold. In this case, the inflationary predictions are given by

$$n_s = 1 - 6\epsilon + 2\eta, \quad r = 16\epsilon, \quad \alpha = 16\epsilon\eta - 24\epsilon^2 - 2\zeta^2, \tag{3.6}$$

where n_s, r and $\alpha \equiv \frac{dn_s}{dlnk}$ are the scalar spectral index, the tensor-to-scalar ratio and the running of the spectral index, respectively, which are evaluated at $\phi = \phi_I$. The Planck 2015 results [20] set an upper bound on the tensor-to-scalar ratio as $r \lesssim 0.11$, while the best fit value for the spectral index (n_s) and the running of spectral index (α) are 0.9655 ± 0.0062 and -0.0057 ± 0.0071, respectively, at 68% CL.

In the SFI scenario, to realize the slow-roll inflation the inflaton potential must exhibit an inflection-point-like behavior, where the potential is very flat.[2] Setting the inflaton value at the horizon in the very flat region $\phi_I = M$ of the potential, we approximate the inflaton potential by the following expansion around $\phi = M$:[3]

$$V(\phi) \simeq V_0 + V_1(\phi - M) + \frac{V_2}{2}(\phi - M)^2 + \frac{V_3}{6}(\phi - M)^3, \tag{3.7}$$

where V_0 is a constant and V_1, V_2 and V_3 are the first, second and third derivatives of the inflaton potential evaluated at $\phi = M$. When V_1 and V_2 are vanishingly small, the inflaton potential exhibits the inflection-point-like behavior. From Eqs. (3.3) and (3.7), the slow-roll parameters are then given by

$$\epsilon(M) \simeq \frac{M_P^2}{2}\left(\frac{V_1}{V_0}\right)^2, \quad \eta(M) \simeq M_P^2\left(\frac{V_2}{V_0}\right), \quad \zeta^2(M) = M_P^4\frac{V_1 V_3}{V_0^2}, \tag{3.8}$$

where we have used the approximation $V(M) \simeq V_0$. Similarly, the power-spectrum $\Delta^2_{\mathcal{R}}$ is

[2]For successful inflation scenario it is not necessary for the potential to realize an *exact* inflection-point. We only require the inflaton potential to exhibit a behavior of almost an inflection-point.

[3]Although our parameterization of the inflaton potential is slightly different, most of analysis in this section overlaps with that in Ref. [8].

expressed as

$$\Delta^2_{\mathcal{R}} \simeq \frac{1}{12\pi^2}\frac{V_0^3}{M_P^6 V_1^2}. \tag{3.9}$$

Using the constraint $\Delta^2_{\mathcal{R}} = 2.195 \times 10^{-9}$ from the Planck 2015 results, we can express V_1 and V_2 as

$$\begin{aligned}
\frac{V_1}{M^3} &\simeq 1961 \left(\frac{M}{M_P}\right)^3 \left(\frac{V_0}{M^4}\right)^{3/2}, \\
\frac{V_2}{M^2} &\simeq -1.725 \times 10^{-2} \left(\frac{1-n_s}{1-0.9655}\right) \left(\frac{M}{M_P}\right)^2 \left(\frac{V_0}{M^4}\right),
\end{aligned} \tag{3.10}$$

where we have used $V(M) \simeq V_0$ and $\epsilon(M) \ll |\eta(M)|$ as will be verified later. For the following analysis we set $n_s = 0.9655$ at the center value from the Planck 2015 results [20].

We define the inflaton value (ϕ_E) at the end of inflation by $\epsilon(\phi_E) = 1$. Using Eq. (3.5), the e-folding number (N) is given by

$$N = \frac{2V_0}{M_P^2\sqrt{-V_2^2 + 2V_1V_3}} \arctan\left(\frac{V_2 + V_3(\phi - M)}{\sqrt{-V_2^2 + 2V_1V_3}}\right)\Big|^{\phi=M}_{\phi=M(1-\delta_E)}, \tag{3.11}$$

where we have parametrized ϕ_E as $\phi_E/M = 1 - \delta_E$ with $0 < \delta_E < 1$. The inflection-point-like behavior of the inflaton potential requires $V_1, V_2 \simeq 0$ and $V3 > 0$, so that we can approximate $-V_2^2 + 2V_1V_3 \simeq 2V_1V_3$. This approximation is justified later. As we will also show later, $V_2, \sqrt{2V_1V_3} \ll V3M\delta_E$ and hence the e-folding number is approximated as

$$N \simeq \frac{2V_0}{M_P^2\sqrt{2V_1V_3}} \arctan\left[\frac{V_3 M\delta_E}{\sqrt{2V_1V_3}}\right] \simeq \pi\frac{V_0}{M_P^2\sqrt{2V_1V_3}}. \tag{3.12}$$

Using Eq. (3.10), V_3 is then given by

$$\frac{V_3}{M} \simeq 6.989 \times 10^{-7} \left(\frac{60}{N}\right)^2 \sqrt{\frac{V_0}{M^2M_P^2}}. \tag{3.13}$$

From Eqs. (3.10) and (3.13), we find $2V_1V_3 \simeq 9.2(60/N)V_2^2$, and $-V_2^2 + 2V_1V_3 \simeq 2V_1V_3$ is a good approximation for $N = 50 - 60$.

Using Eqs. (3.6), (3.8), (3.10), and (3.13), we now express all inflationary predictions in terms V_0, M and N. From Eqs. (3.8) and (3.10), the tensor-to-scalar ratio (r) is given by

$$r = 3.077 \times 10^7 \left(\frac{V_0}{M_P^4}\right). \tag{3.14}$$

The running of the spectral index (α) is found to be

$$\alpha \simeq -2\zeta^2(M) = -2.742 \times 10^{-3} \left(\frac{60}{N}\right)^2. \tag{3.15}$$

Note that this α value is a unique prediction of the inflection-point inflation independently of V_0 and M. This prediction is consistent with the current experimental bound, $\alpha = -0.0057 \pm 0.0071$ [20]. It is expected that the future experiments can reduce the error to ± 0.002 [21], and therefore the prediction of the inflection-point inflation scenario can be tested in the future.

3.3 The Inflection-point U(1)$_X$ Higgs Inflation

The model we will investigate is the anomaly-free U(1)$_X$ extension of the SM, which is based on the gauge group SU(3)$_c$×SU(2)$_L$×U(1)$_Y$×U(1)$_X$. The particle content of the model is listed in Table 4.1. The covariant derivative relevant to U(1)$_Y$× U(1)$_X$ is given by

$$D_\mu \equiv \partial_\mu - i(g_1 Y + \tilde{g} Q_X)B_\mu - i g_X Q_X Z'_\mu, \tag{3.16}$$

where Y (Q_X) are U(1)$_Y$ (U(1)$_X$) charge of a particle, and the gauge coupling $\tilde{g}$ is introduced in association with a kinetic mixing between the two U(1) gauge bosons. Although we set $\tilde{g}$ zero at the $U(1)_X$ symmetry breaking scale, it is generated through the RG evolutions. The particle content includes three generations of right-hand neutrinos N_R^i

	$SU(3)_c$	$SU(2)_L$	$U(1)_Y$	$U(1)_X$
q_L^i	**3**	**2**	1/6	$(1/6)x_H + (1/3)x_\Phi$
u_R^i	**3**	**1**	2/3	$(2/3)x_H + (1/3)x_\Phi$
d_R^i	**3**	**1**	$-1/3$	$(-1/3)x_H + (1/3)x_\Phi$
ℓ_L^i	**1**	**2**	$-1/2$	$(-1/2)x_H - x_\Phi$
e_R^i	**1**	**1**	-1	$(-1)x_H - x_\Phi$
H	**1**	**2**	$-1/2$	$(-1/2)x_H$
N_R^i	**1**	**1**	0	$-x_\Phi$
Φ	**1**	**1**	0	$+2x_\Phi$

Table 3.1: The particle content of the minimal $U(1)_X$ extended SM. In addition to the SM particle content ($i = 1, 2, 3$), the three right-handed neutrinos (N_R^i ($i = 1, 2, 3$)) and the $U(1)_X$ Higgs field (Φ), which is identified with the inflaton, are introduced. The extra $U(1)_X$ gauge group is defined with a linear combination of the SM $U(1)_Y$ and the $U(1)_{B-L}$ gauge groups, and the $U(1)_X$ charges of fields are determined by two real parameters, x_H and x_Φ. Without loss of generality, we fix $x_\Phi = 1$ throughout this Chapter.

and a $U(1)_X$ Higgs field Φ, in addition to the SM particle content. The $U(1)_X$ gauge group is identified with a linear combination of the SM $U(1)_Y$ and the $U(1)_{B-L}$ gauge groups, and hence the $U(1)_X$ charges of fields are determined by two real parameters, x_H and x_Φ. Note that in the model the charge x_Φ always appears as a product with the $U(1)_X$ gauge coupling and it is not an independent free parameter. Hence, we fix $x_\Phi = 1$ throughout this Chapter. In this way, we reproduce the minimal $B - L$ model with the conventional charge assignment as the limit of $x_H \to 0$.[4] The limit of $x_H \to +\infty$ $(-\infty)$ indicates that the $U(1)_X$ is (anti-)aligned to the SM $U(1)_Y$ direction. The anomaly structure of the model is the same as the minimal $B - L$ model and the model is free from all the gauge and the gravitational anomalies in the presence of the three right-handed neutirnos.

The Yukawa sector of the SM is extended to have

$$\mathcal{L}_{Yukawa} \supset -\sum_{i=1}^{3}\sum_{j=1}^{3} Y_D^{ij}\overline{\ell_L^i} H N_R^j - \frac{1}{2}\sum_{k=1}^{3} Y_M^k \Phi \overline{N_R^{k\,C}} N_R^k + \text{h.c.}, \tag{3.17}$$

where the first and second terms are the neutrino Dirac Yukawa coupling and the

[4]For $x_H = -4/5$ and $x_H = -2$, the $U(1)_X$ gauge group can arise from breaking of the SO(10) grand unified gauge group into the Standard Model one via the $SU(5)\times U(1)_X$ for the standard SU(5) and the flipped SU(5) subgroups of the SO(10), respectively.

Majorana Yukawa coupling, respectively. Without loss of generality, the Majorana Yukawa couplings are already diagonalized in our basis. Once the $\mathrm{U}(1)_X$ Higgs field Φ develops non-zero VEV, the $\mathrm{U}(1)_X$ gauge symmetry is broken and the Majorana masses for the right-handed neutrinos are generated. Then, the seesaw mechanism [22] is automatically implemented in the model after the electroweak symmetry breaking.

The renormalizable scalar potential for the SM Higgs doublet (H) and the $\mathrm{U}(1)_X$ Higgs (Φ) fields is given by

$$V = \lambda_H \left(H^\dagger H - \frac{v_h^2}{2} \right)^2 + \lambda_\Phi \left(\Phi^\dagger \Phi - \frac{v_X^2}{2} \right)^2 + \lambda_{\rm mix} \left(H^\dagger H - \frac{v_h^2}{2} \right) \left(\Phi^\dagger \Phi - \frac{v_X^2}{2} \right), \quad (3.18)$$

where all quartic couplings are chosen to be positive. At the potential minimum, the Higgs fields develop their VEVs as

$$\langle H \rangle = \begin{pmatrix} \frac{v_h}{\sqrt{2}} \\ 0 \end{pmatrix}, \quad \langle \Phi \rangle = \frac{v_X}{\sqrt{2}}. \quad (3.19)$$

Associated with the $\mathrm{U}(1)_X$ symmetry breaking (as well as the electroweak symmetry breaking), the $\mathrm{U}(1)_X$ gauge boson (Z' boson), the right-handed Majorana neutrinos, and the $\mathrm{U}(1)_X$ Higgs boson (ϕ) acquire their masses as

$$m_{Z'} = g_X \sqrt{4 v_X^2 + \frac{x_H^2}{4} v_h^2} \simeq 2 g_X v_X, \;\; m_{N^i} = \frac{1}{\sqrt{2}} Y_M^i v_X, \;\; m_\phi = \sqrt{2 \lambda_\Phi} v_X, \quad (3.20)$$

where $v_h = 246$ GeV is the SM Higgs VEV, and we have used the LEP constraint [23] $v_X^2 \gg v_h^2$. Because of the LEP constraint, the mass mixing of the Z' boson with the SM Z boson is very small, and we neglect it in our analysis in this Chapter.

We identify the physical $\mathrm{U}(1)_X$ Higgs field (ϕ) with the inflaton, which is defined as $\Phi = (\phi + v_h)/\sqrt{2}$ in the unitary gauge, and consider the inflation trajectory $\phi \gg v_X, v_h$ and $H = 0$ in the scalar potential in Eq. (3.18). In our analysis, we employ the RG improved

effective potential along this inflation trajectory, which is dominated by the inflaton quartic term and given by

$$V(\phi) = \frac{1}{4}\,\lambda(\phi)\,\phi^4, \tag{3.21}$$

where $\lambda(\phi)$ is the solution to the RG equation listed in Appendix. With the RG improved effective potential, we express the coefficients in the expansion of Eq. (3.7) as

$$\begin{aligned}
\frac{V_1}{M^3} &= \frac{1}{4}\left(4\lambda_\Phi + \beta_{\lambda_\Phi}\right), \\
\frac{V_2}{M^2} &= \frac{1}{4}\left(12\lambda_\Phi + 7\beta_{\lambda_\Phi} + M\beta'_{\lambda_\Phi}\right), \\
\frac{V_3}{M} &= \frac{1}{4}\left(24\lambda_\Phi + 26\beta_{\lambda_\Phi} + 10M\beta'_{\lambda_\Phi} + M^2\beta''_{\lambda_\Phi}\right),
\end{aligned} \tag{3.22}$$

where the prime denotes $d/d\phi$, and β_{λ_Φ} is the beta function of the quartic coupling λ_Φ given by

$$\begin{aligned}
\beta_{\lambda_\Phi} &= \frac{1}{(4\pi)^2}\left[\lambda_\Phi\left\{20\lambda_\Phi + 2\sum_{i=1}^{3}(Y_M^i)^2 - 48\left(\tilde{g}^2 + g_X^2\right)\right\} + 2\lambda_{\rm mix}^2\right. \\
&+ \left. 96\left(\tilde{g}^2 + g_X^2\right)^2 - \sum_{i=1}^{3}(Y_M^i)^4\right],
\end{aligned} \tag{3.23}$$

Using $V_1/M^3 \simeq 0$ and $V_2/M^2 \simeq 0$ to realize the inflection-point like behavior of the inflaton effective potential, we obtain

$$\beta_{\lambda_\Phi}(M) \simeq -4\lambda_\Phi(M), \qquad M\beta'_{\lambda_\Phi}(M) \simeq 16\lambda_\Phi(M). \tag{3.24}$$

For the couplings being in the perturbative regime, we evaluate $M^2\beta''_{\lambda_\Phi}(M) \simeq -M\beta'_{\lambda_\Phi}(M) \simeq -16\lambda_\Phi(M)$ as a good approximation. Hence the last equation

in Eq. (3.22) is simplified to be $V_3/M \simeq 16\,\lambda_\Phi(M)$ and Eq. (3.13) leads to

$$\lambda_\Phi(M) \simeq 4.770 \times 10^{-16} \left(\frac{M}{M_P}\right)^2 \left(\frac{60}{N}\right)^4, \tag{3.25}$$

where we have used $V_0 \simeq (1/4)\lambda_\Phi(M)M^4$. For $M \lesssim M_P$, $\lambda_\Phi(M)$ is found to be very small.

In evaluating $\beta_{\lambda_\Phi}(M)$, we simply assume $\lambda_{\rm mix}(M)$ is negligibly small. Although we have set $\tilde{g}(v_X) = 0$, non-vanishing $\tilde{g}(M)$ is generated through its RG evolution through its beta function consisting of two terms: one is proportional to $\tilde{g}$ and the other is proportional to g_X. However, as we will see later, the inflection-point inflation requires $g_X(M) \ll 1$, and hence $\tilde{g}$ stays negligibly small at any scales. As a result, Eq. (3.24) with Eq. (3.25) leads to $\beta_{\lambda_\Phi}(M) \simeq 0$, and we find

$$Y_M(M) \simeq 32^{1/4} g_X(M), \tag{3.26}$$

where we have taken the degenerate Yukawa couplings for three right-handed neutrinos $Y_M \equiv Y_M^1 = Y_M^2 = Y_M^3$, for simplicity. Therefore, the mass ratio between the right-handed neutrinos and the Z' gauge boson is fixed to realize a successful inflection-point inflation.

Now RG equations for λ_Φ, g_X and Y_M at the 1-loop level are approximately give by

$$\begin{aligned}
16\pi^2 \frac{d\lambda_\Phi}{d\ln\phi} &\simeq 96 g_X^4 - 3Y_M^4, \\
16\pi^2 \frac{dg_X}{d\ln\phi} &= \left(\frac{72 + 64x_H + 41x_H^2}{6}\right) g_X^3, \\
16\pi^2 \frac{dY_M}{d\ln\phi} &\simeq Y_M \left(\frac{5}{2} Y_M^2 - 6 g_X^2\right).
\end{aligned} \tag{3.27}$$

Using the second equation in Eq. (3.24) and Eqs. (3.25)-(3.27), we express the $\mathrm{U}(1)_X$ gauge coupling at $\phi = M$ as

$$g_X(M) \simeq \frac{1.511 \times 10^{-2}}{(93 + 256x_H + 164{x_H}^2)^{1/6}} \left(\frac{M}{M_P}\right)^{1/3} \left(\frac{60}{N}\right)^{2/3}. \tag{3.28}$$

Finally, from Eqs. (3.14) and (3.25), the tensor-to-scalar ratio (r) is given by

$$r \simeq 3.670 \times 10^{-9} \Big(\frac{M}{M_P} \Big)^6, \tag{3.29}$$

which is very small, as expected for the SFI scenario.

At the end of inflation, $\epsilon(\phi_E)$ is explicitly given by

$$\epsilon(\phi_E) = \frac{{M_P}^2}{2V_0^2} \left(V_1 - V_2 \, M\delta_E + \frac{V_3}{2} M^2 {\delta_E}^2 \right)^2 \simeq \frac{{M_P}^2 \, M^6 \, {\delta_E}^2}{2 \, V_0^2} \left(-\frac{V_2}{M^2} + \frac{V_3}{2M} \delta_E \right)^2 . \tag{3.30}$$

We evaluate δ_E from $\epsilon(\phi_E) = 1$. If we assume that the first term dominates in the parenthesis of the final expression above, we find $\delta_E \gg 1$ by using Eqs. (3.10), (3.13), and (3.25), which is inconsistent with $0 < \delta_E < 1$. Therefore, the second term must dominate, and hence we obtain

$$\delta_E \simeq 0.210 \, \Big(\frac{M}{M_P} \Big)^{1/2}, \tag{3.31}$$

by using Eqs. (3.13) and (3.25).

Before presenting our numerical results, let us check the consistency of our analysis. In the previous section we have approximated the inflaton potential by Eq. (3.7), neglecting the higher order terms. For consistency, we need to check if the contribution of higher order terms can actually be neglected in our model. Consider the following expansion of inflaton potential at $\phi = M$,

$$V(\phi) = \sum_{n=0} \frac{V^{(n)}}{n!} (\phi - M)^n, \tag{3.32}$$

where $V^{(n)}$ is the n-th derivative of the potential evaluated at $\phi = M$. As has been discussed in the previous section, $V_1 = V^{(1)}$ and $V_2 = V^{(2)}$ are fixed by the experimental values of the scalar power-spectrum ($\Delta^2_{\mathcal{R}}$) and the spectral index (n_s), respectively. For the

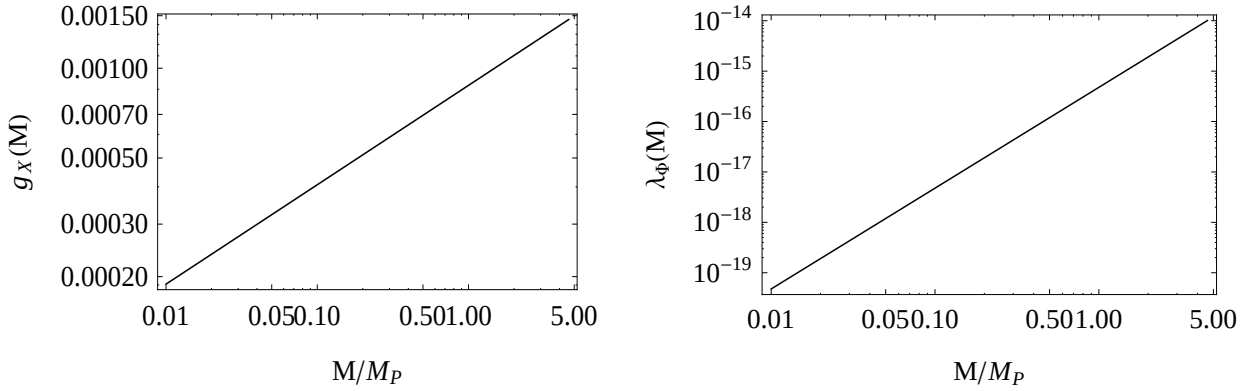

Figure 3.1: Left and right panels show the $\mathrm{U}(1)_X$ gauge coupling ($g_X(M)$) and the inflaton quartic coupling ($\lambda_\Phi(M)$) as a function of M/M_P, respectively, for a fixed $x_H = 400$.

consistency of our previous analysis, we require that the terms $V^{(4)}$ and higher contribute negligibly in determination of δ_E compared to V_3 at the end of inflation. Using Eqs. (3.3) and (3.32), $\epsilon(\phi_E)$ is expressed as

$$\begin{aligned} \epsilon(\phi_E) &\simeq \frac{{M_P}^2}{2V_0^2}\left(\sum_{n=1}\frac{V^{(n)}}{(n-1)!}(\phi - M)^{n-1}\right)^2 \\ &\simeq \frac{{M_P}^2}{2V_0^2}\left(\frac{V_3}{2}M^2{\delta_E}^2 + \sum_{n=4}\frac{V^{(n)}}{(n-1)!}(M\ \delta_E)^{n-1}\right)^2, \end{aligned} \tag{3.33}$$

where we have used $V(\phi_E) \simeq V_0$. This leads to constraint

$${\delta_E}^{(p-3)} < \left|\frac{(p-1)!}{2}\frac{V^{(3)}}{V^{(p)}}M^{3-p}\right|. \tag{3.34}$$

where $p \geq 4$. To proceed further we need to evaluate Eq. (3.34) explicitly for the minimal $\mathrm{U}(1)_X$ model. As has been shown previously in this section, all the higher order derivatives of the potential can be approximately given by $V^{(n)}M^{n-4} \simeq C_n\lambda(M)$, where C_n is a constant. For example, $C_4 = 96$ and $C_5 = 184$. We find that the most severe bound for both cases is from $V^{(4)}$ term. Using Eqs. (3.31) we obtain an upper bound on $M < 5.67M_P$.

Let us now present the numerical results of the inflection-point $\mathrm{U}(1)_X$ Higgs inflation scenario. For the rest of the Chapter, we employ the e-folding number $N = 60$.

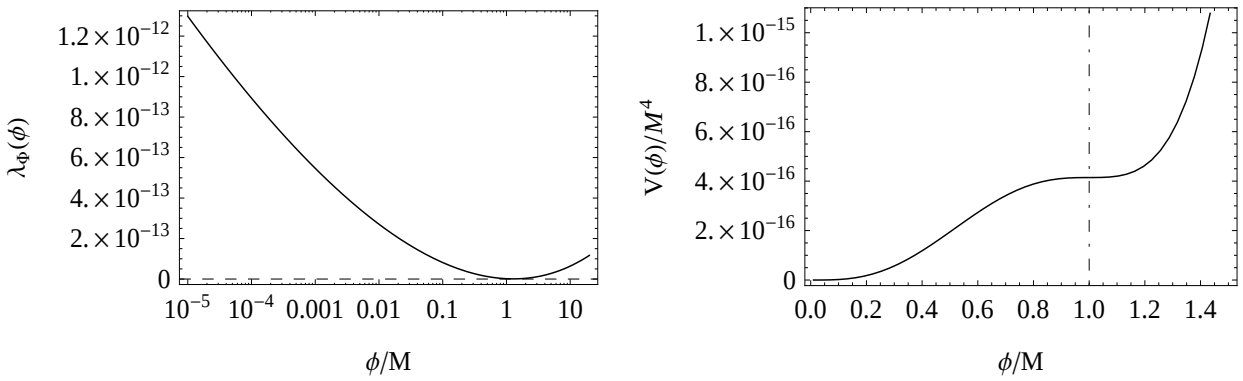

Figure 3.2: Left panel shows the RG running of the $U(1)_X$ Higgs/inflaton quartic coupling plotted against the normalized energy scale ϕ/M. Here we have fixed $M = M_P$ and $x_H = 400$, which corresponds to $g_X(M) = 8.756 \times 10^{-4}$, $Y_M(M) = 2.478 \times 10^{-3}$, and $\lambda_\Phi(M) \simeq 4.770 \times 10^{-16}$. The dashed horizontal line indicates $\lambda = 0$. Right panel shows the corresponding RG improved inflaton potential, where the inflection-point-like point appears at $\phi = M$.

We set $\tilde{g}(v_X) = 0$ and choose $\lambda_{\rm mix}(M)$ to be ${\lambda_{\rm mix}}^2 \ll 48{g_X}^4$, and hence all our results presented in the rest of this section are controlled by only three parameters, M, x_H and v_X.

In Fig. 3.1, we show the $U(1)_X$ gauge coupling (left) and the inflaton quartic coupling (right) at $\phi = M$ as a function of M (see Eqs. (3.25) and (3.26)). Here, we have fixed $x_H = 400$, which is motivated by the LHC phenomenology to be discussed in the next section.

In Fig. 3.2, we plot the running quartic coupling $\lambda_\Phi(\phi)$ (left) and the RG improved effective inflaton/Higgs potential (right). Here we have fixed $M = M_P$ and $x_H = 400$, which corresponds to $g_X(M) = 8.760 \times 10^{-4}$, $Y_M(M) = 2.103 \times 10^{-3}$, and $\lambda_\Phi(M) \simeq 4.770 \times 10^{-16}$. In the left panel, the dashed line indicates $\lambda_\Phi = 0$. In the right panel, we see the inflection-point-like behavior of the inflaton potential around $\phi = M$, marked with a dashed-dotted vertical line.

Here let us look at the inflationary predictions of our scenario. The prediction for the tensor-to-scalar ratio (r) is given by Eq. (3.29). For the upper bound on $M < 5.67 M_P$, the resultant tensor-to-scalar ratio is given by $r < 3.047 \times 10^{-5}$, which is too small to test in the future experiments. However, as discussed in the previous section, the inflection-point

inflation predicts the running of the spectral index to be $\alpha \simeq -2.742 \times 10^{-3}$, independently of M. This predicted value is within the reach of future precision measurements [21].

We now consider the particle mass spectrum of the model at low energies. As we have discussed, the condition of the almost vanishing $\beta_{\lambda_\Phi}(M)$ leads to the relation of $Y_M(M) \simeq 32^{1/4} g_X(M)$. The low energy mass spectrum of the Z' boson and the right-handed neutrinos are obtained by extrapolating the couplings to low energies. From Eq. (3.26) with the upper bound on $M < 5.67 M_P$, we can see $g_X(M) \ll 1$ and hence the RG running effects of the gauge and Yukawa couplings are negligible and $m_N/m_{Z'} \simeq 0.84$ remains almost the same at low energies. On the other hand, the RG evolution of the inflaton quartic coupling significantly changes its value at low energies (as shown in the left panel of Fig. 3.2), since its beta function is controlled by the gauge and Yukawa couplings. Let us approximately solve the RG equations in Eq. (3.27). Since $g_X(M)$, $Y_M(M) \ll 1$, the solutions to their RG equations are approximately given by

$$\begin{aligned} g_X(\mu) &\simeq g_X(M) + \beta_g(M) \ln\left[\frac{\mu}{M}\right], \\ Y_M(\mu) &\simeq Y_M(M) + \beta_Y(M) \ln\left[\frac{\mu}{M}\right], \end{aligned} \tag{3.35}$$

where $\beta_g(M)$ and $\beta_Y(M)$ are their beta-functions evaluated at $\mu = M$. Hence, the beta-function of the quartic coupling is approximately described as

$$\begin{aligned} \beta_{\lambda_\Phi}(\mu) &\simeq 96 g^4(\mu) - 3Y^4(\mu) \\ &\simeq 4\left(96 g_X(M)^3 \beta_g(M) - 3 Y_M(M)^3 \beta_Y(M)\right) \ln\left[\frac{\mu}{M}\right] \\ &\simeq M\beta'_{\lambda_\Phi}(M) \ln\left[\frac{\mu}{M}\right] \simeq 16\lambda_\Phi(M) \ln\left[\frac{\mu}{M}\right], \end{aligned} \tag{3.36}$$

where we have used $M\beta'_{\lambda_\Phi}(M) \simeq 16\lambda_\Phi(M)$ in Eq. (3.24). Then we obtain the approximate

solution to the RG equation as

$$\begin{aligned}\lambda_\Phi(v_X) &\simeq 8\lambda_\Phi(M)\left(\ln\left[\frac{v_X}{M}\right]\right)^2 \\ &\simeq 3.868\times10^{-15}\left(\frac{M}{M_P}\right)^2\left(\ln\left[\frac{v_X}{M}\right]\right)^2,\end{aligned} \tag{3.37}$$

where we have used Eq. (3.25) and $v_X \ll M$. Using $m_{Z'} = 2g(v_X)v_X \simeq 2g(M)v_X$, the mass ratio of the U(1)$_X$ Higgs/inflaton to the Z' boson is given by

$$\frac{m_\phi}{m_{Z'}} \simeq 2.911\times10^{-6}\left(\frac{M}{M_P}\right)^{2/3}\left(87+256x_H+164x_H^2\right)^{1/6}\ln\left[\frac{M}{v_X}\right]. \tag{3.38}$$

3.4 LHC Run-2 Constraints

If kinematically allowed, the Z' boson in the minimal U(1)$_X$ model can be produced at the LHC. The ATLAS and the CMS collaborations have been searching for a narrow resonance with di-lepton final states at the LHC Run-2 and set the upper limits of a Z' boson production cross section [24, 25]. In the analysis by the ATLAS and the CMS collaborations, the so-called sequential SM Z' (Z'_{SSM}) model [26] has been considered as a reference model, where the Z' boson has the same couplings with the SM fermions as the SM Z boson. In this section, we interpret the current LHC constraints on the sequential Z' boson into the U(1)$_X$ Z' boson to identify an allowed parameter region. Then, we examine a consistency of the inflection-point inflation scenario with the LHC Run-2 constraints.

We first calculate the cross section for the process $pp \to Z' + X \to \ell^+\ell^- + X$. The differential cross section with respect to the invariant mass $M_{\ell\ell}$ of the final state di-lepton is given by

$$\frac{d\sigma}{dM_{\ell\ell}} = \sum_{q,\bar{q}}\int_{\frac{M_{\ell\ell}^2}{E_{\rm CM}^2}}^1 dx\frac{2M_{\ell\ell}}{xE_{\rm CM}^2}f_q(x,Q^2)f_{\bar{q}}\left(\frac{M_{\ell\ell}^2}{xE_{\rm CM}^2},Q^2\right)\hat{\sigma}(q\bar{q}\to Z'\to\ell^+\ell^-), \tag{3.39}$$

where f_q is the parton distribution function for a parton (quark) "q", and $E_{\rm CM} = 13$ TeV is

the center-of-mass energy of the LHC Run-2. In our numerical analysis, we employ CTEQ6L [27] for the parton distribution functions with the factorization scale $Q = m_{Z'}$. Here, the cross section for the colliding partons is given by

$$\hat{\sigma}(q\bar{q} \to Z' \to \ell^+\ell^-) = \frac{\pi}{1296}\alpha_X^2 \frac{M_{\ell\ell}^2}{(M_{\ell\ell}^2 - m_{Z'}^2)^2 + m_{Z'}^2\Gamma_{Z'}^2} F_{q\ell}(x_H), \tag{3.40}$$

where $\alpha_X = g_X^2/(4\pi)$, the function $F_{q\ell}(x_H)$ are

$$\begin{aligned} F_{u\ell}(x_H) &= (8 + 20x_H + 17x_H^2)(8 + 12x_H + 5x_H^2), \\ F_{d\ell}(x_H) &= (8 - 4x_H + 5x_H^2)(8 + 12x_H + 5x_H^2) \end{aligned} \tag{3.41}$$

for q being the up-type (u) and down-type (d) quarks, respectively, and the total decay width of Z' boson is given by

$$\Gamma_{Z'} = \frac{\alpha_X}{6} m_{Z'} \left[F(x_H) + 3\left(1 - \frac{4m_N^2}{m_{Z'}^2}\right)^{\frac{3}{2}} \theta\left(\frac{m_{Z'}}{m_N} - 2\right) \right] \tag{3.42}$$

with $F(x_H) = 13 + 16x_H + 10x_H^2$. By integrating the differential cross section over a range of $M_{\ell\ell}$ set by the ATLAS and the CMS analysis, respectively, we obtain the cross section to be compared with the upper bounds obtained by the ATLAS and the CMS collaborations.

In interpreting the 2016 results by the ATLAS and the CMS collaborations into the $\mathrm{U}(1)_X$ Z' boson case, we follow the strategy in [28] (see also [29] for the minimal $B - L$ model). In the Chapter, the cross section for the process $pp \to Z'_{SSM} + X \to \ell^+\ell^- + X$ is calculated and the resultant cross sections are scaled by a k-factor to match with the theoretical predictions presented in the ATLAS and the CMS papers. With the k-factor determined in this way, the cross section for the process $pp \to Z' + X \to \ell^+\ell^- + X$ is calculated to identify an allowed region for the model parameters of α_X, x_H and $m_{Z'}$. See Ref. [28] for the details of the strategy and the k-factors. Our analysis in this section is exactly the same as that in this reference.

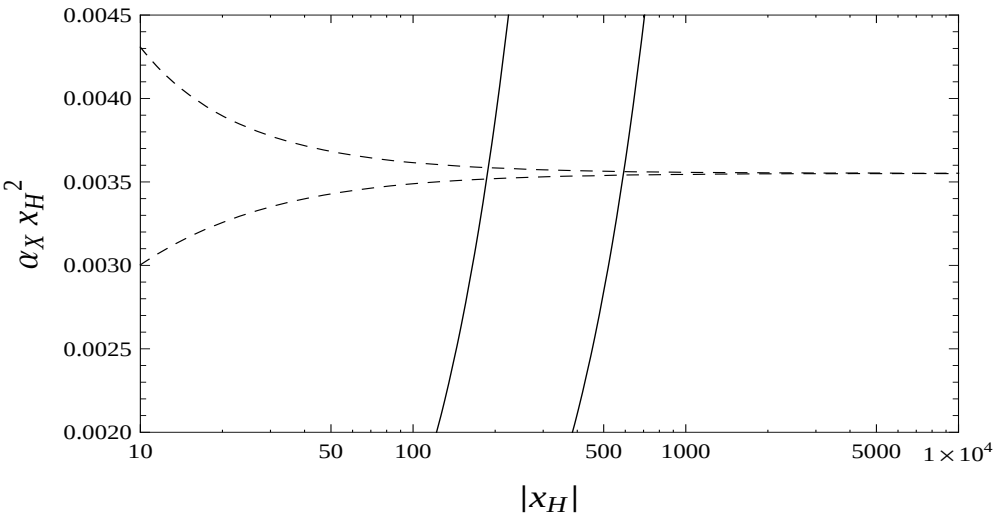

Figure 3.3: The upper bounds on $\alpha_X\, x_H^2$ as a function of x_H from the CMS results on search for a narrow resonance from the combined di-electron and di-muon channels [25]. The lower and upper dashed lines correspond to $x_H > 0$ and $x_H < 0$, respectively. Here we have fixed $m_{Z'} = 4$ TeV. The diagonal solid lines depict Eq. (3.25) for $M = M_P$ (left) and $M = 0.01 M_P$ (right), along which the successful inflection-point inflation is achieved.

For $m_{Z'} = 4$ TeV, we show in Fig. 3.3 the upper bounds on $\alpha_X\, x_H^2$ as a function of x_H from the CMS results on search for a narrow resonance from the combined di-electron and di-muon channels [25]. The lower and upper dashed lines correspond to $x_H > 0$ and $x_H < 0$, respectively. The upper bounds from the ATLAS results [24] are found to be very similar to but slightly weaker than those from the CMS results, and we have shown only the CMS results. As we can see from the cross section formula, the dashed lines approach each other for a large $|x_H|$. The diagonal solid lines depict Eq. (3.25) for $M = M_P$ (left) and $M = 0.01 M_P$ (right), along which the successful inflection-point inflation is achieved. For the diagonal solid lines with a fixed M, the results for $x_H > 0$ and $x_H < 0$ are indistinguishable. From this figure, we find an upper bound on $x_H \lesssim 200$ and $x_H \lesssim 600$, respectively, for $M = M_P$ (left) and $M = 0.01 M_P$ (right). Note that even though the successful inflection-point inflation requires the $\mathrm{U}(1)_X$ gauge coupling to be very small, this scenario can still be tested at the LHC when $|x_H| \gg 1$, in other words, the $\mathrm{U}(1)_X$ gauge symmetry is oriented towards the SM hyper-charge direction.

3.5 Constraints from the Big Bang Nucleosynthesis

Let us now consider a reheating scenario after inflation to connect our inflation scenario with the Standard Big Bang Cosmology. This occurs via inflaton decay into the SM particles during the inflaton oscillates around its potential minimum. We estimate the reheating temperature (T_R) as

$$T_R \simeq 0.55 \left(\frac{100}{g_*}\right)^{1/4} \sqrt{\Gamma_\phi M_P}, \tag{3.43}$$

where Γ_ϕ is the inflaton decay width into the SM particles. For the successful Big Bang Nucleosynthesis (BBN), we impose a model-independent lower bound on the reheating temperature as $T_R \gtrsim 1$ MeV.

In the Higgs potential of Eq. (3.18), a mass matrix between the inflaton (ϕ) and the SM Higgs boson (h) is generated after the $\mathrm{U}(1)_X$ symmetry and the electroweak symmetry breaking:

$$\mathcal{L} \supset -\frac{1}{2} \begin{bmatrix} h & \phi \end{bmatrix} \begin{bmatrix} m_h^2 & \lambda_{\rm mix} v_h v_X \\ \lambda_{\rm mix} v_h v_X & m_\phi^2 \end{bmatrix} \begin{bmatrix} h \\ \phi \end{bmatrix}, \tag{3.44}$$

where $m_\phi = \sqrt{2\lambda_\Phi} v_X$, and $m_h = \sqrt{2\lambda_H} v_h = 125$ GeV. We diagonalize the mass matrix by

$$\begin{bmatrix} h \\ \phi \end{bmatrix} = \begin{bmatrix} \cos\theta & \sin\theta \\ -\sin\theta & \cos\theta \end{bmatrix} \begin{bmatrix} \phi_1 \\ \phi_2 \end{bmatrix}, \tag{3.45}$$

where ϕ_1 and ϕ_2 are the mass eigenstates. The relations among the mass parameters and

the mixing angle (θ) are the following:

$$\begin{aligned} 2v_h v_X \lambda_{\rm mix} &= (m_h^2 - m_\phi^2)\tan 2\theta, \\ m_{\phi_1}^2 &= m_h^2 - \left(m_\phi^2 - m_h^2\right)\tfrac{\sin^2\theta}{1-2\sin^2\theta}, \\ m_{\phi_2}^2 &= m_\phi^2 + \left(m_\phi^2 - m_h^2\right)\tfrac{\sin^2\theta}{1-2\sin^2\theta}\ . \end{aligned} \tag{3.46}$$

Since the inflaton is much lighter than the Z' boson and the heavy neutrinos, it decays to the SM particles mainly through the mixing with the SM Higgs boson. We calculate the inflaton decay width as

$$\Gamma_{\phi_2} = \sin^2\theta \times \Gamma_h(m_{\phi_2}), \tag{3.47}$$

where $\Gamma_h(m_{\phi_2})$ is the SM Higgs boson decay width if the SM Higgs boson mass were m_{ϕ_2}.

There are constraints on the mixing angle. Firstly, we have imposed $\lambda_{\rm mix}^2 \ll 48 g_X^4$ to neglect the contribution of the $\lambda_{\rm mix}$ to β_Φ. Another constraint on the mixing angle is from requiring positive definiteness of mass squared eigenvalues of the mass matrix in Eq. (3.44), which leads to $\lambda_{\rm mix}^2 < 4\lambda_H\lambda_\Phi$. We find that the latter constraint is more severe and requires $\theta \ll 1$. Hence ϕ_1 and ϕ_2 are mostly the SM Higgs and the U(1)$_X$ Higgs mass eigenstates, respectively.

In the following analysis we parameterize $\lambda_{\rm mix}^2 = 4\lambda_H\lambda_\phi\xi$ with a new parameter $0 < \xi < 1$. From Eq. (3.46), we obtain

$$\theta^2 \simeq \xi\left(\frac{m_\phi}{m_h}\right)^2, \tag{3.48}$$

where we have used $m_\phi^2 \ll m_h^2$ from Eq. (3.38) for the parameter region we are interested in, namely $m_{Z'} = \mathcal{O}(1\ \text{TeV})$. We also find that $m_{\phi 2} \simeq m_\phi\sqrt{1-\xi}$. From Eqs. (3.38), (3.43), (3.47) and (3.48), we can express the reheating temperature as a function of M, $m_{Z'}$, x_H and ξ. To simplify our analysis, let us fix $x_H = 400$ and $\xi = 0.1$. In Fig. 3.4, we show the

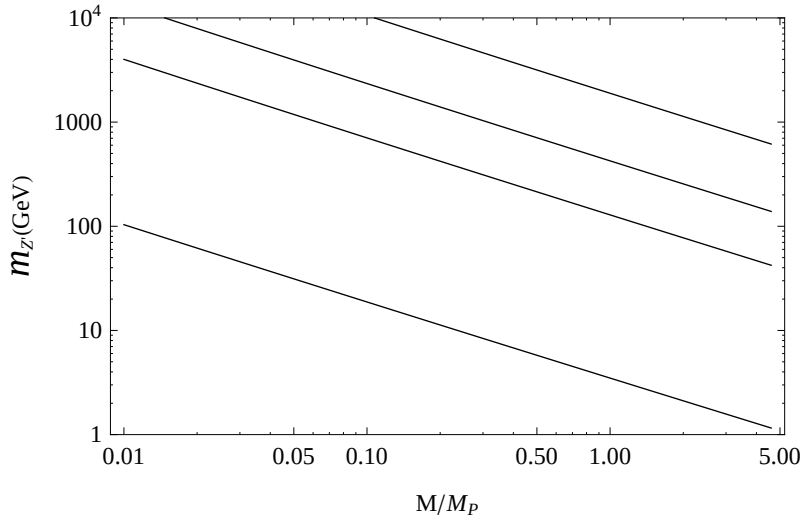

Figure 3.4: The contours corresponding to the reheating temperatures $T_R = 1$ MeV, 1 GeV, 100 GeV, and 1 TeV, from bottom to top, for $x_H = 400$ and $\xi = 0.1$.

contours corresponding to $T_R = 1$ MeV, 1 GeV, 100 GeV, and 1 TeV, from bottom to top.

3.6 Conclusions

From a theoretical point of view, if the inflaton value is trans-Planckian, effective operators suppressed by the Planck mass could significantly affect the inflaton potential during inflation, and hence the inflationary predictions. To avoid this problem, we may consider the SFI, where the inflaton value during inflation is smaller than the Planck mass. In this case, the inflection-point inflation is an interesting possibility to realize a successful slow-roll inflation when inflation is driven by a single scalar field. To realize the inflection-point-like behavior for the RG improved effective $\lambda\phi^4$ potential, the running quartic coupling $\lambda(\phi)$ must exhibit a minimum with an almost vanishing value in its RG evolution, namely $\lambda(\phi_I) \simeq 0$ and $\beta_\lambda(\phi_I) \simeq 0$, where β_λ is the beta-function of the quartic coupling.

From a particle physics perspective, it is more compelling to consider an inflationary scenario, where the inflaton field plays another important role. We may consider a general Higgs model, namely the gauge-Higgs-Yuakwa system, and identify the Higgs field as

inflaton. In this case, the conditions, $\lambda(\phi_I) \simeq 0$ and $\beta_\lambda(\phi_I) \simeq 0$, lead to a relation among the gauge, the Yukawa and the Higgs quartic couplings. Using the relation and requiring the inflationary predictions to be consistent with the Planck 2015 results, we have found that all the couplings (at ϕ_I) depend only on ϕ_I. Hence, the low energy mass spectrum of the model is uniquely determined by only two free parameters, ϕ_I and the inflaton/Higgs VEV, and the inflationary predictions are complementary to the low energy mass spectrum. It is also interesting that the inflection-point inflation provides a unique prediction for the running of the spectral index $\alpha \simeq -2.7 \times 10^{-3}$, which can be tested in the future experiments.

We have investigated the inflection-point inflation in the context of the minimal $\mathrm{U}(1)_X$ extended SM, where the anomaly-free extra gauge symmetry is defined as a linear combination of the SM hyper-charge and the gauged $B - L$ groups. Identifying the $\mathrm{U}(1)_X$ Higgs field with the inflaton, we have obtained a prediction for the mass spectrum for the Z' boson, the right-handed neutrinos, and the $\mathrm{U}(1)_X$ Higgs boson as a function of ϕ_I, x_H, and the inflaton/Higgs VEV. Even though the successful inflection-point inflation requires the $\mathrm{U}(1)_X$ gauge coupling to be very small, we have found that the Z' boson with mass of a few TeV can be explored at the LHC Run-2 when the direction of the $\mathrm{U}(1)_X$ symmetry is oriented towards the SM hyper-charge, or equivalently $|x_H| \gg 1$. This is in sharp contrast to the inflection-point inflation scenario in the minimal $\mathrm{U}(1)_{B-L}$ extended SM previously investigated in Ref. [16]. We have also considered the reheating after inflation and found a large portion of parameter space which can reheat the universe sufficiently high.

3.7 Acknowledgments

S.O. would like to thank the Department of Physics and Astronomy at the University of Alabama for hospitality during her visit for the completion of this work. She would also like to thank FUSUMA Alumni Association at Yamagata University for travel supports for her visit to the University of Alabama. This work is supported in part by the

United States Department of Energy (Award No. DE-SC0013680).

3.8 References

[1] A. A. Starobinsky, "A New Type of Isotropic Cosmological Models Without Singularity," Phys. Lett. B **91**, 99 (1980).

[2] A. H. Guth, "The Inflationary Universe: A Possible Solution to the Horizon and Flatness Problems," Phys. Rev. D **23**, 347 (1981).

[3] A. D. Linde, "Chaotic Inflation," Phys. Lett. B **129**, 177 (1983).

[4] A. Albrecht and P. J. Steinhardt, "Cosmology for Grand Unified Theories with Radiatively Induced Symmetry Breaking," Phys. Rev. Lett. **48**, 1220 (1982).

[5] A. D. Linde, "Hybrid inflation," Phys. Rev. D **49**, 748 (1994) doi:10.1103/PhysRevD.49.748 [astro-ph/9307002].

[6] R. Allahverdi, K. Enqvist, J. Garcia-Bellido and A. Mazumdar, "Gauge invariant MSSM inflaton," Phys. Rev. Lett. **97**, 191304 (2006) doi:10.1103/PhysRevLett.97.191304 [hep-ph/0605035]; R. Allahverdi, K. Enqvist, J. Garcia-Bellido, A. Jokinen and A. Mazumdar, "MSSM flat direction inflation: Slow roll, stability, fine tunning and reheating," JCAP **0706**, 019 (2007) doi:10.1088/1475-7516/2007/06/019 [hep-ph/0610134]; J. C. Bueno Sanchez, K. Dimopoulos and D. H. Lyth, "A-term inflation and the MSSM," JCAP **0701**, 015 (2007) doi:10.1088/1475-7516/2007/01/015 [hep-ph/0608299]; D. Baumann, A. Dymarsky, I. R. Klebanov, L. McAllister and P. J. Steinhardt, "A Delicate universe," Phys. Rev. Lett. **99**, 141601 (2007) doi:10.1103/PhysRevLett.99.141601 [arXiv:0705.3837 [hep-th]]; D. Baumann,

A. Dymarsky, I. R. Klebanov and L. McAllister, "Towards an Explicit Model of D-brane Inflation," JCAP **0801**, 024 (2008) doi:10.1088/1475-7516/2008/01/024 [arXiv:0706.0360 [hep-th]]; M. Badziak and M. Olechowski, "Volume modulus inflection point inflation and the gravitino mass problem," JCAP **0902**, 010 (2009) doi:10.1088/1475-7516/2009/02/010 [arXiv:0810.4251 [hep-th]]; K. Enqvist, A. Mazumdar and P. Stephens, "Inflection point inflation within supersymmetry," JCAP **1006**, 020 (2010) doi:10.1088/1475-7516/2010/06/020 [arXiv:1004.3724 [hep-ph]]; R. Cerezo and J. G. Rosa, "Warm Inflection," JHEP **1301**, 024 (2013) doi:10.1007/JHEP01(2013)024 [arXiv:1210.7975 [hep-ph]]; S. Choudhury, A. Mazumdar and S. Pal, "Low & High scale MSSM inflation, gravitational waves and constraints from Planck," JCAP **1307**, 041 (2013) doi:10.1088/1475-7516/2013/07/041 [arXiv:1305.6398 [hep-ph]]; S. Choudhury and A. Mazumdar, "Reconstructing inflationary potential from BICEP2 and running of tensor modes," arXiv:1403.5549 [hep-th].

[7] G. Ballesteros and C. Tamarit, "Radiative plateau inflation," JHEP **1602**, 153 (2016) doi:10.1007/JHEP02(2016)153 [arXiv:1510.05669 [hep-ph]].

[8] S. M. Choi and H. M. Lee, "Inflection point inflation and reheating," Eur. Phys. J. C **76**, no. 6, 303 (2016) doi:10.1140/epjc/s10052-016-4150-5 [arXiv:1601.05979 [hep-ph]].

[9] F. L. Bezrukov and M. Shaposhnikov, "The Standard Model Higgs boson as the inflaton," Phys. Lett. B **659**, 703 (2008) [arXiv:0710.3755 [hep-th]]; J. Garcia-Bellido, D. G. Figueroa and J. Rubio, "Preheating in the Standard Model with the Higgs-Inflaton coupled to gravity," Phys. Rev. D **79**, 063531 (2009) doi:10.1103/PhysRevD.79.063531 [arXiv:0812.4624 [hep-ph]]; F. Bezrukov, D. Gorbunov and M. Shaposhnikov, "On initial conditions for the Hot Big Bang," JCAP **0906**, 029 (2009) [arXiv:0812.3622 [hep-ph]]; F. L. Bezrukov, A. Magnin and M. Shaposhnikov, "Standard Model Higgs boson mass from inflation," Phys. Lett. B **675**, 88 (2009) [arXiv:0812.4950 [hep-ph]]; F. Bezrukov and M. Shaposhnikov, "Standard Model Higgs

boson mass from inflation: two loop analysis," JHEP **0907**, 089 (2009) [arXiv:0904.1537 [hep-ph]]; F. Bezrukov, A. Magnin, M. Shaposhnikov and S. Sibiryakov, "Higgs inflation: consistency and generalisations," JHEP **1101**, 016 (2011) [arXiv:1008.5157 [hep-ph]]; F. Bezrukov and M. Shaposhnikov, "Higgs inflation at the critical point," Phys. Lett. B **734**, 249 (2014) doi:10.1016/j.physletb.2014.05.074 [arXiv:1403.6078 [hep-ph]]; Y. Hamada, H. Kawai, K. y. Oda and S. C. Park, "Higgs Inflation is Still Alive after the Results from BICEP2," Phys. Rev. Lett. **112**, no. 24, 241301 (2014) doi:10.1103/PhysRevLett.112.241301 [arXiv:1403.5043 [hep-ph]].

[10] A. O. Barvinsky, A. Y. Kamenshchik and A. A. Starobinsky, "Inflation scenario via the Standard Model Higgs boson and LHC," JCAP **0811**, 021 (2008) [arXiv:0809.2104 [hep-ph]]; A. O. Barvinsky, A. Y. Kamenshchik, C. Kiefer, A. A. Starobinsky and C. Steinwachs, "Asymptotic freedom in inflationary cosmology with a non-minimally coupled Higgs field," JCAP **0912**, 003 (2009) [arXiv:0904.1698 [hep-ph]]; "Higgs boson, renormalization group, and naturalness in cosmology," Eur. Phys. J. C **72**, 2219 (2012) [arXiv:0910.1041 [hep-ph]].

[11] A. De Simone, M. P. Hertzberg and F. Wilczek, "Running Inflation in the Standard Model," Phys. Lett. B **678**, 1 (2009) [arXiv:0812.4946 [hep-ph]]; T. E. Clark, B. Liu, S. T. Love and T. ter Veldhuis, "The Standard Model Higgs Boson-Inflaton and Dark Matter," Phys. Rev. D **80**, 075019 (2009) [arXiv:0906.5595 [hep-ph]].

[12] See, for example, M. Sher, "Electroweak Higgs Potentials and Vacuum Stability," Phys. Rept. **179**, 273 (1989).

[13] See, for example, N. Okada, M. U. Rehman and Q. Shafi, "Tensor to Scalar Ratio in Non-Minimal ϕ^4 Inflation," Phys. Rev. D **82**, 043502 (2010) [arXiv:1005.5161 [hep-ph]]; N. Okada, V. N. Senoguz and Q. Shafi, "The Observational Status of Simple Inflationary Models: an Update," arXiv:1403.6403 [hep-ph]; T. Inagaki, R. Nakanishi and

S. D. Odintsov, "Non-Minimal Two-Loop Inflation," Phys. Lett. B **745**, 105 (2015) [arXiv:1502.06301 [hep-ph]].

[14] K. Kannike, G. Hutsi, L. Pizza, A. Racioppi, M. Raidal, A. Salvio and A. Strumia, "Dynamically Induced Planck Scale and Inflation," JHEP **1505**, 065 (2015) doi:10.1007/JHEP05(2015)065 [arXiv:1502.01334 [astro-ph.CO]]; N. Okada and D. Raut, "Running Non-Minimal Inflation with Stabilized Inflaton Potential," PoS DSU **2015**, 013 (2016) [arXiv:1509.04439 [hep-ph]]; K. Kannike, A. Racioppi and M. Raidal, JHEP **1601**, 035 (2016) doi:10.1007/JHEP01(2016)035 [arXiv:1509.05423 [hep-ph]].

[15] R. N. Mohapatra and R. E. Marshak, "Local B-L Symmetry of Electroweak Interactions, Majorana Neutrinos and Neutron Oscillations," Phys. Rev. Lett. **44**, 1316 (1980) Erratum: [Phys. Rev. Lett. **44**, 1643 (1980)]; "Quark - Lepton Symmetry and B-L as the U(1) Generator of the Electroweak Symmetry Group," Phys. Lett. **91B**, 222 (1980); C. Wetterich, "Neutrino Masses and the Scale of B-L Violation," Nucl. Phys. B **187**, 343 (1981); A. Masiero, J. F. Nieves and T. Yanagida, "B^-l Violating Proton Decay and Late Cosmological Baryon Production," Phys. Lett. **116B**, 11 (1982); R. N. Mohapatra and G. Senjanovic, "Spontaneous Breaking of Global B^-l Symmetry and Matter - Antimatter Oscillations in Grand Unified Theories," Phys. Rev. D **27**, 254 (1983); W. Buchmuller, C. Greub and P. Minkowski, "Neutrino masses, neutral vector bosons and the scale of B-L breaking," Phys. Lett. B **267**, 395 (1991).

[16] N. Okada and D. Raut, "Inflection-point Higgs Inflation," arXiv:1610.09362 [hep-ph], to be published in Phys. Rev. D.

[17] B. Schmidt, "The High-Luminosity upgrade of the LHC: Physics and Technology Challenges for the Accelerator and the Experiments," J. Phys. Conf. Ser. **706**, no. 2, 022002 (2016). doi:10.1088/1742-6596/706/2/022002

[18] M. Anelli *et al.* [SHiP Collaboration], "A facility to Search for Hidden Particles (SHiP) at the CERN SPS," arXiv:1504.04956 [physics.ins-det].

[19] T. Appelquist, B. A. Dobrescu and A. R. Hopper, "Nonexotic neutral gauge bosons," Phys. Rev. D **68**, 035012 (2003) [hep-ph/0212073].

[20] P. A. R. Ade *et al.* [Planck Collaboration], "Planck 2015 results. XIII. Cosmological parameters," Astron. Astrophys. **594**, A13 (2016) doi:10.1051/0004-6361/201525830 [arXiv:1502.01589 [astro-ph.CO]].

[21] K. N. Abazajian *et al.*, "Inflation Physics from the Cosmic Microwave Background and Large Scale Structure," Astropart. Phys. **63**, 55 (2015) doi:10.1016/j.astropartphys.2014.05.013 [arXiv:1309.5381 [astro-ph.CO]].

[22] P. Minkowski, Phys. Lett. B **67**, 421 (1977); T. Yanagida, in *Proceedings of the Workshop on the Unified Theory and the Baryon Number in the Universe* (O. Sawada and A. Sugamoto, eds.), KEK, Tsukuba, Japan, 1979, p. 95; M. Gell-Mann, P. Ramond, and R. Slansky, *Supergravity* (P. van Nieuwenhuizen et al. eds.), North Holland, Amsterdam, 1979, p. 315; S. L. Glashow, *The future of elementary particle physics*, in *Proceedings of the 1979 Cargèse Summer Institute on Quarks and Leptons* (M. Lévy et al. eds.), Plenum Press, New York, 1980, p. 687; R. N. Mohapatra and G. Senjanović, "Neutrino Mass and Spontaneous Parity Violation," Phys. Rev. Lett. **44**, 912 (1980); J. Schechter and J. W. F. Valle, "Neutrino Masses in SU(2) x U(1) Theories," Phys. Rev. D **22**, 2227 (1980).

[23] SLD Electroweak Group, SLD Heavy Flavor Group, DELPHI, LEP, ALEPH, OPAL, LEP Electroweak Working Group, L3 Collaboration, "A Combination of preliminary electroweak measurements and constraints on the standard model," hep-ex/0312023; S. Schael *et al.* [ALEPH and DELPHI and L3 and OPAL and LEP Electroweak Collaborations], "Electroweak Measurements in Electron-Positron Collisions at W-Boson-Pair Energies at LEP," Phys. Rept. **532**, 119 (2013) [arXiv:1302.3415 [hep-ex]].

[24] The ATLAS collaboration [ATLAS Collaboration], "Search for new high-mass

resonances in the dilepton final state using proton-proton collisions at $\sqrt{s} = 13$ TeV with the ATLAS detector," ATLAS-CONF-2016-045.

[25] CMS Collaboration [CMS Collaboration], "Search for a high-mass resonance decaying into a dilepton final state in 13 fb^{-1} of pp collisions at $\sqrt{s} = 13$ TeV," CMS-PAS-EXO-16-031.

[26] V. D. Barger, W. Y. Keung and E. Ma, "Doubling of Weak Gauge Bosons in an Extension of the Standard Model," Phys. Rev. Lett. **44**, 1169 (1980).

[27] J. Pumplin, D. R. Stump, J. Huston, H. L. Lai, P. M. Nadolsky and W. K. Tung, "New generation of parton distributions with uncertainties from global QCD analysis," JHEP **0207**, 012 (2002) [hep-ph/0201195].

[28] N. Okada and S. Okada, "Z'-portal right-handed neutrino dark matter in the minimal U(1)$_X$ extended Standard Model," arXiv:1611.02672 [hep-ph], to be published in Phys. Rev. D.

[29] N. Okada and S. Okada, "Z'_{BL} portal dark matter and LHC Run-2 results," Phys. Rev. D **93**, no. 7, 075003 (2016) [arXiv:1601.07526 [hep-ph]].

[30] S. Oda, N. Okada and D. s. Takahashi, "Classically conformal U(1)' extended standard model and Higgs vacuum stability," Phys. Rev. D **92**, no. 1, 015026 (2015) [arXiv:1504.06291 [hep-ph]].

3.A RG equations in the minimal U(1)$_X$ model

In this Appendix we list the one-loop RG equations for the couplings which are used in our analysis. See Appendix in Ref. [30] for a complete list. The RG equations for the

gauge couplings at the one-loop level are given by

$$
\begin{aligned}
\mu\frac{dg_1}{d\mu} &= \frac{g_1}{(4\pi)^2}\left[12\left(\frac{1}{6}g_1+x_q\tilde{g}\right)^2+6\left(\frac{2}{3}g_1+x_u\tilde{g}\right)^2+6\left(-\frac{1}{3}g_1+x_d\tilde{g}\right)^2\right.\\
&+ \left. 4\left(-\frac{1}{2}g_1+x_\ell\tilde{g}\right)^2+2\left(x_\nu\tilde{g}\right)^2+2\left(-g_1+x_e\tilde{g}\right)^2+\frac{2}{3}\left(\frac{1}{2}g_1+x_H\tilde{g}\right)^2+\frac{1}{3}\left(x_\Phi\tilde{g}\right)^2\right],\\
\mu\frac{dg_X}{d\mu} &= \frac{g_X^3}{(4\pi)^2}\left[12x_q^2+6x_u^2+6x_d^2+4x_\ell^2+2x_\nu^2+2x_e^2+\frac{2}{3}x_H^2+\frac{1}{3}x_\Phi^2\right],\\
\mu\frac{d\tilde{g}}{d\mu} &= \frac{1}{(4\pi)^2}\left[\tilde{g}\left\{12\left(\frac{1}{6}g_1+x_q\tilde{g}\right)^2+6\left(\frac{2}{3}g_1+x_u\tilde{g}\right)^2+6\left(-\frac{1}{3}g_1+x_d\tilde{g}\right)^2\right.\right.\\
&+ \left. 4\left(-\frac{1}{2}g_1+x_\ell\tilde{g}\right)^2+2\big(x_\nu\tilde{g}\big)^2+2\big(-g_1+x_e\tilde{g}\big)^2+\frac{2}{3}\left(\frac{1}{2}g_1+x_H\tilde{g}\right)^2+\frac{1}{3}\left(x_\Phi\tilde{g}\right)^2\right\}\\
&+ 2g_X^2\left\{12x_q\left(\frac{1}{6}g_1+x_q\tilde{g}\right)+6x_u\left(\frac{2}{3}g_1+x_u\tilde{g}\right)+6x_d\left(-\frac{1}{3}g_1+x_d\tilde{g}\right)\right.\\
&+ 4x_\ell\left(-\frac{1}{2}g_1+x_\ell\tilde{g}\right)+2x_\nu\big(x_\nu\tilde{g}\big)+2x_e\big(-g_1+x_e\tilde{g}\big)\\
&+ \left.\left.\frac{2}{3}x_H\left(\frac{1}{2}g_1+x_H\tilde{g}\right)+\frac{1}{3}x_\Phi\left(x_\Phi\tilde{g}\right)\right\}\right].
\end{aligned}
\tag{3.49}
$$

Here, x_f is a $\mathrm{U}(1)_X$ charge of a corresponding fermion (f) in Table 4.1. For example, $x_q = (1/6)x_H + (1/3)x_\Phi$, and $x_e = -x_H - x_\Phi$. For the RGEs for the Majorana Yukawa couplings at the one-loop level we have

$$
\mu\frac{dY_M^i}{d\mu} = \frac{Y_M^i}{(4\pi)^2}\left[(Y_M^i)^2+\frac{1}{2}\sum_{j=1}^{3}(Y_M^j)^2+\big(12x_\nu^2-6x_\Phi^2\big)\big(\tilde{g}^2+g_X^2\big)\right]. \tag{3.50}
$$

Finally, the RGEs for the scalar quartic couplings are given by

$$
\begin{aligned}
\mu\frac{d\lambda_\Phi}{d\mu} &= \frac{1}{(4\pi)^2}\Bigg[\lambda_\Phi\Big\{20\lambda_\Phi + 2\sum_{i=1}^{3}(Y_M^i)^2 - 12\big(x_\Phi\tilde{g}\big)^2 - 12\big(x_\Phi g_X\big)^2\Big\} \\
&+ 2\lambda_{\rm mix}^2 - 4\sum_{i=1}^{3}(Y_M^i)^4 + 6\Big\{\big(x_\Phi\tilde{g}\big)^2 + \big(x_\Phi g_X\big)^2\Big\}^2\Bigg], \\
\mu\frac{d\lambda_{\rm mix}}{d\mu} &= \frac{1}{(4\pi)^2}\Bigg[\lambda_{\rm mix}\Bigg\{12\lambda_H + 8\lambda_\Phi + 4\lambda_{\rm mix} + 6y_t^2 + \sum_{i=1}^{3}(Y_M^i)^2 \\
&- \frac{9}{2}g_2^2 - 6\left(\frac{1}{2}g_1 + x_H\tilde{g}\right)^2 - 6\big(x_\Phi\tilde{g}\big)^2 - 6\big(x_H g_X\big)^2 - 6\big(x_\Phi g_X\big)^2\Bigg\} \\
&+ 12\left\{\left(\frac{1}{2}g_1 + x_H\tilde{g}\right)\big(x_\Phi\tilde{g}\big) + \big(x_H g_X\big)\big(x_\Phi g_X\big)\right\}^2\Bigg]. \qquad (3.51)
\end{aligned}
$$

CHAPTER 4

SU(5)×U(1)$_X$ GRAND UNIFICATION WITH MINIMAL SEESAW AND Z'-PORTAL DARK MATTER

4.1 Introduction

Despite its great success, the Standard Model (SM) suffers from several problems. The neutrino mass matrix and a candidate of dark matter (DM) are two major missing pieces of the SM, and they must be supplemented by a framework beyond the SM. The minimal U(1)$_{B-L}$ model [1] is a very simple extension of the SM, where the anomaly-free global $B - L$ (baryon number minus lepton number) symmetry in the SM is gauged and only the three right-handed neutrinos (RHNs) and the U(1)$_{B-L}$ Higgs field in addition to the SM particle content. In the presence of the RHNs, the seesaw mechanism [2] is automatically implemented. Associated with the spontaneous U(1)$_{B-L}$ symmetry breaking by a vacuum expectation value (VEV) of the U(1)$_{B-L}$ Higgs field, the U(1)$_{B-L}$ gauge boson (Z' boson) and the three Majorana RHNs acquire their masses. The SM neutrino mass matrix is generated through the seesaw mechanism after the electroweak symmetry breaking.

Among various possibilities of introducing a DM candidate into the minimal U(1)$_{B-L}$ model, a way proposed in Ref. [3] would be the simplest, where instead of extending the particle content, a Z_2-parity is introduced and a unique Z_2-odd RHN plays the role of DM. The remaining two RHNs work to generate the SM neutrino mass matrix through the seesaw mechanism. Therefore, in this framework, the three RHNs are categorized into one Z_2-odd RHN DM and two Z_2-even RHNs for the so-called Minimal

Seesaw [4], which is the minimal setup to reproduce the neutrino oscillation data with a prediction of one massless eigenstate. In this way, the two missing pieces of the SM are supplemented with no extension of the particle content of the minimal $\mathrm{U}(1)_{B-L}$ model.

The RHN DM communicates with the SM particles in two ways: One is through exchanges of Higgs bosons in their mass basis (Higgs-portal RHN DM), where two physical Higgs bosons are realized as linear combinations of the $\mathrm{U}(1)_{B-L}$ and the SM Higgs bosons. The other is through Z' boson exchange (Z'-portal RHN DM). Phenomenology of the RHN DM has been extensively studied [3, 5, 6], in particular, a complementarity between the RHN DM physics and the LHC physics for the Z'-portal RHN DM scenario has been pointed out in Ref. [6].

The minimal $\mathrm{U}(1)_{B-L}$ model is easily generalized to the minimal $\mathrm{U}(1)_X$ model [7], whose particle content is the same as the one of the minimal $\mathrm{U}(1)_{B-L}$ model. The generalization appears in the $\mathrm{U}(1)_X$ charge assignment for the SM fields: the $\mathrm{U}(1)_X$ charge of an SM field (f) is defined as $Q_X = Y_f\, x_H + Q^f_{B-L}$, where Y_f and Q^f_{B-L} are the hypercharge and the $B-L$ charge of the field, and x_H is a new real parameter (see Table 4.1). With the charge assignment, the minimal $\mathrm{U}(1)_X$ model is free from all the gauge and mixed-gravitational anomalies (see, for example, Ref. [8] for detailed calculations of the anomaly coefficients). The minimal $\mathrm{U}(1)_{B-L}$ model is defined as the limit of $x_H \to 0$. The RHN DM is introduced in exactly the same way for the $\mathrm{U}(1)_{B-L}$ model. In Ref. [9], the minimal $\mathrm{U}(1)_X$ model with the Z'-portal RHN DM has been extensively studied. In the analysis, only four free parameters are involved: the $\mathrm{U}(1)_X$ gauge coupling (α_X), the Z' boson mass ($m_{Z'}$), x_H, and the RHN DM mass (m_{DM}). It has been found in Ref. [9] that $m_{\mathrm{DM}} \simeq m_{Z'}/2$ is required to reproduce the observed DM relic density, and the number of free parameters is effectively reduced to three: α_X, $m_{Z'}$ and x_H. The cosmological constraint from the DM relic density leads to a lower bound on α_X for fixed values of $m_{Z'}$ and x_H. On the other hand, the LHC Run-2 results from the search for a Z' boson resonance provide an upper bound on α_X for fixed values of $m_{Z'}$ and x_H. Therefore, the

DM physics and the LHC Run-2 phenomenology are complementary to narrow down the model parameter space.

In this letter, we propose a grand unified SU(5)×U(1)$_X$ model,[1] into which the minimal U(1)$_X$ model with the RHN DM is embedded. The grand unified theory (GUT) has been attracting a lot of attention since its first proposal in Ref. [11], where all the three gauge interactions in the SM are embedded into the SU(5) gauge group, and all the fermions in the SM are unified into three generations of $\mathbf{5}^*$ and **10**-representations under the SU(5). The picture is not only mathematically beautiful, but also provides the charge quantization for the SM quarks and leptons. It seems natural to regard the GUT as a primary candidate of physics beyond the SM. However, if this is the case, we may require a GUT model to incorporate the neutrino mass matrix and a DM candidate. The model we propose satisfies this requirement with the RHN DM and two RHNs for the minimal type-I seesaw. As in the original proposal in Ref. [11], the SM gauge groups are embedded into the SU(5) group. However, note that the unification of the quarks and leptons into $\mathbf{5}^*$ and **10**-representations is possible only if $x_H = -4/5$. Therefore, the U(1)$_X$ charge is quantized and x_H is no longer a free parameter.

4.2 SU(5)×U(1)$_X$ Unification

In the following, we show that our GUT model is phenomenologically viable. As we will discuss below, the SU(5) gauge symmetry is broken at $M_{\rm GUT} \simeq 4 \times 10^{16}$ GeV, and the minimal U(1)$_X$ model with the RHN DM ($x_H = -4/5$) is realized as low energy effective theory. The U(1)$_X$ symmetry is assume to be broken at the TeV scale. We first review this effective minimal U(1)$_X$ model at the TeV scale, and investigate phenomenological constraints on the model parameters. In our analysis, we follow Ref. [9] and identify an allowed parameter region, which will be found to be very narrow since $x_H = -4/5$ is no

[1] A similar model, but the unification into the flipped SU(5)×U(1) group has been recently proposed in Ref. [10].

	$\mathrm{SU}(3)_C$	$\mathrm{SU}(2)_L$	$\mathrm{U}(1)_Y$	$\mathrm{U}(1)_X$	Z_2
q_L^i	**3**	**2**	$1/6$	$(1/6)x_H + 1/3$	$+$
u_R^i	**3**	**1**	$2/3$	$(2/3)x_H + 1/3$	$+$
d_R^i	**3**	**1**	$-1/3$	$(-1/3)x_H + 1/3$	$+$
ℓ_L^i	**1**	**2**	$-1/2$	$(-1/2)x_H - 1$	$+$
e_R^i	**1**	**1**	-1	$(-1)x_H - 1$	$+$
H	**1**	**2**	$-1/2$	$(-1/2)x_H$	$+$
N_R^j	**1**	**1**	0	-1	$+$
N_R	**1**	**1**	0	-1	$-$
Φ	**1**	**1**	0	$+2$	$+$

Table 4.1: The particle content of the minimal $\mathrm{U}(1)_X$ extended SM with Z_2-parity. In addition to the SM particle content ($i = 1, 2, 3$), the three RHNs (N_R^j ($j = 1, 2$) and N_R) and the $\mathrm{U}(1)_X$ Higgs field (Φ) are introduced. The unification into $\mathrm{SU}(5)\times\mathrm{U}(1)_X$ is achieved only for $x_H = -4/5$, and x_H is quantized in our model.

longer a free parameter. Next, we discuss that the SM gauge couplings are successfully unified at $M_{\rm GUT}$ with some extra fermions at the TeV scale, which originate one $\mathbf{5} + \mathbf{5}^*$ and one $\mathbf{10} + \mathbf{10}^*$ multiplets under the SU(5) gauge group. After the SU(5) breaking, a kinetic mixing between the $\mathrm{U}(1)_Y$ and $\mathrm{U}(1)_X$ gauge bosons is generated through the renormalization group (RG) evolution. We also discuss that this mixing is negligibly small and has little effect on our analysis.

We first define the minimal $\mathrm{U}(1)_X$ model by the particle content listed in Table 4.1. The minimal $B - L$ model is reproduced as the limit of $x_H \to 0$. The model is free from all the gauge and the gravitational anomalies in the presence of the three RHNs. Because of the Z_2-parity assignment shown in Table 4.1, the N_R is a unique (cold) DM candidate. Fixing $x_H = -4/5$, we can see the unification of quarks and lepton into $\mathrm{SU}(5)\times\mathrm{U}(1)_X$ multiplets: $\overline{F_5}^i$ of $(\mathbf{5}^*, -3/5) \supset (d_R^i)^c \oplus \ell_L^i$, and F_{10}^i of $(\mathbf{10}, 1/5) \supset q_L^i \oplus (u_R^i)^c \oplus (e_R^i)^c$.

The Yukawa sector of the SM is extended to have

$$\mathcal{L}_{Yukawa} \supset -\sum_{i=1}^{3}\sum_{j=1}^{2} Y_D^{ij}\overline{\ell_L^i} H N_R^j - \frac{1}{2}\sum_{k=1}^{2} Y_N^k \Phi \overline{N_R^{k\,C}} N_R^k - \frac{1}{2} Y_N \Phi \overline{N_R^C} N_R + \text{H.c.}, \quad (4.1)$$

where the first term is the neutrino Dirac Yukawa coupling, and the second and third terms

are the Majorana Yukawa couplings. Without loss of generality, the Majorana Yukawa couplings are already diagonalized in our basis. Note that only the two Z_2-even RHNs are involved in the neutrino Dirac Yukawa coupling. After the $\mathrm{U}(1)_X$ and the electroweak symmetry breakings, the Z' boson mass, the Majorana masses for the RHNs, and the neutrino Dirac masses are generated:

$$\begin{aligned} m_{Z'} &= g_X \sqrt{4v_\Phi^2 + \frac{1}{4}x_H^2 v_h^2} \simeq 2 g_X v_\Phi, \\ m_{N^i} &= \frac{Y_N^i}{\sqrt{2}} v_\Phi, \quad m_{\mathrm{DM}} = \frac{Y_N}{\sqrt{2}} v_\Phi, \quad m_D^{ij} = \frac{Y_D^{ij}}{\sqrt{2}} v_h, \end{aligned} \tag{4.2}$$

where g_X is the $\mathrm{U}(1)_X$ gauge coupling, $\langle \Phi \rangle = v_\Phi/\sqrt{2}$, $v_h = 246$ GeV is the SM Higgs VEV, and we have used the LEP constraint [12]${v_\Phi}^2 \gg {v_h}^2$.

4.3 Z'-portal Dark Matter

Now we investigate phenomenological constraints for the minimal $\mathrm{U}(1)_X$ model with the RHN DM. We follow Ref. [9] for our analysis, where only four free parameters, $\alpha_X = g_X^2/(4\pi)$, $m_{Z'}$, x_H and m_{DM}. However, the grand unification to $\mathrm{SU}(5)\times\mathrm{U}(1)_X$ requires to fix $x_H = -4/5$, and hence the resultant allowed parameter space is more restricted.

Let us first evaluate the DM relic density by integrating the Boltzmann equation given by [13]

$$\frac{dY}{dx} = -\frac{xs\langle \sigma v_{\mathrm{rel}} \rangle}{H(m_{\mathrm{DM}})} \left(Y^2 - Y_{EQ}^2 \right), \tag{4.3}$$

where $x = m_{\mathrm{DM}}/T$ is the ratio of the DM mass to the temperature of the Universe (T), $H(m_{\mathrm{DM}})$ is the Hubble parameter at $T = m_{\mathrm{DM}}$, Y is the yield (the ratio of the DM number density to the entropy density s) of the DM, and Y_{EQ} is the yield of the DM particle in thermal equilibrium. The thermal average of the DM annihilation cross section times

relative velocity, $\langle \sigma v_{\rm rel} \rangle$, is calculated from the total cross section of the DM pair annihilation process $NN \to Z' \to f\bar{f}$ (f denotes the SM fermions) given by

$$\sigma(s) = \frac{\pi}{3}\alpha_X^2 \frac{\sqrt{s(s-4m_{\rm DM}^2)}}{(s-m_{Z'}^2)^2 + m_{Z'}^2\Gamma_{Z'}^2} F(x_H), \tag{4.4}$$

where

$$F(x_H) = 10\left(x_H + \frac{4}{5}\right)^2 + \frac{33}{5}, \tag{4.5}$$

and the total decay width of Z' boson is given by

$$\Gamma_{Z'} \;=\; \frac{\alpha_X}{6} m_{Z'} \left[F(x_H) + \beta^3 \theta(\beta^2)\right], \tag{4.6}$$

where $\beta = \sqrt{1-4m_{\rm DM}^2/m_{Z'}^2}$, $\theta(z)$ is the unit step function, and the masses of all SM fermions are neglected. Here, we have assumed $m_{N_R^{1,2}} > m_{\rm DM}$, $m_{Z'}/2$, for simplicity. By solving the Boltzmann equation numerically, the present DM relic density is evaluated by

$$\Omega_{DM}h^2 = \frac{m_{\rm DM}\, s_0\, Y(\infty)}{\rho_c/h^2}, \tag{4.7}$$

where $s_0 = 2890$ cm^{-3} is the entropy density of the present Universe, and $\rho_c/h^2 = 1.05 \times 10^{-5}$ GeV/cm^3 is the critical density. We identify a parameter region to reproduce the observed DM relic density in the range of $0.1183 \leq \Omega_\chi h^2 \leq 0.1213$ (68% confidence level), measured by the Planck satellite experiment [14]. As shown in Ref. [9], an enhancement of the DM pair annihilation cross section via the Z' boson resonance in the s-channel is necessary to reproduce the observed DM density. Hence, we always find $m_{\rm DM} \simeq m_{Z'}/2$, and thus our results are effectively described by only two free parameters: α_X and $m_{Z'}$.

Next we consider the current LHC constraints from the search for a narrow

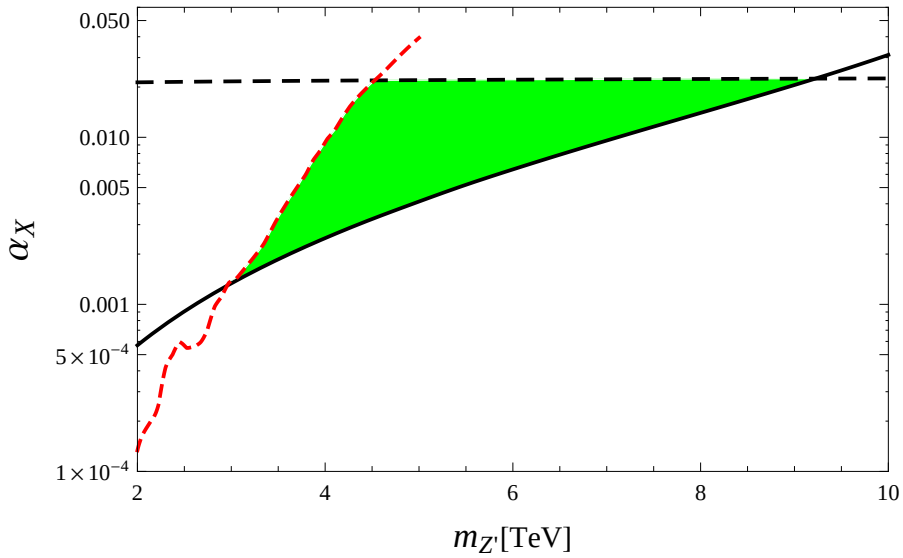

Figure 4.1: Allowed parameter region (green shaded) for the Z'-portal RHN DM scenario in the context of our SU(5)×U(1)$_X$ model ($x_H = -4/5$). The (black) solid line denotes the lower bound on α_X as a function of $m_{Z'}$ to reproduce the observed DM relic abundance. The diagonal dashed line (in red) shows the upper bound on α_X obtained from the search results for a Z' boson resonance at the LHC, which is applicable to $m_{Z'} \leq 5.0$ TeV. The perturbativity bound (see the discussion around Eq. (4.15)) is depicted by the horizontal dashed line. Combining all three constraints, we obtain the Z' boson mass bound in the range of $3.0 \leq m_{Z'}[\text{TeV}] \leq 9.2$.

resonance with dilepton final states at the LHC Run-2. In the analysis by the ATLAS and CMS collaborations, the so-called sequential SM Z' (Z'_{SSM}) has been studied as a reference model. We interpret the current LHC constraints on the Z'_{SSM} boson into the Z' boson in our U(1)$_X$ model to identify an allowed parameter region. Although our analysis follows that in Ref. [9], we will update the LHC constraints presented in Ref. [9] by employing the latest ATLAS results in 2017 [15].

The cross section for the process $pp \to Z' + X \to \ell^+\ell^- + X$ is given by

$$\sigma = 2 \sum_{q,\bar{q}} \int dM_{\ell\ell} \int_{\frac{M^2_{\ell\ell}}{s}}^1 dx \frac{2M_{\ell\ell}}{xs} f_q(x,Q^2) f_{\bar{q}} \left(\frac{M^2_{\ell\ell}}{xs}, Q^2 \right) \hat{\sigma}(q\bar{q} \to Z' \to \ell^+\ell^-), \quad (4.8)$$

where $M_{\ell\ell}$ is the invariant mass of a final state dilepton, f_q is the parton distribution function for a parton (quark) "q", and $\sqrt{s} = 13$ TeV is the center-of-mass energy of the LHC Run-2. In our numerical analysis, we employ CTEQ6L [16] for the parton distribution functions with the factorization scale $Q = m_{Z'}$. The cross section for the colliding partons is given by

$$\hat{\sigma}(q\bar{q} \to Z' \to \ell^+\ell^-) = \frac{\pi}{1296} \alpha_X^2 \frac{M^2_{\ell\ell}}{(M^2_{\ell\ell} - m^2_{Z'})^2 + m^2_{Z'}\Gamma^2_{Z'}} F_{q\ell}(x_H), \quad (4.9)$$

where the function $F_{q\ell}(x_H)$ is given by

$$\begin{aligned} F_{u\ell}(x_H) &= (8 + 20x_H + 17x_H^2)(8 + 12x_H + 5x_H^2), \\ F_{d\ell}(x_H) &= (8 - 4x_H + 5x_H^2)(8 + 12x_H + 5x_H^2) \end{aligned} \quad (4.10)$$

for q being the up-type (u) and down-type (d) quarks, respectively. By integrating the differential cross section over a range of $M_{\ell\ell}$ set by the ATLAS analysis, we obtain the cross section to be compared with the upper bounds obtained by the ATLAS collaboration. Only two free parameters, α_X and $m_{Z'}$, are involved in our analysis.

In Figure 4.1, we show our combined results from the DM relic abundance and the

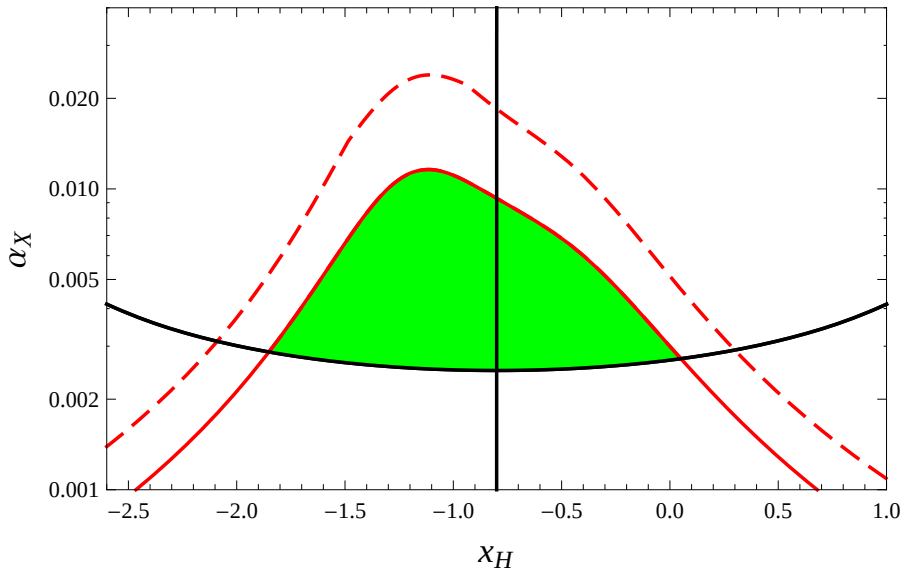

Figure 4.2: Allowed parameter region (green shaded) as a function of x_H, for $m_{Z'} = 4$ TeV in the minimal U(1)$_X$ model with the Z'-portal RHN DM. For the grand unified model, $x_H = -4/5$ is indicated by a vertical solid line. The (black) solid line shows the cosmological lower bound on α_X as a function of x_H. The dashed line (in red) shows the upper bound on α_X obtained in Ref. [9] by employing the LHC data with a 13/fb luminosity. Our update of the results by employing the ATLAS results with 36/fb is shown by the (red) solid line.

search results for a Z' boson resonance at the LHC. We can see these two constraints are complementary to narrow down the allowed parameter region. In Figure 4.1, we also show the perturbativity bound (see the discussion around Eq. (4.15)), which provides the upper bound on the U(1)$_X$ gauge coupling. Combining all three constraints, we have obtained the Z' boson mass bound in the range of $3.0 \leq m_{Z'}[\text{TeV}] \leq 9.2$.

Although in our grand unified model $x_H = -4/5$ is not a free parameter, we present the combined results as a function of x_H in Figure 4.2 for $m'_Z = 4$ TeV, in order to show that $x_H = -4/5$ has an interesting phenomenological implication. The (black) convex-downward solid line shows the cosmological lower bound on α_X as a function of x_H. The (red) convex-upward dashed line shows the upper bound on α_X presented in Ref. [9], where the results are obtained from the LHC 2016 data with a 13/fb luminosity. We have updated the results by employing the latest ATLAS results with 36/fb [15], and our result is shown by the (red) convex-upward solid line. The (green) shaded region is the final result

for the allowed parameter space after combining the cosmological and the LHC constraints when x_H is a free parameter. Interestingly, the plot indicates that $x_H = -4/5$ required by the grand unification into $\mathrm{SU}(5)\times\mathrm{U}(1)_X$ is almost the best value within the allowed region.

4.4 Gauge Coupling Unification

Let us now consider the gauge coupling unification. To realize the grand unification picture, the SM gauge coupling must be unified at a high energy scale. It has been shown in Ref. [17] that the SM gauge couplings are successfully unified around $M_{\rm GUT} \simeq 4 \times 10^{16}$ GeV in the presence of two pairs of vector-like quarks, $D_L + D_R$ and $Q_L + Q_R$, with their mass of $\mathcal{O}(1$ TeV) in the representations of $(\mathbf{3}, \mathbf{1}, 1/3)$ and $(\mathbf{3}, \mathbf{2}, 1/6)$, respectively, under the SM gauge group of $\mathrm{SU}(3)_C\times\mathrm{SU}(2)_L\times\mathrm{U}(1)_Y$. Here, we adopt this simple case to our scenario with a common mass (M) for $D_L + D_R$ and $Q_L + Q_R$. We simply take $M = m_{Z'}/2$ not to change the Z' boson decay width that we have used in our DM analysis. The unification scale leads to proton lifetime to be $\tau_p \simeq 10^{38}$ years, which is consistent with the current experimental lower bound obtained by the Super-Kamiokande [18], $\tau_p(p \to \pi^0 e^+) \gtrsim 10^{34}$ years.

In the grand unified $\mathrm{SU}(5)\times\mathrm{U}(1)_X$ picture, $D_L + D_R^C$ and $Q_L + Q_R^C$ are unified into $F_5 + \overline{F_5} = (\mathbf{5}, 3/5) + (\mathbf{5}^*, -3/5)$ and $F_{10} + \overline{F_{10}} = (\mathbf{10}, 1/5) + (\mathbf{10}^*, -1/5)$, respectively. The way to realize the mass splittings among the components in the SU(5) multiplets and leave only $D_L + D_R$ and $Q_L + Q_R$ light is analogous to the triplet-doublet mass splitting for the **5**-plet Higgs field in the usual SU(5) GUT model. We introduce the Yukawa couplings and the mass terms such as

$$\mathcal{L}_Y = \overline{F_5}(Y_5\Sigma - M_5)F_5 + \mathrm{tr}\left[\overline{F_{10}}(Y_{10}\Sigma - M_{10})F_{10}\right], \tag{4.11}$$

where $Y_{5,10}$ are Yukawa coupling constants, $M_{5,10}$ are masses for the vector-like fermions, Σ is a $\mathrm{U}(1)_X$ charge-neutral SU(5) adjoint Higgs field, whose VEV of

$\langle\Sigma\rangle = v_{\rm GUT}\,{\rm diag}(1,1,1,-3/2,-3/2)$ breaks the SU(5) gauge group into the SM ones, and we have used antisymmetric 5×5 matrices to express F_{10} and $\overline{F_{10}}$. We tune the Yukawa coupling to realize $Y_5 v_{\rm GUT} - M_5 = \mathcal{O}(1\text{ TeV})$ for $F_5 + \overline{F_5}$, so that the vector-like $\mathrm{SU}(3)_C$ color triplets $(D_L + D_R)$ become light, while the vector-like $\mathrm{SU}(2)_L$ doublets in the multiplets are heavy with mass of $(5/2)M_5$. By tuning Y_{10} to realize $Y_{10}v_{\rm GUT} + 4M_{10} = \mathcal{O}(1$ TeV) for F_{10} and $\overline{F_{10}}$, we obtain $Q_L + Q_R$ light, while the rest in the **10**-plets are heavy with mass of $5M_{10}$. Taking suitable values for $Y_{5,10} = \mathcal{O}(1)$, we can obtain the common TeV scale mass for $D_L + D_R$ and $Q_L + Q_R$, while the other components have GUT-scale masses.

Once the SU(5) symmetry is broken to the SM gauge groups at $M_{\rm GUT}$, a kinetic mixing between the $\mathrm{U}(1)_Y$ and the $\mathrm{U}(1)_X$ gauge bosons is generated at low energies through the RG evolutions. Following standard techniques in Ref. [19], we generally set a basis where the gauge boson kinetic terms are diagonalized and a covariant derivative of a field is defined as

$$D_\mu = \partial_\mu - (Y\ Q_X)\begin{pmatrix} g_Y & g_{\rm mix} \\ 0 & g_X \end{pmatrix}\begin{pmatrix} B_\mu \\ Z'_\mu \end{pmatrix}. \tag{4.12}$$

Here, Y and Q_X are $\mathrm{U}(1)_Y$ and $\mathrm{U}(1)_X$ charges of the field, respectively, B_μ is the SM $\mathrm{U}(1)_Y$ gauge field, and g_Y is the $\mathrm{U}(1)_Y$ gauge coupling. Originating from the gauge kinetic mixing, a new parameter, namely, "mixed gauge coupling" $g_{\rm mix}$ is introduced. In this basis, the RG evolution of the SM $\mathrm{U}(1)_Y$ gauge coupling remains the same as the SM one at the one-loop level, while g_X and $g_{\rm mix}$ evolve according to their coupled RG equations. At the one-loop level, the coupled RG equations for $\mu > \mathcal{O}(\text{TeV})$ are given by

$$\mu\frac{dg_X}{d\mu} = \frac{\beta_{g_X}}{16\pi^2}, \quad \mu\frac{dg_{\rm mix}}{d\mu} = \frac{\beta_{g_{\rm mix}}}{16\pi^2}, \tag{4.13}$$

where

$$\begin{aligned}
\beta_{g_X} &= \frac{1}{6} g_X \left[\left(80 + 64 x_H + 45 x_H^2\right) g_X^2 + 2 \left(32 + 45 x_H\right) g_X g_{\rm mix} + 45 g_{\rm mix}^2 \right], \\
\beta_{g_{\rm mix}} &= \frac{5}{3} g_Y^2 \left[\left(\frac{32}{5} + 9 x_H \right) g_X + 9 g_{\rm mix} \right] \\
&+ \frac{1}{6} g_{\rm mix} \left[(80 + 64 x_H + 45 x_H^2) g_X^2 + 2 (32 + 45 x_H) g_X g_{\rm mix} + 45 g_{\rm mix}^2 \right]. \qquad (4.14)
\end{aligned}$$

Here we have taken into account all particle contributions to the beta functions at the TeV scale. Numerically solving the RG equations with $g_{\rm mix} = 0$ and various values of g_X at $\mu = M_{\rm GUT}$, we have found that $g_{\rm mix}/g_X \simeq 0.034$ at the TeV scale for any input values of g_X at $M_{\rm GUT}$. Therefore, we can safely neglect effects of $g_{\rm mix}$ in our analysis and set $g_{\rm mix} = 0$ as a good approximation.

Neglecting $g_{\rm mix}$ in the RG equations, we find the following analytic solution for the $\mathrm{U}(1)_X$ gauge coupling:

$$\alpha_X(m_{Z'}) = \frac{\alpha_X(M_{\rm GUT})}{1 + \alpha_X(M_{\rm GUT}) \frac{b_X}{2\pi} \ln \left[\frac{M_{\rm GUT}}{m_{Z'}} \right]}, \qquad (4.15)$$

where $b_X = \left(80 + 64 x_H + 45 x_H^2\right)/6 = 48/5$ for $x_H = -4/5$. Since the running $\mathrm{U}(1)_X$ gauge coupling $\alpha_X(\mu)$ is asymptotically non-free, we now impose the "perturbativity bound" that $\alpha_X(M_{\rm GUT})$ must be in the perturbative regime. Adopting a condition of $\alpha_X(M_{\rm GUT}) \leq 4\pi$, we find $\alpha_X(m_{Z'}) \leq 0.022$ for $m_{Z'} \leq 10$ TeV. In Figure 4.1, we see that this perturbativity bound is more severe than the LHC bound for $m_{Z'} \gtrsim 4.5$ TeV.

4.5 Conclusion and Discussion

We have proposed a grand unified $\mathrm{SU}(5) \times \mathrm{U}(1)_X$ model, where the standard SU(5) grand unified theory is supplemented by minimal seesaw and a right-handed neutrino dark matter with an introduction of a global Z_2-parity. With three right-handed neutrinos (RHNs), the model is free from all gauge and mixed-gravitational anomalies. The SU(5)

symmetry is broken into the Standard Model (SM) gauge group at $M_{\rm GUT} \simeq 4 \times 10^{16}$ GeV in the standard manner, while the $U(1)_X$ symmetry breaking occurs at the TeV scale, which generates the TeV-scale mass of the $U(1)_X$ gauge boson (Z' boson) and the three Majorana RHNs. A unique Z_2-odd RHN is stable and serves as the dark matter (DM) in the present Universe, while the remaining two RHNs generate the SM neutrino masses through the minimal seesaw. We have investigated the Z'-portal RHN DM scenario in this model context. We have shown that the constraints from the DM relic abundance, and the Z' boson search at the Large Hadron Collider (LHC), and the perturbativity bound on the $U(1)_X$ gauge coupling are complementary to narrow down the allowed parameter region in the range of $3.0 \leq m_{Z'}[\text{TeV}] \leq 9.2$ for the Z' boson mass. The allowed region for $m_{Z'} \leq 5$ TeV will be fully covered by the future LHC experiments.

Finally, our grand unified $SU(5) \times U(1)_X$ model can also account for the origin of the Baryon asymmetry in the Universe through leptogenesis [20] with two Z_2-even RHNs if they are almost degenerate (resonant leptogenesis [21]). Introducing non-minimal gravitational couplings, the $U(1)_X$ Higgs field plays the role of inflaton. We can achieve the successful cosmological inflation scenario with a suitable choice of the non-minimal gravitational coupling constant. See, for example, Ref. [22].

4.6 Acknowledgments

This work of N.O. is supported in part by the U.S. Department of Energy (DE-SC0012447).

4.7 References

[1] R. N. Mohapatra and R. E. Marshak, "Local B-L Symmetry of Electroweak Interactions, Majorana Neutrinos and Neutron Oscillations," Phys. Rev. Lett. **44**, 1316 (1980) Erratum: [Phys. Rev. Lett. **44**, 1643 (1980)]; R. E. Marshak and R. N. Mohapatra, "Quark - Lepton Symmetry and B-L as the U(1) Generator of the

Electroweak Symmetry Group," Phys. Lett. **91B**, 222 (1980); C. Wetterich, "Neutrino Masses and the Scale of B-L Violation," Nucl. Phys. B **187**, 343 (1981); A. Masiero, J. F. Nieves and T. Yanagida, "B^-l Violating Proton Decay and Late Cosmological Baryon Production," Phys. Lett. **116B**, 11 (1982); R. N. Mohapatra and G. Senjanovic, "Spontaneous Breaking of Global $B - L$ Symmetry and Matter - Antimatter Oscillations in Grand Unified Theories," Phys. Rev. D **27**, 254 (1983); W. Buchmuller, C. Greub and P. Minkowski, "Neutrino masses, neutral vector bosons and the scale of B-L breaking," Phys. Lett. B **267**, 395 (1991).

[2] P. Minkowski, "$\mu \to e\gamma$ at a Rate of One Out of 10^9 Muon Decays?," Phys. Lett. **67B**, 421 (1977); T. Yanagida, "Horizontal Symmetry and Masses of Neutrinos," Prog. Theor. Phys. **64**, 1103 (1980); J. Schechter and J. W. F. Valle, "Neutrino Masses in SU(2) $\otimes$ U(1) Theories," Phys. Rev. D **22**, 2227 (1980); T. Yanagida, in Proceedings of the Work- shop on the Unified Theory and the Baryon Number in the Universe (O. Sawada and A. Sugamoto, eds.), KEK, Tsukuba, Japan, 1979, p. 95; M. Gell-Mann, P. Ramond, and R. Slansky, Supergravity (P. van Nieuwenhuizen et al. eds.), North Holland, Amsterdam, 1979, p. 315; S. L. Glashow, The future of elementary particle physics, in Proceedings of the 1979 Carg'ese Summer Institute on Quarks and Leptons (M. Levy et al. eds.), Plenum Press, New York, 1980, p. 687; R. N. Mohapatra and G. Senjanovic, "Neutrino Mass and Spontaneous Parity Violation," Phys. Rev. Lett. **44**, 912 (1980).

[3] N. Okada and O. Seto, "Higgs portal dark matter in the minimal gauged $U(1)_{B-L}$ model," Phys. Rev. D **82**, 023507 (2010) [arXiv:1002.2525 [hep-ph]].

[4] S. F. King, "Large mixing angle MSW and atmospheric neutrinos from single right-handed neutrino dominance and U(1) family symmetry," Nucl. Phys. B **576**, 85 (2000) [hep-ph/9912492]; P. H. Frampton, S. L. Glashow and T. Yanagida,

"Cosmological sign of neutrino CP violation," Phys. Lett. B **548**, 119 (2002) [hep-ph/0208157].

[5] N. Okada and Y. Orikasa, "Dark matter in the classically conformal B-L model," Phys. Rev. D **85**, 115006 (2012) [arXiv:1202.1405 [hep-ph]]; T. Basak and T. Mondal, "Constraining Minimal $U(1)_{B-L}$ model from Dark Matter Observations," Phys. Rev. D **89**, 063527 (2014) [arXiv:1308.0023 [hep-ph]].

[6] N. Okada and S. Okada, "Z'_{BL} portal dark matter and LHC Run-2 results," Phys. Rev. D **93**, no. 7, 075003 (2016) [arXiv:1601.07526 [hep-ph]].

[7] T. Appelquist, B. A. Dobrescu and A. R. Hopper, "Nonexotic neutral gauge bosons," Phys. Rev. D **68**, 035012 (2003) [hep-ph/0212073].

[8] S. Oda, N. Okada and D. s. Takahashi, "Classically conformal U(1)' extended standard model and Higgs vacuum stability," Phys. Rev. D **92**, no. 1, 015026 (2015) [arXiv:1504.06291 [hep-ph]].

[9] N. Okada and S. Okada, "Z'-portal right-handed neutrino dark matter in the minimal $U(1)_X$ extended Standard Model," Phys. Rev. D **95**, no. 3, 035025 (2017) [arXiv:1611.02672 [hep-ph]]; S. Oda, N. Okada and D. s. Takahashi, "Right-handed neutrino dark matter in the classically conformal U(1)' extended standard model," Phys. Rev. D **96**, no. 9, 095032 (2017) [arXiv:1704.05023 [hep-ph]].

[10] H. Y. Chen, I. Gogoladze, S. Hu, T. Li and L. Wu, "The Minimal GUT with Inflaton and Dark Matter Unification," arXiv:1703.07542 [hep-ph].

[11] H. Georgi and S. L. Glashow, "Unity of All Elementary Particle Forces," Phys. Rev. Lett. **32**, 438 (1974).

[12] M. Carena, A. Daleo, B. A. Dobrescu and T. M. P. Tait, "Z' gauge bosons at the Tevatron," Phys. Rev. D **70**, 093009 (2004) [hep-ph/0408098]; J. Heeck, "Unbroken B-L symmetry," Phys. Lett. B **739**, 256 (2014) [arXiv:1408.6845 [hep-ph]].

[13] E. W. Kolb and M. S. Turner, *The Early Universe* (Addison-Wesley, Reading, MA, 1990).

[14] P. A. R. Ade *et al.* [Planck Collaboration], "Planck 2015 results. XIII. Cosmological parameters," Astron. Astrophys. **594**, A13 (2016) [arXiv:1502.01589 [astro-ph.CO]].

[15] M. Aaboud *et al.* [ATLAS Collaboration], "Search for new high-mass phenomena in the dilepton final state using 36 fb^{-1} of proton-proton collision data at $\sqrt{s} = 13$ TeV with the ATLAS detector," JHEP **1710**, 182 (2017) [arXiv:1707.02424 [hep-ex]].

[16] J. Pumplin, D. R. Stump, J. Huston, H. L. Lai, P. M. Nadolsky and W. K. Tung, "New generation of parton distributions with uncertainties from global QCD analysis," JHEP **0207**, 012 (2002) [hep-ph/0201195].

[17] U. Amaldi, W. de Boer, P. H. Frampton, H. Furstenau and J. T. Liu, "Consistency checks of grand unified theories," Phys. Lett. B **281**, 374 (1992); J. L. Chkareuli, I. G. Gogoladze and A. B. Kobakhidze, Phys. Lett. B **340**, 63 (1994); Phys. Lett. B **376**, 111 (1996) [hep-ph/9602399]; D. Choudhury, T. M. P. Tait and C. E. M. Wagner, "Beautiful mirrors and precision electroweak data," Phys. Rev. D **65**, 053002 (2002) [hep-ph/0109097]; D. E. Morrissey and C. E. M. Wagner, "Beautiful mirrors, unification of couplings and collider phenomenology," Phys. Rev. D **69**, 053001 (2004) [hep-ph/0308001]; I. Gogoladze, B. He and Q. Shafi, "New Fermions at the LHC and Mass of the Higgs Boson," Phys. Lett. B **690**, 495 (2010) [arXiv:1004.4217 [hep-ph]].

[18] M. Miura [Super-Kamiokande Collaboration], "Search for Nucleon Decay in Super-Kamiokande," Nucl. Part. Phys. Proc. **273-275**, 516 (2016).

[19] F. del Aguila, G. D. Coughlan and M. Quiros, "Gauge Coupling Renormalization With Several U(1) Factors," Nucl. Phys. B **307**, 633 (1988) Erratum: [Nucl. Phys. B **312**, 751 (1989)].

[20] M. Fukugita and T. Yanagida, "Baryogenesis Without Grand Unification," Phys. Lett. B **174**, 45 (1986).

[21] A. Pilaftsis, "CP violation and baryogenesis due to heavy Majorana neutrinos," Phys. Rev. D **56**, 5431 (1997); A. Pilaftsis and T. E. J. Underwood, Nucl. Phys. B **692**, 303 (2004) [hep-ph/0309342].

[22] N. Okada, M. U. Rehman and Q. Shafi, "Non-Minimal B-L Inflation with Observable Gravity Waves," Phys. Lett. B **701**, 520 (2011) [arXiv:1102.4747 [hep-ph]]; N. Okada and D. Raut, "Running non-minimal inflation with stabilized inflaton potential," Eur. Phys. J. C **77**, no. 4, 247 (2017) [arXiv:1509.04439 [hep-ph]]; S. Oda, N. Okada, D. Raut and D. s. Takahashi, "Non-minimal quartic inflation in classically conformal $U(1)_X$ extended Standard Model," arXiv:1711.09850 [hep-ph].

CHAPTER 5

CONCLUSION

Despite the tremendous success of the SM in explaining most of the phenomena currently observed in nature, the SM does not include viable candidates to account for the cosmological inflation, observed DM relic abundance, and neutrino masses. Hence, we need to extend the SM beyond its current framework. With a motivation to address these issues, we have considered anomaly free minimal $\mathrm{U}(1)_X$ extended SM, where in addition to the particles in the SM, we have three generations of RHNs, a new $B-L$ Higgs field to break the $\mathrm{U}(1)_X$ gauge symmetry, and a $\mathrm{U}(1)_X$ gauge boson (Z'). The $\mathrm{U}(1)_X$ charges of the particles are defined by a single free parameter x_H. This model is a generalization of the minimal $B-L$ model, and is identical to the minimal $B-L$ model in the limit of $x_H = 0$

From a theoretical point of view, if the inflaton value is trans-Planckian ($\phi_I > M_{Pl}$) during the inflaton, effective operators suppressed by the Planck mass (M_{Pl}) could significantly affect the inflaton potential during the inflation, and hence the inflationary predictions. In chapters 2 [19], we have shown that the inflection-point inflation is an interesting possibility to realize a successful slow-roll inflation when inflation is driven by a single scalar field with initial inflaton value less than Planck mass ($\phi_I < M_{Pl}$). To realize the inflection-point-like behavior for the RG improved effective $\lambda\phi^4$ potential, we have shown that the running quartic coupling $\lambda(\phi)$ must exhibit a minimum with an almost vanishing value in its RG evolution, namely $\lambda(\phi_I) \simeq 0$ and $\beta_\lambda(\phi_I) \simeq 0$, where β_λ is the beta-function of the quartic coupling. Imposing the consistency of the inflationary predictions with the observed Planck measurements, we have shown that the conditions,

$\lambda(\phi_I) \simeq 0$ and $\beta_\lambda(\phi_I) \simeq 0$, lead to relations among the gauge, the Yukawa and the Higgs quartic couplings at ϕ_I. Interestingly, inflection-point inflation provides a unique prediction for the running of the spectral index $\alpha \simeq -2.7 \times 10^{-3}$, independently of the other model parameters.

From a particle physics perspective, it is more compelling to consider an inflationary scenario, where the inflaton/scalar field plays the role of a Higgs field which spontaneously breaks a gauge symmetry of the model. As an example, in Chapters 2 and 3, Refs. [19] and [20], respectively, we have considered the inflection-point inflation with the identification of $\mathrm{U}(1)_X$ Higgs field to be the inflaton field. Requiring the inflationary predictions to be consistent with the cosmological observation, the conditions $\lambda(\phi_I) \simeq 0$ and $\beta_\lambda(\phi_I) \simeq 0$, uniquely fixes the mass ratios among the Z' boson, RHNs, and the $\mathrm{U}(1)_X$ Higgs field, which is determined by only two free parameters, ϕ_I and x_H. After considering the reheating at the end of inflation and imposing the BBN constraint as well as the current collider experimental bounds, we have shown that the inflationary predictions are complimentary to Z' boson searches at the LHC to identify the allowed parameter regions. In Chapter 2 [20], we have considered $\mathrm{U}(1)_X$ Higgs inflation at the $B - L$ limit ($x_H = 0$), to show that the entire parameter region for $m_{Z'} < 500$ GeV can be tested by the future collider experiments such as the High Luminosity (HL)-LHC and the SHiP experiments. In Chapter 3 [21], we have considered $\mathrm{U}(1)_X$ Higgs inflation for $|x_H| \gg 1$. Although the inflationary predictions requires gauge coupling to be very small, we have shown that Z' mass of a few TeV can be explored at the LHC Run-2. This is in sharp contrast with the previous case with $x_H = 0$, where only $m_{Z'} < 500$ GeV can be explored in the future.

In the same model context, in Chapter 4 [24], we have also considered $\mathrm{SU}(5)\times\mathrm{U}(1)_X$, where the SM quarks and lepton are unified into SU(5) for fixed $x_H = -4/5$. Hence, the $\mathrm{U}(1)_X$ charge is quantized for $x_H = -4/5$. With the introduction of a global Z_2 symmetry, we have assigned Z_2-odd parity to one of the RHNs which is stable and serves as the DM in our setup. We have investigated the Z'-portal RHN DM

scenario, where the RHN DM candidate interacts with the SM particles through the Z' boson mediated processes. For the Z' boson mass < 5 TeV, we have found that the constraints from the DM relic abundance and the search results for a Z' boson resonance at the LHC with di-lepton final states are complementary to narrow down the allowed parameter region. The allowed parameter region will be fully covered by the future HL-LHC experiment. Also, with two additional pairs of vector-like quarks, all the SM gauge coupling are successfully unified around $M_{\rm GUT} \simeq 4 \times 10^{16}$ GeV.

In addition, in Refs. [25, 26], we have shown that this model can also explain the origin of observed neutrino masses. Using a realistic choice of parameters to reproduce the neutrino oscillation data, we have shown that the model provides significant enhancement of the production cross section of the RHNs from Z' boson decay, which is crucial for the discovery of RHNs in the future LHC experiments.

In conclusion, we have shown that the $\mathrm{U}(1)_X$ extended SM is a very well motivated extension of the SM framework. Even with a minimal extension of the SM particle content, we have shown that the model can accommodate the cosmological inflation scenario, the DM particle as well as the masses for the neutrinos. Hence, this model can address all three major shortcomings of the SM. Importantly, we have established interesting complementarities between cosmological observations of the inflationary scenario and the DM physics with the new physics searches at the collider experiments. Hence, the model can be tested in the future.

REFERENCES

[1] T. Moori, C. S. Lim, and S. N. Mukheree, "The physics of the standard model and beyond (2016)".

[2] C. P. Burgess and G. D. Moore, "The standard model: A primer (Cambridge University Press, 2016)".

[3] C. Patrignani *et al.* [Particle Data Group], "Review of Particle Physics," Chin. Phys. C **40**, no. 10, 100001 (2016).

[4] E. W. Kolb and M. S. Turner, "The Early Universe," Front. Phys. **69**, 1 (1990).

[5] S. Weinberg, "Cosmology (Oxford University Press, 2008)".

[6] D. Baumann, "Inflation," arXiv:0907.5424 [hep-th].

[7] G. Hinshaw *et al.* [WMAP Collaboration], "Nine-Year Wilkinson Microwave Anisotropy Probe (WMAP) Observations: Cosmological Parameter Results," Astrophys. J. Suppl. **208**, 19 (2013) [arXiv:1212.5226 [astro-ph.CO]].

[8] P. A. R. Ade *et al.* [Planck Collaboration], "Planck 2015 results. XIII. Cosmological parameters," Astron. Astrophys. **594**, A13 (2016) [arXiv:1502.01589 [astro-ph.CO]].

[9] M. Lisanti, "Lectures on Dark Matter Physics," arXiv:1603.03797 [hep-ph].

[10] T. Appelquist, B. A. Dobrescu and A. R. Hopper, "Nonexotic neutral gauge bosons," Phys. Rev. D **68**, 035012 (2003) [hep-ph/0212073].

[11] R. N. Mohapatra and R. E. Marshak, "Local B-L Symmetry of Electroweak Interactions, Majorana Neutrinos and Neutron Oscillations," Phys. Rev. Lett. **44**, 1316 (1980) Erratum: [Phys. Rev. Lett. **44**, 1643 (1980)].

[12] R. E. Marshak and R. N. Mohapatra, "Quark - Lepton Symmetry and B-L as the U(1) Generator of the Electroweak Symmetry Group," Phys. Lett. **91B**, 222 (1980).

[13] C. Wetterich, "Neutrino Masses and the Scale of B-L Violation," Nucl. Phys. B **187**, 343 (1981).

[14] A. Masiero, J. F. Nieves and T. Yanagida, "B^{-}l Violating Proton Decay and Late Cosmological Baryon Production," Phys. Lett. **116B**, 11 (1982).

[15] R. N. Mohapatra and G. Senjanovic, "Spontaneous Breaking of Global $B - L$ Symmetry and Matter - Antimatter Oscillations in Grand Unified Theories," Phys. Rev. D **27**, 254 (1983).

[16] W. Buchmuller, C. Greub and P. Minkowski, "Neutrino masses, neutral vector bosons and the scale of B-L breaking," Phys. Lett. B **267**, 395 (1991).

[17] S. Oda, N. Okada and D. s. Takahashi, "Classically conformal U(1)' extended standard model and Higgs vacuum stability," Phys. Rev. D **92**, no. 1, 015026 (2015) [arXiv:1504.06291 [hep-ph]].

[18] H. S. Lee and S. Yun, "Mini force: The $(B-L)+xY$ gauge interaction with a light mediator," Phys. Rev. D **93**, no. 11, 115028 (2016) [arXiv:1604.01213 [hep-ph]].

[19] N. Okada and D. Raut, "Inflection-point $B-L$ Higgs Inflation," Phys. Rev. D **95**, no. 3, 035035 (2017) [arXiv:1610.09362 [hep-ph]].

[20] N. Okada, S. Okada and D. Raut, "Inflection-point inflation in hyper-charge oriented $\mathrm{U}(1)_X$ model," Phys. Rev. D **95**, no. 5, 055030 (2017) [arXiv:1702.02938 [hep-ph]].

[21] S. Oda, N. Okada, D. Raut and D. s. Takahashi, "Nonminimal quartic inflation in classically conformal $\mathrm{U}(1)_X$ extended standard model," Phys. Rev. D **97**, no. 5, 055001 (2018) [arXiv:1711.09850 [hep-ph]].

[22] N. Okada and S. Okada, "Z'_{BL} portal dark matter and LHC Run-2 results," Phys. Rev. D **93**, no. 7, 075003 (2016) [arXiv:1601.07526 [hep-ph]].

[23] N. Okada and S. Okada, "Z'-portal right-handed neutrino dark matter in the minimal $\mathrm{U}(1)_X$ extended Standard Model," Phys. Rev. D **95**, no. 3, 035025 (2017) [arXiv:1611.02672 [hep-ph]].

[24] N. Okada, S. Okada and D. Raut, "$\mathrm{SU}(5)\times\mathrm{U}(1)_X$ grand unification with minimal seesaw and Z'-portal dark matter," Phys. Lett. B **780**, 422 (2018) [arXiv:1712.05290 [hep-ph]].

[25] A. Das, N. Okada and D. Raut, "Enhanced pair production of heavy Majorana neutrinos at LHC," arXiv:1710.03377 [hep-ph].

[26] A. Das, N. Okada and D. Raut, "Heavy Majorana neutrino pair productions at the LHC in minimal U(1) extended Standard Model," arXiv:1711.09896 [hep-ph].

[27] M. Anelli *et al.* [SHiP Collaboration], "A facility to Search for Hidden Particles (SHiP) at the CERN SPS," arXiv:1504.04956 [physics.ins-det].

[28] R. N. Mohapatra and A. Y. Smirnov, "Neutrino Mass and New Physics," Ann. Rev. Nucl. Part. Sci. **56**, 569 (2006) [hep-ph/0603118].